UNIVERSIDADE FEDERAL DO PARÁ
INSTITUTO DE GEOCIÊNCIAS
PROGRAMA DE PÓS-GRADUAÇÃO EM GEOLOGIA E GEOQUÍMICA

TESE DE DOUTORADO Nº 140

O MAR EPICONTINENTAL ITAITUBA NA REGIÃO CENTRAL DA BACIA DO AMAZONAS: PALEOAMBIENTE E CORRELAÇÃO COM OS EVENTOS PALEOCLIMÁTICOS E PALEOCEANOGRÁFICOS DO CARBONÍFERO

Tese apresentada por:

PEDRO AUGUSTO SANTOS DA SILVA
Orientador: Prof. Dr. Afonso César Rodrigues Nogueira (UFPA)

BELÉM
2019

Universidade Federal do Pará
Instituto de Geociências
Programa de Pós-Graduação em Geologia e Geoquímica

O MAR EPICONTINENTAL ITAITUBA NA REGIÃO CENTRAL DA BACIA DO AMAZONAS: PALEOAMBIENTE E CORRELAÇÃO COM OS EVENTOS PALEOCLIMÁTICOS E PALEOCEANOGRÁFICOS DO CARBONÍFERO

Tese apresentada por

PEDRO AUGUSTO SANTOS DA SILVA

Como requisito parcial à obtenção de Grau de Doutor em Ciências na Área de GEOLOGIA

Data de Aprovação: 14 / 03 / 2019

Banca Examinadora:
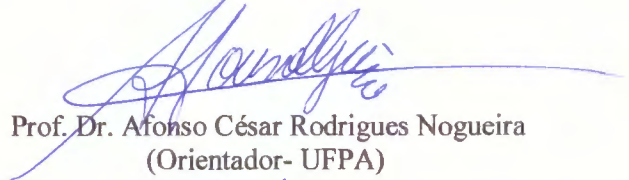
Prof. Dr. Afonso César Rodrigues Nogueira
(Orientador- UFPA)

Prof.ª Dr.ª Ana Maria Góes
(Membro-USP)
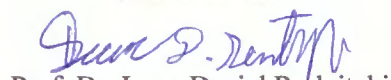
Prof. Dr. Isaac Daniel Rudnitzki
(Membro-UFOP)

Prof. Dr. Werner Truckenbrodt
(Membro-UFPA)
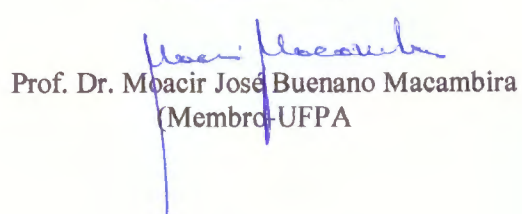
Prof. Dr. Moacir José Buenano Macambira
(Membro-UFPA

Ao meu pai Seu Bandeira (*In memoriann*)
Pelos sacrifícios e o imenso amor e dedicação

AGRADECIMENTOS

À Deus por suas diferentes formas de mostrar o mundo.

A família por ter compreendido o isolamento e o estresse causado durante esses anos todos de pós-graduação, agradeço por cada um de vocês terem me ensinados lições que levo para toda a vida, obrigado por se fazerem presente em minha vida, mesmo que houvesse distância em muitos momentos, serei sempre grato à minha querida mãe Denyse, aos meus tios e primos: José Bandeira Jr., Kely, Cecylia, Júnior, Ronaldo e em especial a minha vó Landa.

Ao programa de pós-graduação em geologia e geoquímica da Universidade Federal do Pará (PPGG-UFPA) pela infraestrutura, apoio financeiro e logístico.

À Cleida Freitas e Joanice Lopes, secretárias do PPGG, por todo auxílio e suporte fornecidos nesses anos de pós-graduação.

A CAPES e ao CNPQ pela concessão da bolsa de doutorado.

Ao grande amigo e orientador Prof. Dr. Afonso Nogueira, obrigado pelos ensinamentos da geologia sedimentar e todos os conselhos de vida. Serei sempre grato a quem há exatos 11 anos atrás, acreditou que mais um Silva poderia trilhar um caminho mais longo na vida, muito obrigado mestre!!!

Ao grande amigo Dr. José Bandeira, por me incentivar e mostrar o maravilhoso mundo da geologia, obrigado por tudo, pelos conselhos e paciência em momentos difíceis no desenrolar deste trabalho.

Ao projeto "Rochas calcárias da Bacia do Amazonas e Plataforma Bragantina: Avaliação de áreas potenciais para insumos agrícolas do Estado do Pará, regiões de Santarém-Uruará e do Salgado" Coordenado pelo Prof. Dr. Afonso Nogueira, pelo financiamento as etapas de campo na região de Monte Alegre.

Ao projeto "Estudo das ocorrências de minerais industriais–carbonatos, fosfatos e evaporitos – na região de Santarém–Itaituba (PA), Carbonífero da Bacia do Amazonas" (Edital MCT/CT-Mineral/CNPq Nº 44/2010) coordenado pelo Prof. Moacir Macambira, pelo financiamento a etapa de campo da região do Rio Tapajós, em Itaituba.

Às professoras Drª. Ana Karina Scomazzon e Drª. Luciane Profs Moutinho por todo auxilio na etapa de campo em Monte Alegre, a todas as discussões a cerca dos conodontes e foraminíferos e os demais fósseis do Pensilvaniano.

Aos professores Dr. Rômulo Angélica, Dr. Moacir Macambira e Drª. Rosemery Nascimento pelas valiosas discussões nas etapas de campo. Ao amigo Dr. Isaac Salém pela valiosa ajuda nas coletas de amostra e as conversas sobre os ricos paleoambientes deposicionais da Bacia do Amazonas.

Existem muitas hipóteses em ciências que estão erradas.
Isso é perfeitamente aceitável,
elas são a abertura para achar as que estão certas
Carl Sagan

RESUMO

A paleogeografia do Carbonífero de Gondwana Ocidental foi dominada por mares epicontinentais ligados ao Oceano Panthalassa a Oeste. Uma sucessão transgressiva Pensilvaniana mista siliciclástica-carbonática, com 50m de espessura, foi estudada em afloramentos e testemunhos de sondagem utilizando uma combinação de análises faciológicas, estratigráficas com a estratigrafia isotópica de C e O. Trinta e quatro fácies representativas dos sistemas deposicionais costeiros a plataformais são agrupadas em três associações de fácies (AF): AF1 depósito desértico costeiro constituídos de arenitos finos a médios, pelitos e dolomitos finos a arenosos que correspondem a uma complexa associação de dunas arenosas eólicas, lençóis de areia, interduna, canais fluviais e depósitos lagunares bioturbados pelos traços fósseis *Palaeophycus*, *Lockeia*, *Thalassinoides* e *Rosselia.* AF2) planície de maré mista constituída por arenitos finos a médios, pelitos, folhelhos, siltitos e dolomitos finos, interpretados como depósitos de supramaré, de canais de maré, delta de marés e lagunas com fósseis de braquiópodes e equinodermas. AF3) depósitos carbonáticos de plataforma constituídos por *lime mudstones, wackestones, packstones, grainstones* com aloquímicos (oóides e pelóides), grãos terrígenos e abundantes e diversificados organismos bentônicos marinhos rasos como: restos de peixes, foraminíferos, braquiópodes, equinodermas, gastrópodes, briozoários, trilobitas, corais, ostracodes e conodontes, interpretados como barras bioclásticas e plataforma carbonática. As espécies de conodontes *Neognathodus symmetricus, Streptognathodus sp.* e *Ellisonia sp.* em AF3 indicam uma idade Baskiriana-Moscoviana para estes depósitos. A dolomitização afetou os calcários e arenitos de AF1 e AF2 substituindo a matriz micrítica e ocorrendo como dolomita em sela, indicando mistura de águas meteóricas e marinhas e soterramento respectivamente. O neomorfismo da matriz micrítica opaca e em conchas de bivalves são constatadas pelo crescimento de mosaico de cristais xenotópicos. Em contraste, o cimento calcítico secundário é equigranular, fibroso, *bladed* e espático. A micritização é encontrada nas conchas de bioclastos exibindo envelope micrítico. A autigênese de quartzo e pirita de origem biogênica é comumente encontrada em AF2 e AF3. A compactação mecânica e química nos calcários causou a redução da porosidade, cimentação, fraturas e o desenvolvimento de *dissolution seams* e estilólitos. Os arenitos foram cimentados por quartzo, calcita e óxidos e hidróxidos de ferro e mostram contatos de grãos côncavos-convexos e suturados. A predominância de feições eodiagenéticas e subordinadamente mesodiagenéticas na sucessão Monte Alegre-Itaituba indicou um arcabouço menos modificado pelos processos diagenéticos, que corrobora com a assinatura original dos valores de $\delta^{13}C$

variando de ~-2‰ a +5, 28‰. Esta tendência enriquecida se coaduna com a alta produtividade orgânica, desencadeada pelo florescimento maciço de organismos bentônicos de controle eufótico, principalmente em AF3. Cinco tipos de ciclos de raseamento ascendente e assimétricos caracterizam a sucessão Monte Alegre-Itaituba. Ciclos de perimaré em deserto costeiro (ciclo I) foram formados pela alternância de dolomitos e arenitos com valores de $\delta^{13}C$ variando de -1, 5‰ a +0, 3‰. Os ciclos II consistem em intercalações de arenito pelito e arenito floatstone e o ciclo III é composto por alternância de dolomitos e arenitos. Estes ciclos como depósitos de planície de maré e laguna com valores de $\delta^{13}C$ alcançando de +3, 98‰ a +4, 62‰. O ciclo IV é um ritmito formado por pares de *wackestone/lime mudstone,* enquanto o ciclo V consiste na alternância de *grainstones, wackestones* e *lime mudstones* (ciclicidade ABC) passando para ciclos compostos por *wackestones* e *lime mudstones* (ciclicidade AB). Os ciclos IV e V são depósitos de plataforma com valores de $\delta^{13}C$ variando de +3, 65‰ a 5, 28‰. O empilhamento de 53 ciclos com espessuras médias de 1,1 m, combinados com o diagrama de *Fisher plot,* indicou um padrão de empilhamento agradacional a retrogradacional inserido em um trato de sistema transgressivo inicial (ciclos I-III) e o trato de sistema transgressivo tardio (ciclos IV e V). A sucessão foi depositada em ~13 Ma e os ciclos individuais acumulados em aproximadamente 0, 25 Ma, típicos de ciclos de quarta ordem relacionados a flutuações do nível do mar de alta frequência. Estes dados foram correlacionados com as curvas globais de $\delta^{13}C$ e nível do mar que posicionaram a sucessão Monte Alegre-Itaituba no Serpukhoviano Superior ao Moscoviano inferior. A influência da glaciação Mississispiana Superior foi insignificante nestes depósitos, mas a transgressão pós-glacial associada a lenta subsidência da Bacia do Amazonas gerou os ciclos I, IV e V. Os ciclos II e III foram formados por processos autóctones durante um período de equilíbrio entre o suprimento e a glacioeustasia. A sucessão Monte Alegre-Itaituba é o registro de um grande mar epicontinental amazônico que estava diretamente ligado ao Oceano Panthalassa durante o Pensilvaniano.

Palavras-chave: Pensilvaniano, Bacia do Amazonas, Sucessão Monte Alegre-Itaituba, ciclicidade de alta frequência, isótopos estáveis de $\delta^{13}C$ e $\delta^{18}O$

ABSTRACT

The Carboniferous paleogeography of the West Gondwana was dominated by epicontinental seas connected with the Panthalassa Ocean to the west. 50m-thick Pennsylvanian mixed siliciclastic-carbonate transgressive succession of the Amazonas Basin, Northern Brazil, were studied in outcrops and cores using facies and stratigraphic analysis in combination with O- and C-isotopic stratigraphy. Thirty-four facies, representative of coastal to shelf depositional systems grouped in three facies associations (FA): FA1) coastal desertic deposits, consisting of fine to medium-grained sandstone, mudstone and fine-grained dolostone that corresponds to a complex association of aeolian dunes, sand sheets, interdunes, fluvial channels and lagoon deposits bioturbated by *Palaeophycus*, *Lockeia*, *Thalassinoides* and *Rosselia* trace fossils; FA2) mixed tidal flat setting, constituted by fine to medium-grained sandstone, mudstone, shale, siltstone, lime mudstone and fine dolostone interpreted as supratidal, tidal channel, tidal delta and lagoon deposits with some brachiopod and echinoderm body fossils; and FA3) carbonate shelf deposits, consisting of lime mudstone, wackestone, packstone and grainstone with allochems (ooids and peloids), terrigenous grains and abundant and diversified open shallow marine benthic organisms, including, fish remains, foraminifers, brachiopods, echinoderms, gastropods, bryozoans, trilobites, corals, ostracodes, and conodonts, interpreted as bioclastic bars and carbonate shelf deposits. The conodonts species *Neognathodus symmetricus, Streptognathodus sp.* and *Ellisonia sp*. in the FA3 indicate the Baskirian-Moscovian age. The dolomitization affected the limestone and sandstone of AF1 and AF2 replacing the micritic matrix and occur as saddle dolomite indicating mixed of meteoric and marine waters and late burial. The neomorphism of opaque micritic matrix and bivalve shells are indicated by the growing of xenotopic mosaic of calcite crystals. In contrast, the secondary calcite cement is equant, fiber, bladed and espatic. Micritization is found in the bioclast shells exhibiting micritic coatings. The autigenesis of quartz and biogenic pyrite is commonly found in FA2 and FA3. The mechanic and chemical compaction in limestone caused the porosity reduction, cementation, fractures and development of dissolution seams and stylolite. The sandstones were cemented by quartz, calcite and iron hydroxides/oxides and show concave-convex and sutured contacts between quartz grains. The predominance of eodiagenetic and subordinate mesodiagenetic features in the Monte Alegre-Itaituba succession indicated less modified framework by the diagenesis corroborating the pristine signature of δ^{13}C values ranging from ~ -2 to ~+5.28‰. This enriched trend upsection coadunate with high organic productivity triggered by massive flourishment of euphotic-controlled benthic organisms mainly in the FA3.

Five types of shallowing upward asymmetric cycles characterize the Monte Alegre-Itaituba succession. Peritidal cycles in coastal desertic (Cycle I) were formed by alternance of dolostone and sandstone with $\delta^{13}C$ values ranging from -1.5 to +0.3‰. Cycles II consist in interbedded of sandstone-mudstone and sandstone-mudstone-floatstone rhythmites and the Cycle III constitute dolostone interbedded with sandstone. These cycles II and III were interpreted as tidal flat and lagoon deposits with $\delta^{13}C$ values ranging from +3,98‰ to +4, 62‰. The Cycle IV is a rhythmite formed by *wackestones/mudstones* couplets while the Cycle V consists of alternance of *grainstones*, *wackestones* and lime *mudstone* (ABC cyclicity) passing upsection for cycles composed by *wackestones* and lime *mudstone* (AB cyclicity). The cycles IV and V are shelf deposits with $\delta^{13}C$ values ranging from +3,65‰ a +5,28‰. The stacking of 53 cycles with average thickness of 1,1 m, combined with Fisher plot diagram, indicated an aggradational to retrogradational stacking pattern inserted in the lowstand to early transgressive system tract (Cycles I-III) and late transgressive system tract (Cycles IV and V). The succession was deposited in ~13 Ma and individual cycles accumulated in an approximately 0.25 my typical of fourth order cycles related to high-frequency fluctuations of relative sea level. These data were correlated to the global $\delta^{13}C$ and sea-level curves that positioned the Monte Alegre-Itaituba succession in the Late Serpukhovian to Early Moscovian age. The influence of Late Misssipian glaciation was negligible in these deposits but the post-glacial transgression combined with slow subsidence of the Amazonas basin caused the generation of allogenic cycles I, IV and V. The cycles II and III were formed by autochthonous processes during a period of equilibrium between supply and glacioeustasy. The Monte Alegre-Itaituba succession is the record of a large Amazonia epicontinental sea that was directly connected with the Panthalassa Ocean during Pennsylvanian.

Key-Words: Pennsylvanian, Amazonas Basin, Monte Alegre- Itaituba Succession, high frequency cyclicity, δC^{13} e δO^{18} stable isotopes

LISTA DE FIGURAS

Capítulo 4

Capítulo 5

LISTA DE TABELAS

SUMÁRIO

CAPÍTULO 1-INTRODUÇÃO

1.1 APRESENTAÇÃO

O Carbonífero foi um período entre 358,9 ± 0,4 Ma e 298,9 ± 0,2 Ma subdividido em dois subsistemas, o Mississipiano e Pensilvaniano, que incluem sete estágios globais: Tournasiano, Viseano, Serpukhoviano, Bashikiriano, Moscoviano, Kasimoviano e Gzheliano (Davydov *et al.* 2012). Estes estágios serão adotados neste trabalho seguindo a carta cronoestratigráfica internacional. Este período foi influenciado principalmente pelos processos de amalgamação que precederam a formação do supercontinente Pangea, que causou grandes alterações paleoceanográficas, aumento das taxas de intemperismo continental, aumento e diminuição das geleiras que afetaram o Gondwana acompanhadas de expressivas oscilações globais do nível do mar, gerando amplos desertos e a deposição de sucessões marinhas cíclicas desenvolvidas principalmente em mares epicontinentais (Ross & Ross 1985, 1987, Davydov *et al.* 2012, Smith & Read 2000, Saltzman & Thomas 2012) . O alto bioprovincialismo foi acompanhado pela rápida diversificação de répteis, anfíbios, plantas terrestres, insetos sem asas, braquiópodes, crinóides, corais rugosos, radiolários, amonóides, moluscos, foraminíferos bentônicos, tubarões e conodontes. Conodontes e foraminíferos são os principais fósseis para a cronoestratigrafia carbonífera, propiciando a correlação regional e global das sucessões dessa idade. (Lockzy 1966, Caputo & Crowell 1985, Rowley 1985, Wopfner 1999, Davydov *et al.* 2012, Lupia & Armitage 2013).

Os registros do Carbonífero são encontrados principalmente nas bacias sedimentares do Gondwana Oeste, como aqueles expostos na Bacia do Amazonas, Norte do Brasil, que apresenta depósitos siliciclásticos-carbonáticos que ainda são pouco estudados do ponto de vista estratigráfico e quimioestratigráfico, que tem limitado a correlação global dos eventos deste período. Esta limitação advém também das condições de exposições de rochas desta idade na região amazônica, onde a densa cobertura vegetal e os intensos processos intempéricos prejudicam a investigação geológica contínua destes depósitos. Mares epicontinentais dominavam a paleogeografia do Gondwana e os registros destes mares na Bacia do Amazonas, são representados pelas formações Monte Alegre e Itaituba, porção basal do Grupo Tapajós (Cunha *et al*. 1994). As rochas das formações Monte Alegre e Itaituba, objeto deste estudo, foram previamente interpretadas como uma sucessão flúvio-eólica e plataforma marinha carbonática com influência de maré, respectivamente, oriundas de ciclos transgressivos-regressivos influenciados por períodos de glaciação que afetaram diferentes bacias ao longo do

Paleozoico Superior (Figueiras 1983, Caputo 1984, Figueiras & Truckenbrodt 1987, Cunha *et al.* 1994, Matsuda, 2002, Cunha *et al.* 2007, Lima, 2010, Matsuda *et al.* 2010, Silva 2014, Silva *et al.* 2015).

Existem poucos trabalhos que abordam as características de depósitos associados a mares epicontinentais durante o Carbonífero da Bacia do Amazonas (Anelli 1999, Matsuda 2002, Lima 2010). Estudos fossilíferos com base em conodontes obtidos de fácies carbonáticas do topo da Formação Monte Alegre e da base da Formação Itaituba, posicionaram estas unidades no intervalo Bashikiriano e Moscoviano (Scomazzon 2004, Scomazzon *et al.* 2016, Moutinho *et al.* 2016). Os conodontes descritos em trabalhos anteriores para o topo da Formação Itaituba posiciona esta unidade para o intervalo Atokano, correspondente ao atual Moscoviano Médio (Fúlvaro 1965, Lemos & Medeiros 1989, Lemos 1990, Lemos 1992, Lemos & Medeiros 1996). Na borda Sul da Bacia do Amazonas conodontes não foram observados no contato entre essas unidades o que dificulta a correlação estratigráfica regional desta unidade, demonstrando a necessidade da utilização de outros métodos de datação, como por exemplo estudos de isótopos de C e O.

O estudo realizado neste doutoramento utilizou a análise de fácies estratigráfica, combinada com dados de isótopos de C e O em uma sucessão de 50m de espessura de rochas siliciclásticas e carbonáticas, pertencentes as formações Monte Alegre e Itaituba da Bacia do Amazonas. Estas unidades foram refinadas do ponto de vista paleoambiental, cronoestratigráfico e quimioestratigráfico permitindo a correlação destes depósitos com os eventos globais do Carbonífero contribuindo com o entendimento dos processos paleocanográficos e paleoclimáticos, além de tecer considerações sobre a reconstrução paleogeográfica de mares epicontinentais do Gondwana Oeste durante o Pensilvaniano.

1.2. OBJETIVO

O objetivo geral desta tese de doutorado consistiu em caracterizar os depósitos siliciclásticos-carbonáticos das formações Monte Alegre e Itaituba, para a melhor compreensão dos ambientes e sua relação com os eventos globais do Carbonífero Superior. Para se chegar a esta conclusão foram cumpridos os seguintes objetivos específicos: i) a reconstituição paleoambiental e paleogeográfica da sucessão siliciclástica-carbonática da porção basal do Grupo tapajós; ii) definição das microfácies carbonáticas, tipologia dos arenitos e da sequência dos eventos diagenéticos da sucessão Monte Alegre-Itaituba; iii) origem da ciclicidade da sucessão e sua relação com os eventos de glacioeustasia e tectônicos do Pensilvaniano; e iv) discutir o significado das excursões isotópicas de carbono e oxigênio e sua correlação com os eventos paleoambientais e paleoceanográficos do Pensilvaniano.

1.3 ÁREA DE ESTUDO

A área de estudo se concentrou na porção Oeste do Estado Pará, nos municípios de Itaituba, Uruará, Aveiro e Monte Alegre (figura 1.1). Os principais afloramentos são pedreiras e escarpas fluviais nas bordas Norte e Sul da Bacia do Amazonas e ao longo do Rio Tapajós, adjacentes a cidade de Itaituba. O estudo de afloramentos foi combinado com a observação da sucessão em testemunhos de sondagem realizados no município de Uruará, borda sul da bacia, com acesso através da rodovia transamazônica (BR-230) e na região de Aveiro próximo a margem do Rio Tapajós. Na borda Norte da Bacia do Amazonas os afloramentos estudados são cortes de estradas e pedreiras ao longo das rodovias PA-255 e PA-423 nas proximidades do município de Monte Alegre.
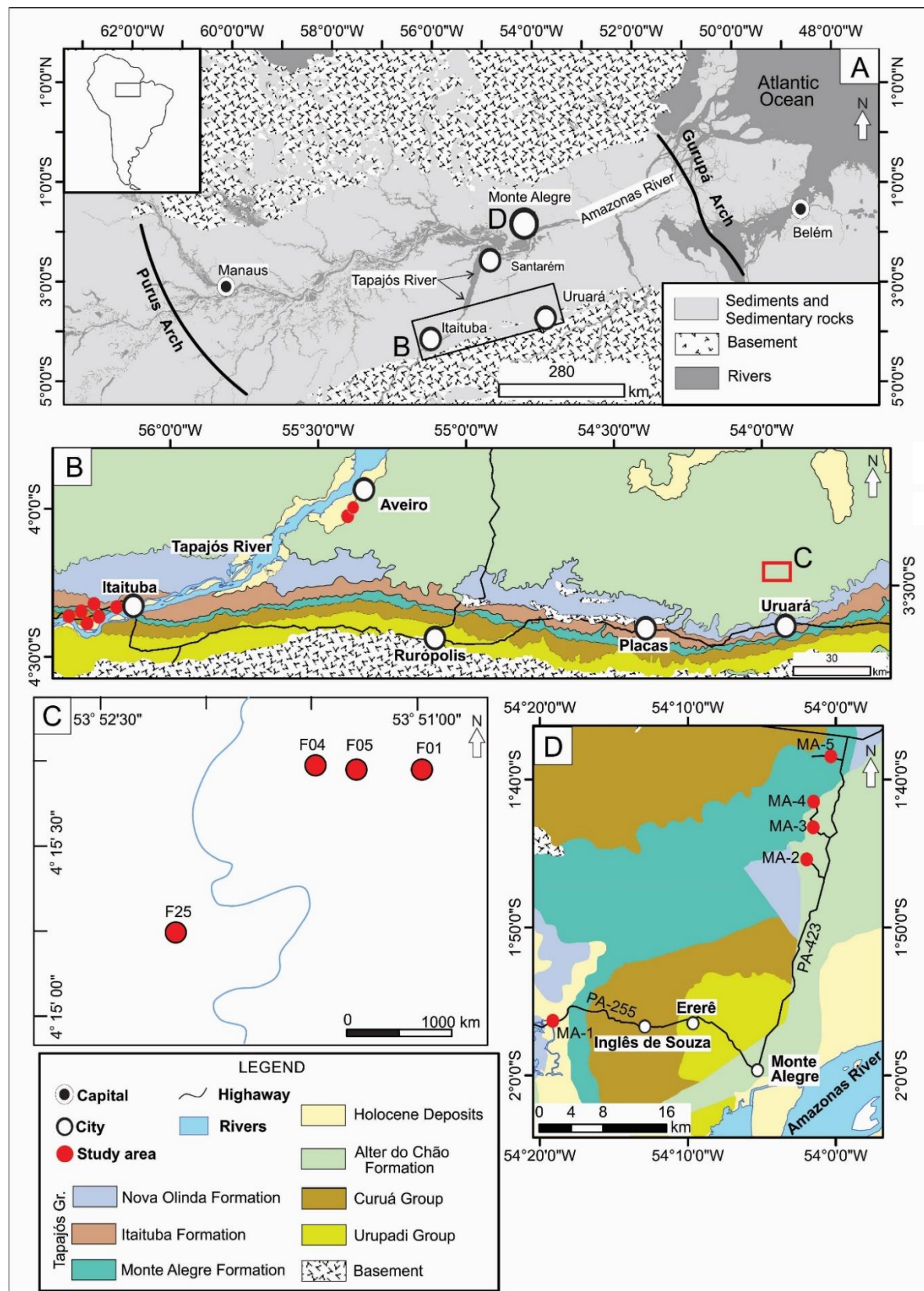
Figura 1.1- Geologia da Amazônia Central, Norte do Brasil. A) Mapa geológico mostrando os limites estruturais (arcos e escudos cratônicos) da Bacia do Amazonas com indicação das áreas de estudo próximas as cidades de Itaituba, Uruará e Monte Alegre. B) Geologia da região de Itaituba-Uruará onde ocorrem os afloramentos clássicos em escarpas do Rio Tapajós. C) Localização dos sítios onde foram realizados os testemunhos de sondagem (F1-F25) na região de Uruará. D) Localização dos cortes de estrada (MA1-MA 5) e pedreiras (MA 3 and MA 4) da região de Monte Alegre.

1.4 GEOLOGIA REGIONAL

1.4.1. Bacia do Amazonas

A Bacia do Amazonas localiza-se na região Norte do Brasil, englobando os estados do Amazonas e Pará. A bacia está limitada ao Norte pelo Escudo das Guianas, ao Sul pelo Cráton do Guaporé, a Leste pelo arco de Gurupá e a Oeste pelo Arco de Purus (figura 1a). Possui uma área de 500.000 km^2 e um preenchimento sedimentar máximo de até 6 km de espessura em seu depocentro, seu formato é alongado e estreito de direção WSW-ENE (Cunha *et al.* 1994, Costa 2002, Zálan 2004, Cunha *et al.* 2007).

A gênese da bacia está ligada aos processos distensivos, oriundos do fechamento do Ciclo Brasiliano (Cunha *et al.* 1994, Pereira *et al.* 2012). Estes esforços estariam associados a uma zona de alívio desenvolvida a partir da Faixa Móvel Araguaia-Tocantins e corresponderia ao *rift* precursor da Bacia do Amazonas, tendo se propagado de leste para oeste devido à reativação de zonas de fraquezas pré-cambrianas (Wanderley Filho 1991). Após o evento distensivo ocorreu o resfriamento magmático, gerando subsidência termal e o posterior estabelecimento de uma sinéclise intracontinental (Cunha *et al.* 1994, Zálan 2004, Cunha *et al.* 2007).

1.4.2. Preenchimento Sedimentar

A geração do *rift* inicial da bacia foi sucedida pela acumulação de unidades sedimentares e vulcanosedimentares no final do Ciclo Brasiliano (700 a 470 Ma), com idades neoproterozoicas (Almeida & Hasui 1984). Estas unidades afloram contiguamente ao longo do Arco de Purus e são representadas pelos arenitos fluviais da Formações Prosperança e carbonatos de planície de maré da Formação Acari, ambas estão inseridas no Grupo Purus (Cunha *et al.* 2007).

As unidades litoestratigráficas da Bacia do Amazonas foram reavaliadas seguindo os conceitos da estratigrafia de sequências, e foram agrupadas em duas megassequências de primeira ordem, a Paleozoica e a Mesozoica-Cenozoica (Cunha *et al.* 2007, Matsuda *et al.* 2010). A megassequência paleozoica é dividida em quatro sequências de segunda ordem: ordovício-devoniana, devono-tournasiana, neoviseana e pensilvaniana-permiana. Estas sequências deposicionais são separadas entre si por discordâncias regionais (Anexo).

A sequência ordovício-devoniana foi depositada em um evento transgressivo-regressivo, com os sedimentos originados de ambientes marinhos e glaciais, correspondendo ao Grupo Trombetas. Este grupo se divide da base para o topo nas formações Autás-Mírim, constituída de arenitos e folhelhos, Nhamundá, composta de arenitos e diamictitos, Pitinga, representada por folhelhos e diamictitos, Manacapuru, formada por arenitos e pelitos e Jatapu, constituída de arenitos e siltitos. O topo da sequência é truncado por uma discordância originada por soerguimentos gerados pela Orogenia Caledoniana (Cunha *et al* 1994, Cunha *et al.* 2007).

A sequência Devono-Tournasiana foi depositada em um evento transgressivo, decorrente da subsidência tectônica e posterior invasão marinha, seguido de um pulso regressivo. Durante esses eventos depositaram-se os grupos Urupadi e Curuá, interpretados como depósitos marinhos de plataforma rasa. O Grupo Urupadi é dividido nas formações Maecuru, constituída de arenitos e pelitos e Ererê, composta por siltitos, folhelhos e arenitos, enquanto o Grupo Curuá é constituído das formações Barreirinhas, composta por folhelhos, Curiri, que consiste em argilitos, siltitos e diamictitos e Oriximiná, constituída por uma intercalação de siltitos e folhelhos. O topo desta sequência encerra-se com o truncamento da unidade por uma discordância regional gerada durante a Orogenia Acadiana (Cunha *et al.* 1994, Cunha *et al.* 2007).

Após a deposição da sequência Devono-Tournasiana há um intenso processo tectônico responsável pelo soerguimento e erosão das unidades, configurando um período de 14Ma de hiato deposicional. Após está interrupção na sedimentação, há um novo evento de subsidência restrita que gera a sequência Neoviseana, correspondente a Formação Faro, constituída de arenitos e pelitos. Esta sequência encerra-se no topo por uma discordância regional originaria da Orogenia Eo-Herciniana resultando em uma grande erosão da unidade (Cunha *et al.* 2007).

A sequência Pensilvaniana–Permiana deposita-se após um hiato de 15 Ma e corresponde a um depósito transgressivo-regressivo, com a invasão marinha vinda de oeste e ultrapassando o arco de Purus (Matsuda *et al.* 2010, Cunha *et al.* 1994). Durante essa sequência formou-se o Grupo Tapajós, que engloba as formações Monte Alegre, constituída de arenitos, siltitos, folhelhos, dolomitos e calcários, Itaituba, composta de calcários, dolomitos, evaporitos, arenitos e folhelhos fossilíferos, Nova Olinda, representada por calcários e evaporitos e Andirá, constituída de arenitos, siltitos e folhelhos avermelhados (Cunha *et al.* 2007, Matsuda *et al.* 2004).

O evento que sucedeu a sequência Pensilvaniana–Permiana foi o estabelecimento da Orogenia Gondwanides, originária da colisão da Laurásia e Gondwana, resultando em fraturamentos regionais no Escudo das Guianas, passando pela Bacia do Amazonas provocando soerguimentos e erosões das unidades. Posteriormente a estes acontecimentos a tectônica intraplaca formou esforços distensivos de direção leste-oeste, seguido de magmatismo básico na forma de enxame de diques e soleiras de rochas básicas (Cunha *et al.* 2007, Wanderley Filho *et al.* 2006).

Os processos tectônicos que resultaram na abertura do Oceano Atlântico e a consolidação da zona de subducção andina promoveram também a reativação de estruturas tectônicas pretéritas, de direções ENE–WSW e WNW–ESE, chamado de Diastrofismo Juruá (Zálan 2004). Em seguida ao Diastrofismo Juruá um relaxamento tectônico estabeleceu-se, gerando uma zona de subsidência para a acumulação da megassequência Mesozoica-Cenozoica, constituída pelas sequências cretácea e terciária que constituem o Grupo Javari, representado pelas formações Alter do Chão, composta de conglomerados, arenitos, argilitos, siltitos e folhelhos, e Solimões, de composição arenosa e pelítica. Durante o Cretáceo houve o estabelecimento de um sistema fluvial que corria de leste para oeste, porém devido ao soerguimento andino ocorrido no limite Cretáceo/Terciário os rios cretáceos transformaram-se em lagos rasos de água doce, contendo restos vegetais e conchas de moluscos (Nogueira 2008, Bezerra 2018). Após o completo desenvolvimento dos Andes durante o Mioceno, a Bacia do Amazonas passou a ser suprida pelos sedimentos oriundos desta cadeia de montanhas e o fluxo passou a correr para leste em direção ao Oceano Atlântico (Nogueira *et al.* 2013).

1.4.3. Grupo Tapajós

O Grupo Tapajós possui uma espessura máxima de 2800 m, depositados durante o intervalo Pensilvaniano ao Permiano (Cunha *et al.* 2007, Matsuda *et al.* 2004). O Grupo Tapajós está associado diretamente a eventos transgressivos responsáveis pela deposição das unidades basais e com um evento regressivo registrado nas unidades de topo. O Grupo é subdividido, da base para o topo, em quatro formações: Monte Alegre, Itaituba, Nova Olinda e Andirá (figura 1.2).

1.4.3.1 Formação Monte Alegre

A primeira descrição dos arenitos correspondentes a Formação Monte Alegre foi feita por Albuquerque (1922) que identificou camadas de arenitos basais aos calcários da região do Rio Jatapu, Estado do Amazonas, a qual denominou de arenito Forno, devido a área situar-se em uma pedreira de mesmo nome. Somente a partir de Freydank (1957) que estes arenitos basais passaram a ser formalizados como Formação Monte Alegre, este autor identificou camadas de arenitos recobertas por carbonatos, na região do munícipio de Monte Alegre. A Formação Monte Alegre apresenta contato gradacional com os carbonatos sotopostos da Formação Itaituba, onde se intercalam formando pequenos ciclos de alternância de arenitos e dolomitos bioturbados.
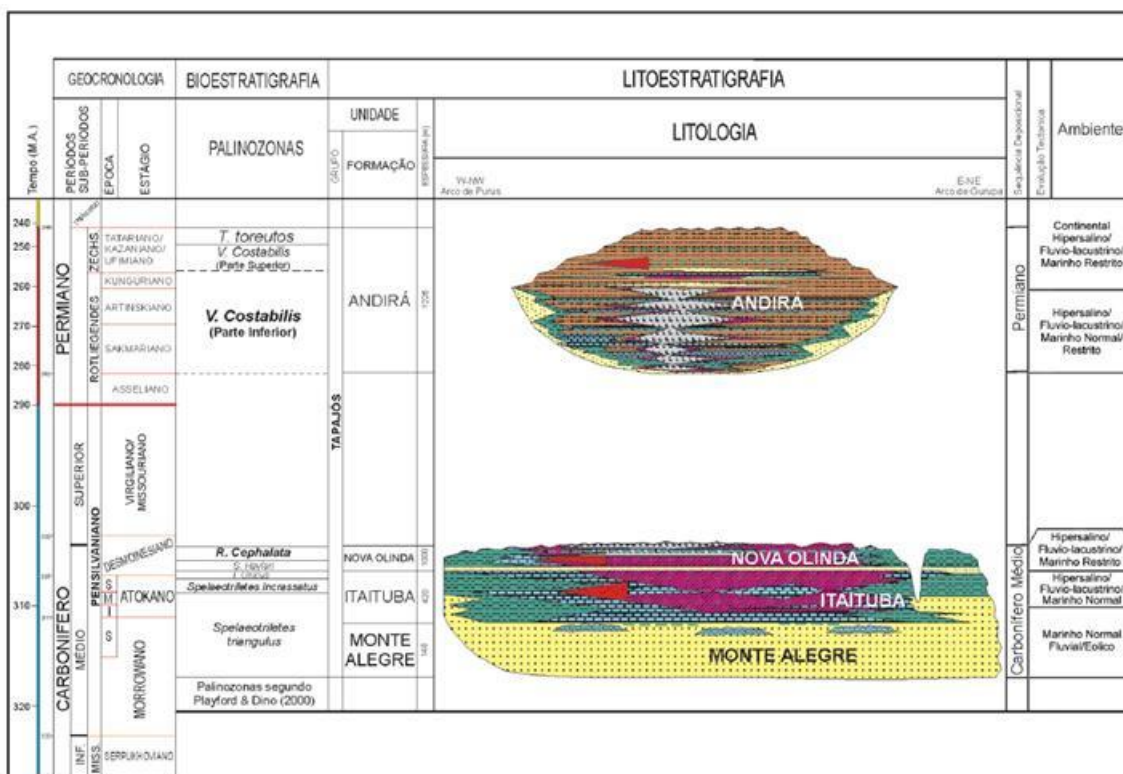
Figura 1.2: Carta litoestratigráfica do Grupo Tapajós, mostrando as palinozonas correspondentes às formações Monte Alegre, Itaituba, Nova Olinda e Andirá, posicionando-as no limite Morrowano-Atokano, equivalente ao limite Bashikiriano-Moscoviano. Fonte: Matsuda *et al.* (2004).

A Formação Monte Alegre é interpretada como um sistema eólico composto por campo de dunas e *wadis* constituídos por arenitos e intercalados com folhelhos e siltitos de lagos e interdunas (Cunha *et al.* 1994). Kremer (1956) e Torres (1989) descrevem um sistema desértico na região do Rio Tapajós, este último associando-o diretamente com os carbonatos da Formação Itaituba, caracterizando um ciclo transgressivo-regressivo. A unidade possui espessura média de 80 m, entretanto em seu depocentro pode apresentar até 150 m de espessura

máxima (Torres 1989), além disso nota-se através de métodos sísmicos que se acunha em direção ao Arco de Gurupá (Caputo *et al.* 1971, Caputo 1984). Costa & Selbach (1981) sugerem ambiente litorâneo devido a presença de carbonatos intercalados com arenitos eólicos.

A Formação Monte Alegre é considerada do Pensilvaniano inferior, devido aos dados micropaleontológicos obtidos da porção carbonática de topo da formação que se baseiam em palinomorfos, foraminíferos e conodontes (Daemon & Contreiras 1971, Playford & Dino 2000, Lemos & Scomazzon 2001, Matsuda *et al.* 2004, Scomazzon 2004). Recentemente através do uso da bioestratigrafia de conodontes e de foraminíferos pôde-se chegar a um refinamento estratigáfico, posicionando a Formação Monte Alegre no limite Bashikiriano-Moscoviano (Moutinho *et al.* 2016a, Scomazzon *et al.* 2016).

1.4.3.2 Formação Itaituba

Segundo Caputo (1984) a primeira menção a rochas carbonáticas na bacia do Amazonas foi feita por Hart (1874), a qual denominou estas rochas de "série Itaituba", que acabou sendo extrapolada para todas as demais camadas de calcários da bacia. Somente a partir dos estudos da Petrobrás na região do município de Itaituba que a unidade passou a ser formalizada como uma formação. A Formação Itaituba é composta por calcários, dolomitos, arenitos siltitos, folhelhos e evaporitos interpretados como depósitos de planície de maré (Cunha *et al.* 1994, Matsuda 2002, Cunha *et al.* 2007), plataforma carbonática rasa com influencia de maré (Figueiras 1983, Figueiras & Truckenbrodt 1987, Caputo 1984, Lima 2010, Silva 2014) e planície de maré mista que grada para uma plataforma carbonática representativa de um mar raso (Silva *et al.* 2015).

A máxima espessura da Formação Itaituba é da ordem de 420 m no depocentro da bacia, onde grande parte destas rochas são carbonáticas (Cunha *et al.* 2007). Apresenta um contato gradacional com a Formação Monte Alegre, representada pela intercalação de arenitos e dolomitos (Matsuda *et al.* 2010). Sua porção superior também apresenta contato gradacional com a Formação Nova Olinda, com a intercalação de carbonatos com espessas camadas de evaporitos (Cunha *et al.* 2007, Pereira *et al.* 2012). A Formação Itaituba possui um amplo registro fossilífero na bacia do Amazonas, são compostos por algas, braquiópodes, briozoários, bivalves, cefalópodes, corais, esponjas, equinodermas, foraminíferos, gastrópodes e trilobitas, além de peixes, conodontes e plantas, esta varidade de organismos é posicionada no Neocorbonífero (Daemon & Contreiras 1971). Estudos mais específicos baseados em conodontes refinam o posicionamento da unidade e a inserem no intervalo Morrowano a

Atokano correspondentes aos estágios Bashikiriano-Moscoviano (Scomazzon 2004, Scomazzon *et al.* 2005, Moutinho 2006, Nascimento *et al.* 2010). Esta unidade foi posicionada no intervalo Bashikiriano-Moscoviano devido a ocorrência de *Neognathoddus atokensis, Diplognathodus ellemerensis* e *Idiognathodues incurvus*, organismos de águas rasas muito comuns em mares epicontinentais de idade pensilvaniana (Scomazzon *et al.* 2016).

1.5. MARES EPICONTINENTAIS

Os mares epicontinentais possuem uma ampla história de distribuição no tempo geológico, sendo registrados desde o Proterozoico até o Mesozoico, com alguns autores extendendo sua ocorrência até o Neógeno (Jipa & Olariu 2013). Correspondem a uma massa de água rasa, com profundidades médias de 50 a 60 m, com limite máximo de 100 m (Harries 2011, Flügel 2004). Estas massas de água oceânica invadem as regiões cratônicas interiores dos continentes devido às flutuações marinhas e a subsidência tectônica (figura 1.3), formando mares com centenas de quilômetros quadrados de extensão (Wilson 1975, Witzki 1986). Os mares interiores são ausentes nos dias atuais devido a alguns fatores, tais como: a) as regiões continentais serem mais elevadas que as regiões cratônicas do passado geológico; b) o ritmo das atividades tectônicas presentes serem muito mais lentas que no passado; e c) o volume das massas de águas oceânicas serem mais reduzidos devido a glaciações continentais observadas atualmente na Antártida e Groenlândia, além de glaciações em regiões polares compostas apenas por massa de água oceânica, como ocorre com o atual Pólo Norte (Harries 2011).
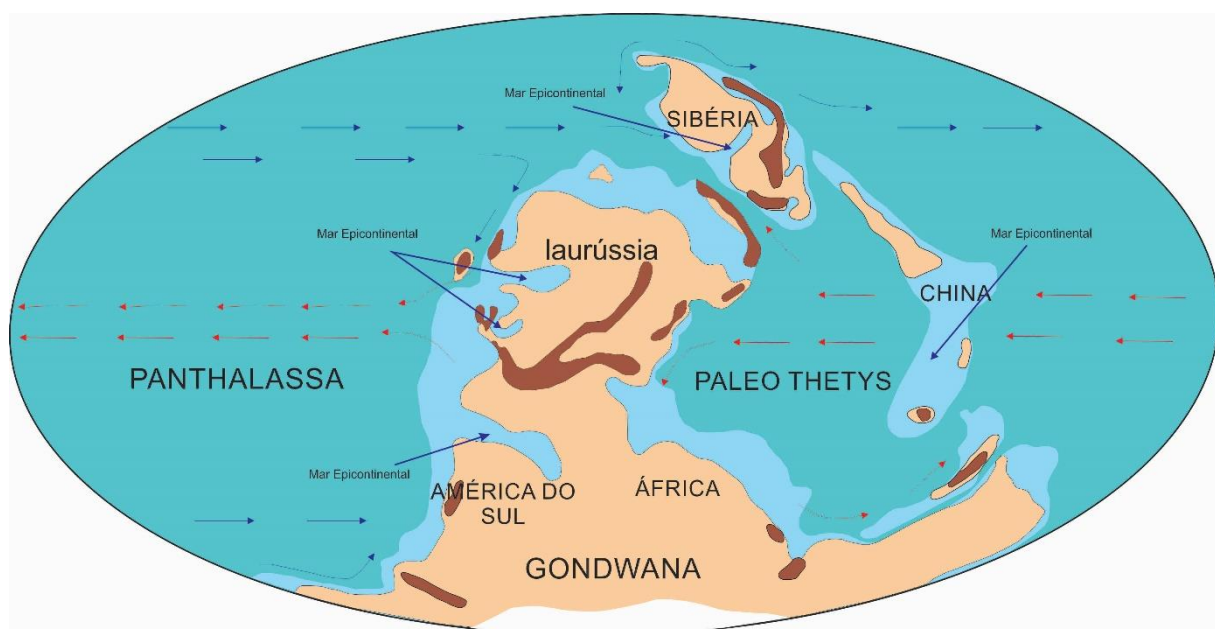
Figura 1.3: Mapa paleogeográfico do Pensilvaniano, em detalhes os principais mares epicontinentais encontrados neste período, destaque para o mar da América do Sul, o mar interior de Laurússia, o mar interior da Sibéria e o mar interior da China. Fonte: Scotese (2001).

Quanto a composição sedimentológica podem ser constituídos tanto de sedimentos siliciclásticos quanto de sedimentos evaporíticos e carbonáticos, configurando uma baixa energia na sua sedimentação. O influxo de terrígenos para as porções marinhas são advindos da porção continental, dependem da posição paleogeográfica na qual o continente se encontra, podendo gerar desde mares rasos equatoriais de clima quente até mares austrais de clima glacial (Witzki 1986, Harries 2011, Holmden *et al.* 2012). Os mares epicontinentais com sedimentação siliciclástica são gerados a partir de fontes proximais, onde as bordas apresentam sedimentação grosseira formando canais que desaguavam em massas de águas costeiras e, a medida que estas encontram-se mais afastadas, geram depósitos dominados por silte e lama. Estes mares são descritos amplamente no Paleozoico inferior como o mar de Mohawkian, de idade Ordoviciana (Panchuk *et al.* 2005). Estes mares também apresentam sedimentação evaporítica e carbonática, como é descrito para a Formação Nova Olinda da Bacia do Amazonas (Palagi 2009). A sedimentação carbonática é bastante comum nos mares em posição equatorial, sendo dominadas pela ação de ondas (Irwin 1965, Laporte 1969, Richards *et al.* 2009, Purkis *et al.* 2015) e por vezes a ação de maré é registrada nas bordas dos mares, formando as típicas sequências de planícies de maré mistas de sedimentação siliciclástica nas bordas e a precipitação carbonática ao centro (Ginsburg 1971, Pratt & James 1986, Chell & Leckie 1992, Lee & Chough 2011).

CAPÍTULO 2. MATERIAIS E MÉTODOS

2.1. ANÁLISE DE FÁCIES SEDIMENTAR

A análise de fácies sedimentares seguiu o modelo proposto por Walker (1992), a qual definiu o procedimento a partir da individualização e descrição da fácies, baseados nas suas características, como a composição, litologia, geometria, textura, estruturas sedimentares, conteúdo fossilífero e padrões de paleocorrentes. Juntamente com as descrições de fácies, a compreensão dos processos sedimentares geradores das fácies se faz necessário para agrupar em associações de fácies contemporâneas e cogenéticas, com o intuito de determinar o paleoambiente deposicional da área de estudo. As fácies foram codificadas seguindo o padrão proposto por Miall (1977), em que a letra inicial maiúscula corresponde a litologia e as letras seguintes representam a estrutura sedimentar, caso ocorra mais de uma estrutura sedimentar associada, a sigla da estrutura dominante é inserida. As descrições e caracterizações foram auxiliadas por perfis estratigráficos colunares para determinar as variações verticais e laterais das fácies.

2.2. ANÁLISE ESTRATIGRÁFICA DE ALTA FREQUÊNCIA

A análise dos ciclos sedimentares dos depósitos de Pensilvanianos da Bacia do Amazonas foi baseada nas proposições de Posamentier & James (1993) e Strasser *et al.* (2006) para os conceitos básicos de ciclicidade e sua identificação. O termo "ciclo" aqui adotado foi proposto por Kerans & Tinker (1997) que considera uma seqüência de 4ª e 5ª ordem como ciclos de alta frequência geralmente observada em escala de afloramento, de 0,2 a 0,5 milhões de anos, inseridos em seqüências de terceira ordem 0,5 a 3 milhões de anos. Ciclos de pequena escala variando de 0,5 a 10 m de espessura são típicos dos ambientes de plataforma / rampa de carbonato aberta, laguna e planícies de maré (Tucker 1991, Tucker & Harland 2010).

A avaliação dos padrões cíclicos considera mudanças de fácies/microfacias, tendência ascendente, variações de espessura e frequências e padrões de ciclos (progradacional, agradacional e retrogradacional), bem como a identificação de superfícies-chave, como superfícies de inundação máxima, paraseqüência e limites de seqüência (Strasser 1991, Schwarzacher 1993, Perlmutter & Azambuja Filho 2005, Cateneanu 2006, Tucker & Harland 2010). O gráfico de gráficos de Fischer foi usado para avaliar melhor as flutuações do nível do mar relacionadas aos ciclos de perimaré (Fischer 1964, Sadler *et al.* 1993, Bosence *et al.* 2009). O gráfico exibe partições cumulativas obtidas a partir da espessura média contra o número de

ciclos, modelando a taxa de acomodação e sua correlação com as mudanças no nível do mar, caracterizando os sistemas (Goldhammer 1987, Goldhammer *et al.* 1991, Kerans & Tinker 1997, Bosence *et al.* 2009). O padrão de variação de espessura foi construído usando o programa Fischerplot excel (Husinec *et al.* 2008). A análise da ciclicidade em carbonatos Pensilvanianos favoreceu a reconstrução dos processos de controle da sedimentação, bem como as causas da repetição contínua dos pares de camadas e sua relação com uma origem autocíclica e/ou alocíclica.

2.3. ANÁLISE PETROGRÁFICA

As análises das fácies carbonáticas fundamentaram-se nas descrições petrográficas, e são chamadas de microfácies (Flügel 2004). Foram realizadas a descrição delâminas delgadas de carbonatos, arenitos e siltitos, tanto em testemunhos de sondagem, quanto em afloramentos, com o intuito de definir a composição dos constituintes das rochas e suas feições diagenéticas (Folk 1974). Para os carbonatos utilizou-se as descrições de matriz, cimento, bioclastos, aloquímicos, grãos terrígenos para estabelecer a nomenclatura da rocha com base no trabalho de Dunham (1962) e Embry & Klovan (1971) (figura 2.1). O tamanho dos cristais foi estabelecido segundo Folk (1962) e os processos diagenéticos embasados nos compêndios de Choquette & Pray (1970), Barthrust (1971), McIlreath & Morrow (1990), Tucker & Wrigth (1990), Tucker (1992), Scholle & Scholle (2003) e Flügel (2004).

As amostras seguiram o padrão de contagem estabelecido por Flügel (2004), com o estabelecimento de 300 pontos em cada lâmina para determinar a porcentagem dos constituintes de cada rocha e os tipos de contato (Anexo II). As seções delgadas com conteúdo carbonático foram tingidas com Alizarina vermelho S para estabelecer o conteúdo carbonático, calcítico ou dolomíticos, além do tingimento com Ferrocianeto de Potássio para distinção entre calcita ferrosa e calcita magnesiana (Adams *et al* 1984, Tucker 1988). Foram elaboradas pranchas com as fotomicrografias das microfácies, bem como seus constituintes e suas principais feições diagenéticas.

Deposicional				Biológico		
Suportado por matriz (frações argila e silte)		Suportado por grãos		Organismos In-situ		
< 10% de grãos	> 10% de grãos	com matriz	sem matriz	Encrustados	Suspensão	Rígidos
Mudstone	Wackestone	Packstone	Grainstone	Boundstone	Bafflestone	Framestone

				Diâmetro dos cristais	Constituintes autigênicos
	Floatstone		Rudstone	> 4 mm	Cristais extremamente grossos
				1 mm - 4 mm	Cristais muito grossos
				0.25 mm - 1 mm	Cristais grossos
				0.062 mm - 0.25 mm	Cristais médios
Grãos > 2 mm				0.016 mm - 0.062 mm	Cristais finos
				0.004 mm - 0.016 mm	Cristais muito finos
				< 0.004 mm	Afanocristalino Folk (1962)

Figura 2.1: Classificação das rochas carbonáticas propostas por Dunham (1962), Embry e Klovan (1971), juntamente com a classificação proposta por Folk (1962) para a classificação dos diferentes tamanhos dos cristais carbonáticos.

2.4. CATODOLUMINESCÊNCIA

A análise de catodoluminescência em carbonatos foi realizada no Laboratório de Catodoluminescência do Instituto de Geociências da UFPa no equipamento composto de microscópio ótico Leica modelo DM 4500 P LED acoplado ao aparelho Optical cathodoluminescence CL 8200 MK5-2. As imagens foram feitas em lâminas delgadas polidas, submetidas à luminescência gerada pelo impacto de elétrons energéticos, revelando as estruturas que são invisíveis à luz natural branca ou polarizada. Esta análise proveu informações sobre o crescimento e as gerações dos cimentos calcíticos, através dos diferentes padrões de cores gerados a partir da luminosidade, onde as cores amarela, laranja e vermelha representam diferentes tipos de calcita e consequentemente gerações de cimento diferentes, já as dolomitas apresentam coloração vermelha escura (Solomon & Walkden 1985, Tucker 1988, Scholle & Scholle 2003, Boggs Jr. & Krinsley 2006).

2.5. MICROSCOPIA ELETRÔNICA DE VARREDURA

A análise mineralógica por MEV foi realizada no laboratório de microscopia de varredura (LABMEV) do Instituto de Geociências da UFPA sob orientação do Prof. Dr. Cláudio Lamarão. As amostras foram efetuadas em arenitos e carbonatos no equipamento modelo LEO-1430, sendo as condições de análises para as imagens de elétrons secundários: corrente do feixe de elétrons=90 µA, voltagem de aceleração constante=20 kv, distância de trabalho=10 mm. As imagens revelaram a textura e a composição das amostras selecionadas,

caracterizando a mineralogia de algumas fases de cimento e o tipo de mineral opaco precipitado nos carbonatos.

2.6. ISÓTOPOS DE C e O

A análise isotópica fundamentou-se na coleta sistemática de amostras da região de Monte Alegre, na Pedreira Caltarém, pertencentes a porção superior da Formação Monte Alegre e na porção basal da Formação Itaituba. As amostras foram coletadas em intervalos de 50 cm em 50 cm, sendo pulverizadas em graal e pistilo de ágata, evitando-se fraturas, porções cimentadas, rochas alteradas pela ação intempérica e por diagênese. As amostras foram enviadas ao laboratório de geocronologia da Universidade de Brasília (UnB) sob coordenação da Prof^a. Dr^a. Lucieth Cruz Vieira, onde 30 amostras foram selecionadas e pulverizadas com cerca de 10 g do pó da matriz da rocha. A assinatura do isótopo de carbono e oxigênio foi obtida das amostras após reação com 100% de H_3PO_4 a 25 °C durante pelo menos 1 hora. A composição isotópica do CO_2 liberado foi determinada usando um espectrômetro de massa Finnigan DELTA Plus Advantage. A reprodutibilidade analítica dos valores de $\delta^{13}C$ e $\delta^{18}O$, baseada nas réplicas dos padrões NBS-18 e NBS-19 com erro associado de 0,05 para $\delta^{13}C$ e 0,10 para $\delta^{18}O$. Os resultados são apresentados em notação convencional per mil (‰) em relação ao padrão VPDB (Vienna Pee Dee Belemnite). VPDB é uma escala reconhecida pelo Instituto Nacional de Padrões e Tecnologia (NIST) que é usada para relatar as abundâncias relativas de $\delta^{13}C$ ou $\delta^{18}O$ através da notação delta.

2.7. ANÁLISE MICROPALEONTOLÓGICA

Para a análise micropaleontológica foram selecionadas amostras das associações de fácies de planíce de maré e de plataforma epicontinental e correspondentes a rochas carbonáticas. Estas amostras foram enviadas ao Laboratório de Micropaleontologia, do departamento de paleontologia e estratigrafia da UFRGS sob tutela da Prof^a. Dr^a. Ana Karina Scomazzon. A metodologia seguiu o proposto por Scomazzon (2004) e consistiu em desagregar 500 g de carbonato colocando-o em uma solução de 5 l de água para 500 ml de ácido acético glacial, a mistura é colocada em um recipiente para que ocorra a reação do soluto com a solução ácida diluída durante 10 dias. Com a reação já ocorrida as amostras são lavadas e peneiradas com auxílio da peneira de 80 *mesh* e de 200 *mesh*, para posterior triagem e identificação dos conodontes e fauna associada em lupa.

CAPÍTULO 3 PENNSYLVANIAN MIXED SILICICLASTIC-CARBONATE DEPOSITS OF THE AMAZONAS BASIN: THE RECORD OF EPICONTINENTAL SEA IN THE WESTERN GONDWANA

Pedro Augusto Santos da Silva[1], Afonso César Rodrigues Nogueira[1] Joelson Lima Soares[1] José Bandeira Silva[1] Ana Karina Scomazzon[2] Sara Nascimento[2] Luciane Profs Moutinho[2] Sanmya Karoline Dias[1]

[1]Programa de Pós-Graduação em Geologia e Geoquímica - PPGG, Instituto de Geociências, Universidade Federal do Pará – UFPA, Rua Augusto Corrêa, s/n, CEP 66075-110, Belém, Pará, Brasil (pedrogeologia8@hotmail.com ; anogueira@ufpa.br; jlsoares@ufpa.br; jotabandeira@gmail.com; sanmyadias.geo@outlook.com)

[2]Universidade Federal do Rio Grande do Sul- UFRGS- Av. Bento Gonçalves, 9500, Prédio 43127, Sala 211, CEP 91501-970, Porto Alegre, Rio Grande do Sul, Brasil (akscomazzon@yahoo.com.br; luci.profs@gmail.com)

ABSTRACT

Epicontinental seas dominated the Central Amazonia during the Carboniferous configurating a singular paleogeography of the West Gondwana connected to the Panthalassa Ocean. The Pennsylvanian record in the Amazonas Basin is represented by 1,7 km-thick of mixed siliciclastic-carbonate-evaporite sedimentation resulted of a complete transgressive-regressive megacycle. Outcrop and core-based stratigraphic and facies analysis carried out in 50m-thick mixed siliciclastic-carbonate transgressive succession of the Amazonas Basin identified thirty-four facies, representative of coastal to shelf depositional systems grouped in three facies associations: 1) coastal desertic deposits, consisting of fine to medium-grained sandstone, lime mudstone and fine-grained dolostone that corresponds to a complex association of aeolian dunes, sand sheets, interdunes, fluvial channels and lagoon deposits bioturbated *Palaeophycus*, *Lockeia*, *Thalassinoides, Rosselia* and meniscate trace fossils; 2) mixed tidal flat setting, constituted by fine to medium-grained sandstone, mudstone, shale, siltstone and limestone interpreted as supratidal, tidal channel, tidal delta and lagoon settings with evidence of subaerial exposure, tidal currents with restricted biological activity indicated by brachiopod and echinoderm body fossils mainly in lagoon deposits; and 3) carbonate shelf deposits, consisting of lime mudstone, wackestone, packstone and grainstone with allochems (ooids and peloids), terrigenous grains and abundant and diversified open shallow marine benthic organisms, including, fish remains, foraminifers, brachiopods, echinoids, gastropods, bryozoans, trilobites, corals, ostracodes, and conodonts, interpreted as bioclastic bars and carbonate shelf deposits. The Bashkirian-Moscovian age is suggested based on conodonts, particularly the species *Neognathodus symmetricus, Streptognathodus sp.* and *Ellisonia sp.*. These mixed siliciclastic-carbonate deposits are correlate with several successions recorded in the west and east Amazonia and sub-Andean basins in South America confirming the paleogeography of Itaituba epicontinental sea directly connected with the Panthalassa Ocean during Pennsylvanian.

Keywords: Bashikirian-Moscovian, Monte Alegre-Itaituba succession, Epicontinental Itaituba Sea, Western, Gondwana, Panthalassa Ocean

1.INTRODUCTION

The Pennsylvanian is marked by geological events such as global climatic variations, the development of ice caps in the Southern of Gondwana, sea level changes, the evolution and diversification of continental plants, the advent of Pre-Pangea continental deserts and the increase of thick carbonate accumulations in addition to epicontinental seas (Caputo and Crowley 1985, Caputo 1984, Ross and Ross 1985, Lupia and Armitage 2013, Wopfner 1999, Lockzy 1966, Harrington 1962, Davydov *et al.* 2012). The development of Pre-Pangea deserts, climatic variations, sea-level fluctuations, epicontinental seas, and thick accumulations of carbonate sediments are observed in the Pennsylvanian record of the Amazonas Basin comprising a succession of transgressive deposits (Caputo 1984, Cunha *et al.* 1994, Matsuda 2002, Cunha *et al.* 2007).

These transgressive deposits are widely recorded in the Pennsylvanian as well in the Permian and represent over fifty deposits with the substitution of continental sedimentation by marine sedimentation (Ross and Ross 1985). In the Amazon Basin this is represented by the base of the Tapajós Group, by the Monte Alegre and Itaituba formations, previously interpreted as aeolian and marine carbonate paleoenvironments, respectively. In the last decades, these deposits have been studied mainly based on lithostratigraphy, paleontology and geochemistry. In the same way, the rare facies and depositional system analysis (Matsuda 2002, Lima 2010, Scomazzon *et al*. 2016, Silva *et al.* 2015) do not allow to define a precise paleoenvironmental and stratigraphic framework that can propitiate a correlation with global events of the Carboniferous. In addition, the scarcity of continuous outcrops due to the dense vegetation and intense weathering typical of Amazonia region not allow the complete recognition of the depositional systems and sequences. For solve this difficulty we used outcrops and cores to refine the stratigraphy and facies analysis of the Monte Alegre and Itaituba formations exposed on the northern and southern margins of the Amazonas Basin, Brazil. The identification of 50m-thick mixed siliciclastic-carbonate transgressive succession allowed the paleoenvironmental, paleoclimatic and paleogeographic reconstruction of an epicontinental sea implanted in the Western Gondwana during Pennsylvanian (Figure 1).
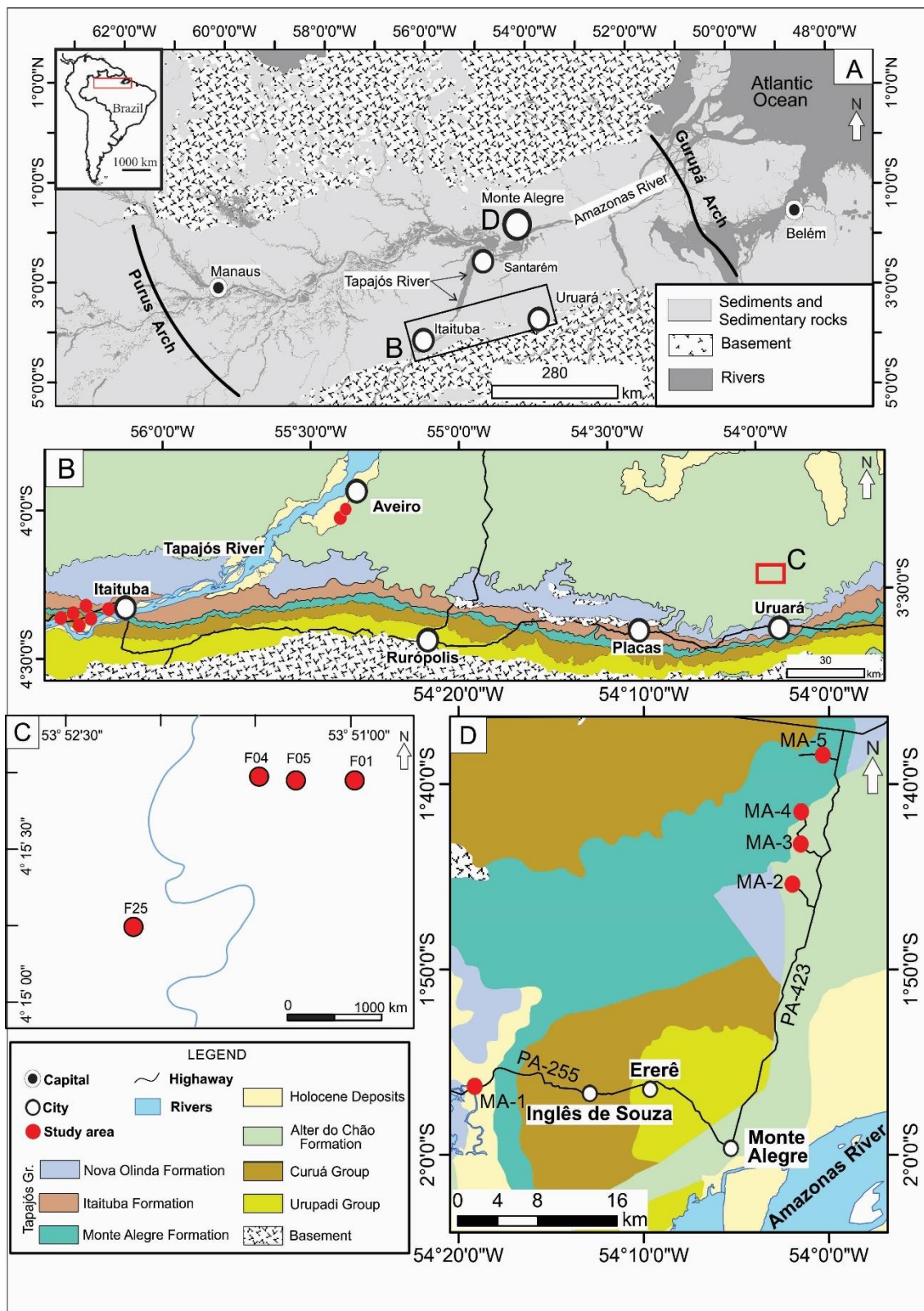
Figure 1- The Central Amazonas Basin, Northern Brazil. A) Geological map showing the structural limits (arches and cratonic shields) of the Amazon Basin with indication of studied areas near to Itaituba, Uruará and Monte Alegre cities. B) Detailed geological map of the Itaituba-Uruará region where the classical outcrops occur in fluvial scarps of the Tapajós River. C) Location of drill cores sites (F1-F25) in the Uruará region. D) Location of studied outcrops in road cuts (MA1-MA 5) and quarries (MA 3 and MA 4) in the Monte Alegre region.

2. REGIONAL GEOLOGY

The Amazonas Basin is situated in the Northern of Brazil. It is limited to the North by the Guianas Shield, to the South by the Brazilian Shield, to the East by the Gurupá Arch, and to the West by the Purus Arch (Figure 1a). It has an area of 500.000 km^2, and a sedimentary in-fill of about 6000 m thick (Caputo 1984, Cunha *et al.* 1994). This sedimentary in-fill consists of two first order mega-sequences: Palaeozoic and Meso-Cenozoic (Cunha *et al.* 1994, Cunha *et al.* 2007). In addition, the sedimentary in-fill, there are diabase intrusions in the form of dykes and sills of Triassic age in the basin (Issler *et al.* 1974, Wanderley Filho *et al.* 2006). The Palaeozoic mega-sequence consists of four second order sequences: Ordovician-Devonian, Devonian-Tournasian, Neovisean and Pennsylvanian-Permian. The Pennsylvanian-Permian sequence is represented by the Tapajós Group, originating from a transgressive-regressive cycle involving sea-level variations (Cunha *et al.* 2007, Matsuda *et al.* 2010).

The Tapajós Group consists of the Monte Alegre, Itaituba, Nova Olinda and Andirá formations, and records the passage of continental environments to marine (Cunha *et al.* 2007). The Monte Alegre and Itaituba formations correspond to the basal part of this group, and represent a fluvial-aeolian environment, which passes, concordantly, to a mixed tidal flat environment, thence grading into a carbonate shelf (Matsuda 2002, Matsuda *et al.* 2010, Lima 2010, Silva *et al.* 2015). This environmental transition is observed by the change in the sedimentation, which begins by siliciclastic of aeolian origin to subaqueous marine with the proliferation of invertebrates typical of shallow water and the precipitation of carbonate (Caputo *et al.* 1971, Caputo 1984, Matsuda *et al.* 2004, Lima 2010, Moutinho *et al.* 2016a).

In terms of age, these units are positions at the base of the Pennsylvanian, although the Monte Alegre Formation was considered to be Morrowan (Lemos and Scomazzon 2001), on the basis of the *Spelaeotriletes triangulus* palinozone. However, Scomazzon *et al.* (2016) placed the upper part of the Monte Alegre Formation in the Bashikirian interval based on the presence of the conodonts *Idiognatjoides sinuatus* and *Neognathodus symmetricus*. Moutinho *et al.* (2016b) used foraminifera, conodonts and palinomorphs to position the upper succession of the Monte Alegre Formation in the Bashikirian–Moscovian interval. In consideration of the age of the Itaituba Formation, Matsuda *et al.* (2004) cited palinozones to identify the same Bashikirian–Moscovian interval. Moutinho *et al.* (2016a) studied marine invertebrates and conodonts in the contact between the two units and positioned the contact in the Bashikirian. Scomazzon *et al.* (2016) using biostratigraphy cited the presence of the conodonts

Idiognathodus incurvus and *Diplognathodus coloradensis* of Bashikirian–Moscovian age in the contact, and in the basal part of the unit as Moscovian.

3. METHODOLOGY

In this paper we followed the method proposed by Walker (1992) for facies description, which involves: *i)* the recognition and definition of the sedimentary facies noting the characteristics of the geometry, lithology, sedimentary structures, paleontological content and information on the paleo currents; *ii)* understand the sedimentary processes that formed the structures; *iii)* group the cogenetic and contemporaneous facies in facies associations and thus determine the different environments and sub- environments. The facies were codified following Miall (1977), and represented by stratigraphic columns.

Petrography was used to determine the carbonate microfacies observed in 235 thin sections with emphasis on: descriptions of the allochemical constituents, bioclastic and terrigenous content; b) classification of the microfacies following Dunham (1962), Folk (1962), Embry and Klovan (1971) and Wright (1992); c) staining the thin sections with Alizarin Red S to separate calcite and dolomite, and potassium ferrocyanide to separate magnesian calcite from ferroan calcite; d) the counting of 300 points in the thin sections to determine the constituents and their relative content; e) create reference displays of photomicrographs showing the main constituents of each facies/microfacies.

The age determination was based on the method proposed by Scomazzon (2004), and consists of weighing 500 g of sample of disaggregated carbonate adding 500 ml of acetic acid (CH_3 COOH) and 4.5 l of water. This mixture remains in solution until completely boiled, which take about 10 days. Following this stage, the remaining material is washed and dried, and sieved to 80 mesh (0.177 mm) and then to 200 mesh (0.074 mm). Following this, the sample is stored on a tray where the conodonts and associated fauna are collected and identified.

The biostratigraphic positioning was carried out according to the established international zones by comparing the data obtained with the work of Lane and Straka (1974) and Wang and Qi (2002). The correlation with the biostratigraphic zonation for the Amazonas Basin was carried out by the comparison with the data obtained by Lemos and Medeiros (1996) and Nascimento (2008).

4. FACIES ASSOCIATIONS

4.1 The Monte Alegre and Itaituba facies associations

Seventeen stratigraphic columns were assembled (Figure 2), of which five were from the Municipality of Monte Alegre, six sections along the Tapajós River near of Itaituba city and four sections from drill core from the neighbourhood of the Uruará city: drill core 1, 4, 5 and 25, and two cores from Aveiro: AV-01 and AV-02 (Figure 2).

The distinction between the Monte Alegre and Itaituba formations is based on the interpretation of the facies associations as well as on the differentiated sedimentary structures, lithology and fossil content. The outcrops are up to 8 m thick, but exposures in some of the quarries may be as much as 30 m. These consist of siliciclastic and mixed (carbonate/siliciclastic) sediments. The drill cores show that the thickness of the carbonate beds increases vertically, as does the fossil assemblage characteristically consisting of marine organisms. These beds may be up to 50 m thick, and show the largest paleoenvironmental variations.

A total of 35 facies/microfacies, grouped into three facies associations were identified from the stratigraphic sections: coastal desert (FA1), mixed tidal flat (FA2), and epicontinental carbonate shelf (FA3) (Table 1). These three associations are gradationally related without there occurring direct erosional contacts, except in some channels.

4.1.2 Facies association coastal desert (FA1)

This association consists of sandstone with medium-scale trough cross-bedding (Scb), sandstone with low angle cross-bedding (Sla), sandstone with even-parallel stratification (Sep), massive sandstone (Sm), sandstone with tangential cross-bedding (St), sandstone/mudstone with supercritical climbing ripple cross-lamination (Smc), massive dolostone (Dm) and sandy dolostone (Ds).
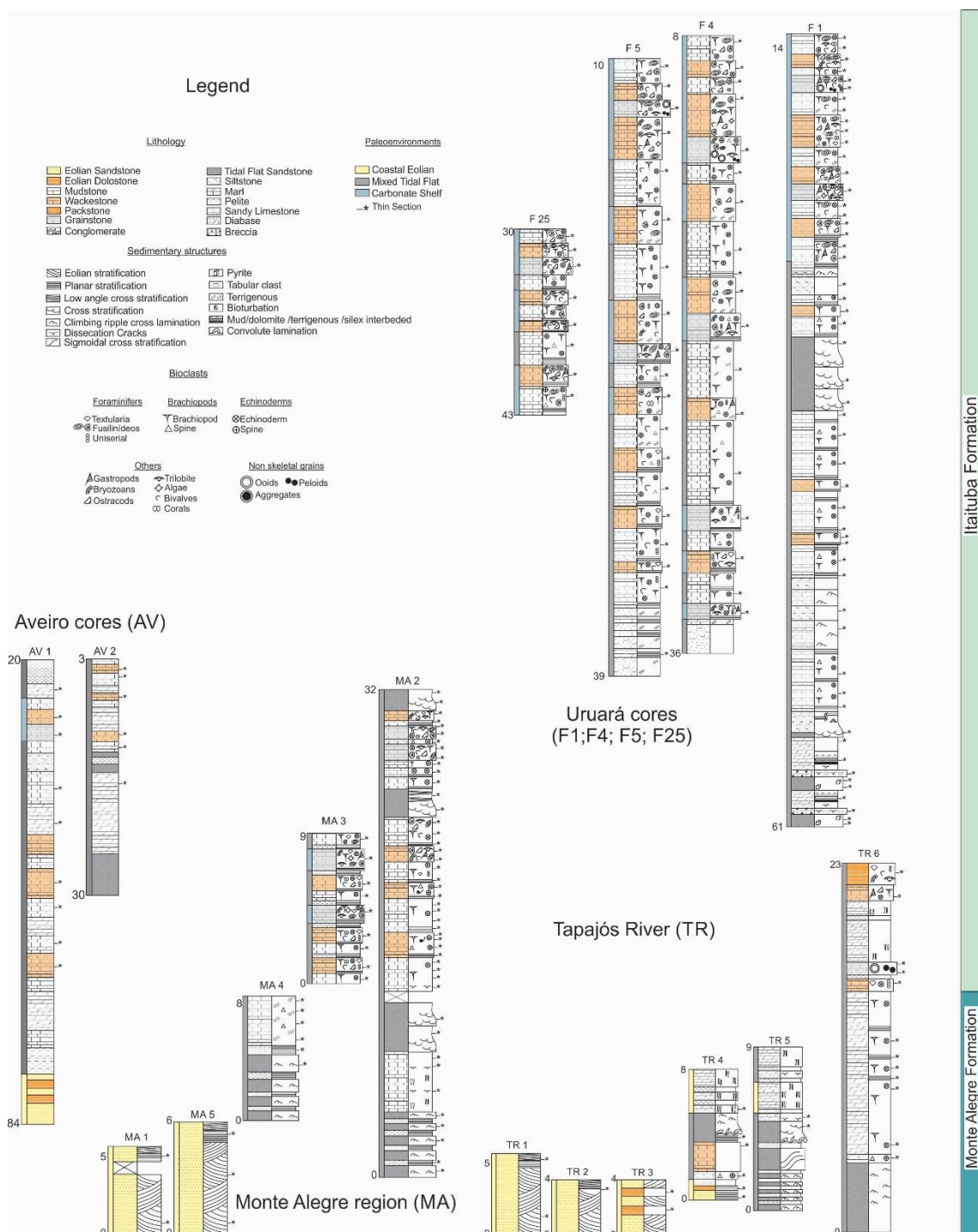
Figure 2- Stratigraphic sections of Pennsylvanian deposits of Amazonas Basin. Location of outcrops and cores are found in the figure 1.

Facies/microfacies	Structures	Process
Sandstone with cross-bedding (Scb)	Medium -scale trough cross-bedding	Aeolian dune migration formed by unidirectional flow
Sandstone with even-parallel bedding (Sp)	Even-parallel bedding	Traction processes caused by high velocity winds
Sandstone with low angle cross-bedding (Sla)	Low angle cross-bedding	Ripple mark migration by unidirectional traction currents
Massive sandstone (Sm)	Massive and adhesion warts	Grain migration over a wet surface and obliteration of the internal structure
Sandstone with tangential cross-bedding (St)	Tangential cross-bedding and convolutions	Sand wave migration by lower flow regime over a flat surface
Sandstone/mudstone with climbing cross-lamination (Smc)	Supercritical climbing cross-lamination and planar lamination	Traction currents, deceleration and suspension processes
Massive dolostone (Dm)	Massive	Biochemical precipitation in a confined environment
Sandy dolostone (Ds)	Massive, bioturbated with terrigenous material in the matrix	Biochemical precipitation in a confined environment and the proliferation of organisms
Massive dolostone (Dm)	Massive	Biochemical precipitation with a difference in the size of the crystals
Dolostone with terrigenous material (Dt)	Massive	Biochemical precipitation in influx of terrigenous material by traction currents
Massive sandstone (Sm)	Massive	Rapid deposition and carbonate cementation obliterating the original structure
Dolomitic Breccia (Bd)	Mud cracks	Subaerial exposure and dolomitization
Silicified dolostone with terrigenous fragments (Dts)	Planar lamination, locally undulating and with micro fractures	Dolomitization and influx by traction currents of terrigenous material including silt and fine-grained sand and subsequent silicification
Massive conglomerate (Cm)	Massive with quartz clasts	Migration of bed forms by unidirectional high energy flow
Sandstone with wavy lamination (Sw)	Wavy cross-lamination	Traction and suspension by marine currents
Siltstone with cross-lamination (Scl)	Low angle cross-lamination, wavy and convolute lamination	Alternating traction currents and suspension in oscillating currents, load cast and liquefaction
Marl with climbing cross-lamination (Mcr)	Supercritical climbing cross-lamination	Biochemical precipitation and traction processes originating from oscillating currents
Sandstone with tidal bundle (Stb)	Tidal bundle and mud drapes	Traction and suspension by the action of marine currents
Sandstone with trough cross-bedding (St)	Trough cross-bedding	Migration of subaqueous dunes and sinuous crests
Sandstone with swash cross-bedding (Ssw);	Swash cross-bedding	Swash and backwash wave flows

Sandstone with climbing cross-lamination (Scr)	Supercritical climbing ripple cross-lamination	Traction and suspension by subaqueous currents
Massive mudstone (Mm)	Massive	Deposition by decantation
Sandstone with sigmoidal cross-bedding (Ss)	Sigmoidal cross-bedding	Migration of bed forms of straight crests, unidirectional flow with rapid deceleration
Massive siltstone (Sim)	Massive	Rapid deposition from suspension
Massive shale (Shm)	Massive with pyrite crystals	Deposition by decantation, rapid tractive subaqueous influx and precipitation of pyrite
Massive lime mudstone (Lm)	Massive	Biochemical precipitation and preservation of bioclasts of brachiopods echinoderms
Wackestone with terrigenous (Wt)	Massive	Biochemical precipitation and preservation of rare bioclasts and traction influx
Floatstone with brachiopods (Fb)	Massive with pseudo lamination	Biochemical precipitation, preservation of brachiopods larger than 2 mm
Oolitic Grainstone with bioclastic (Gbo)	Massive	Biochemical precipitation and migrating ripple marks with bioclastic fragments
Bioclastic Grainstone with terrigenous fragments (Gbt)	Planar to massive lamination	Biochemical precipitation and migration of ripple marks with the predominance of terrigenous fragments
Carbonate-rich sandstone with cross-lamination (Scc)	Cross lamination	Migration of the form of sinuous crest bed and carbonate precipitation
Marl with cross-lamination (Mcl)	Climbing ripple-cross lamination	Biochemical cross-lamination, traction originated by oscillating currents
Bioclastic wackestone, bioclastic (Wb)	Massive	Biochemical precipitation and preservation of bioclasts in addition to diagenetic processes
Bioclastic wackestone with terrigenous (Wbt);	Massive	Biochemical precipitation, preservation of bioclasts and influx of terrigenous particles by traction currents
Bioclastic packstone (Pb)	Massive	Biochemical precipitation and preservation of bioclasts
Bioclastic packstone with terrigenous fragments (Pbt)	Massive	Biochemical precipitation and preservation of bioclasts, cemented and silicified
Bioclastic lime mudstone (Lb)	Massive	Biochemical precipitation with the preservation of bioclasts in addition to diagenetic processes

Table 1: Facies/microfacies of the Monte Alegre and Itaituba formations with descriptions, processes and respective facies associations, in addition to individualized units, in light grey FA 1, dark grey FA2 and White FA3.

The Scb facies (Figure 3a) may be traced laterally for hundreds of metres. It has a maximum stratigraphic thickness of 8 m, is exposed along the Tapajós River in the proximity of Monte Alegre and is observed in the Aveiro drill core. This facies is whitish in colour, and consists of very fine and fine-grained sandstone. It is bimodal, and the grains follow the bedding (NW-SE). In thin section the rock is seen to consist of microcrystalline quartz, plagioclase and microcline, cemented by silica and carbonate. Where it is intercalated with Ds the rock is partially dolomitized (Figure 4e). The crystals of dolomite is fine in size, and displays a *dirty cloudy* texture, which may corrode the margins of some terrigenous grains.

The Sla facies has a maximum stratigraphic thickness of 60 cm (Figure 3b) and is exposed in the Monte Alegre region as well as along the Tapajós River. This facies is whitish, and consists of very fine and fine-grained sandstone. The grains are bimodal, moderately well sorted, and each bed dips up to about 8°. The minerals consist of monocrystalline quartz, polycrystalline quartz, plagioclase, microcline and fragments of chert. The cement is silica and iron oxide and hydroxide.

The Sep facies has a stratigraphic thickness of about 90 cm (Figure 3b). It is exposed in the Monte Alegre region as well as along the Tapajós River and in the vicinity of Aveiro. This facies is associated with the Sla facies, and the bedding becomes plane laterally. The colour of the facies is whitish, and it consists of fine to medium-gained sandstone. These sediments are poorly sorted, with the predominance of angular and subangular grains. The grains are frosted and the sediment is bimodal. The minerals consist of monocrystalline quartz, chert fragments and plagioclase. The grains are cemented by overgrowths of silica and iron oxide and hydroxide.

The Sm facies is found only in the Monte Alegre region (Figure 3c). It is whitish in colour, and may attain a stratigraphic thickness of 50 cm. It is discontinuous laterally, and consists of very fine to fine-grained sandstone. The grains are subangular to sub-rounded, and the sediment is moderately well sorted (Figure 3.3d). Adhesion warts are observed on the tops of the beds, and the minerals consist of monocrystalline quartz, plagioclase and pyrite (Figure 3d). The matrix consists of iron oxide and hydroxide, which give the rock a reddish colour.

The St facies is discontinuous laterally, and has a maximum stratigraphic thickness of 1 m (Figure 3e). It is exposed only in the Monte Alegre region. This facies is whitish in colour, and consists of medium to coarse-grained sandstone, displaying medium-scale tangential cross-bedding. At the base of the beds there are coarser grains (Figure 3.3i), locally up to granule-

size. The minerals consist of monocrystalline quartz and a few fragments of chert. The cement is silica and iron oxide and hydroxide.

The Smc facies is discontinuous, and is exposed only at Monte Alegre, it has a maximum thickness of 60 cm (Figure 3f). The sandstone is whitish, and the grain-size is very fine to fine-grained. It displays supercritical climbing cross-lamination, and consists of quartz, feldspar and chert fragments. The sandstone facies is intercalated with mudstone. The mudstone is yellowish in colour, and is quite variable. The mudstone shows even-parallel lamination, and consists of clay mineral, iron oxide and hydroxide and detrital quartz in silt-sized particles.

The Dm facies is exposed along the Tapajós River (Figure 3g), where it is locally intercalated with beds of massive mudstone (Mm). It is whitish in colour. It is massive and continuous laterally. It is 50 cm thick. Petrographically, it consists of a very fine to fine-grained dolomitic matrix (90%). There are rare monocrystalline quartz grains (8%), silt to fine sand in size. Subordinately, there are grains of pyrite (2%) observed to be disseminated in the matrix. The crystals are subhedral to anhedral, and reach a maximum of 40 µm. The Mm facies is greyish in colour, massive and centimetric thicknesses are observed to be intercalated in the Dm, and it is composed of clay mineral, detrital quartz and iron oxide and hydroxide.

The Ds microfacies is locally intercalated with the Scb facies. It is exposed only along the Tapajós River and at Aveiro. Macroscopically, it is massive, and is bioturbated by: *Palaeophycus*, *Lockeia*, *Thalassinoides, Rosselia* and meniscate trace fossils. In thin section the matrix is seen to be composed of fine crystal of dolomite (80%), quartz monocrystals (17%) and plagioclase (3%). In general, the grains are subangular to angular, and are observed to the partially corroded, locally. or substituted by a dolomitic matrix, the grains of which vary in size from silt to very fine-grained sand-size (Figure 4f).
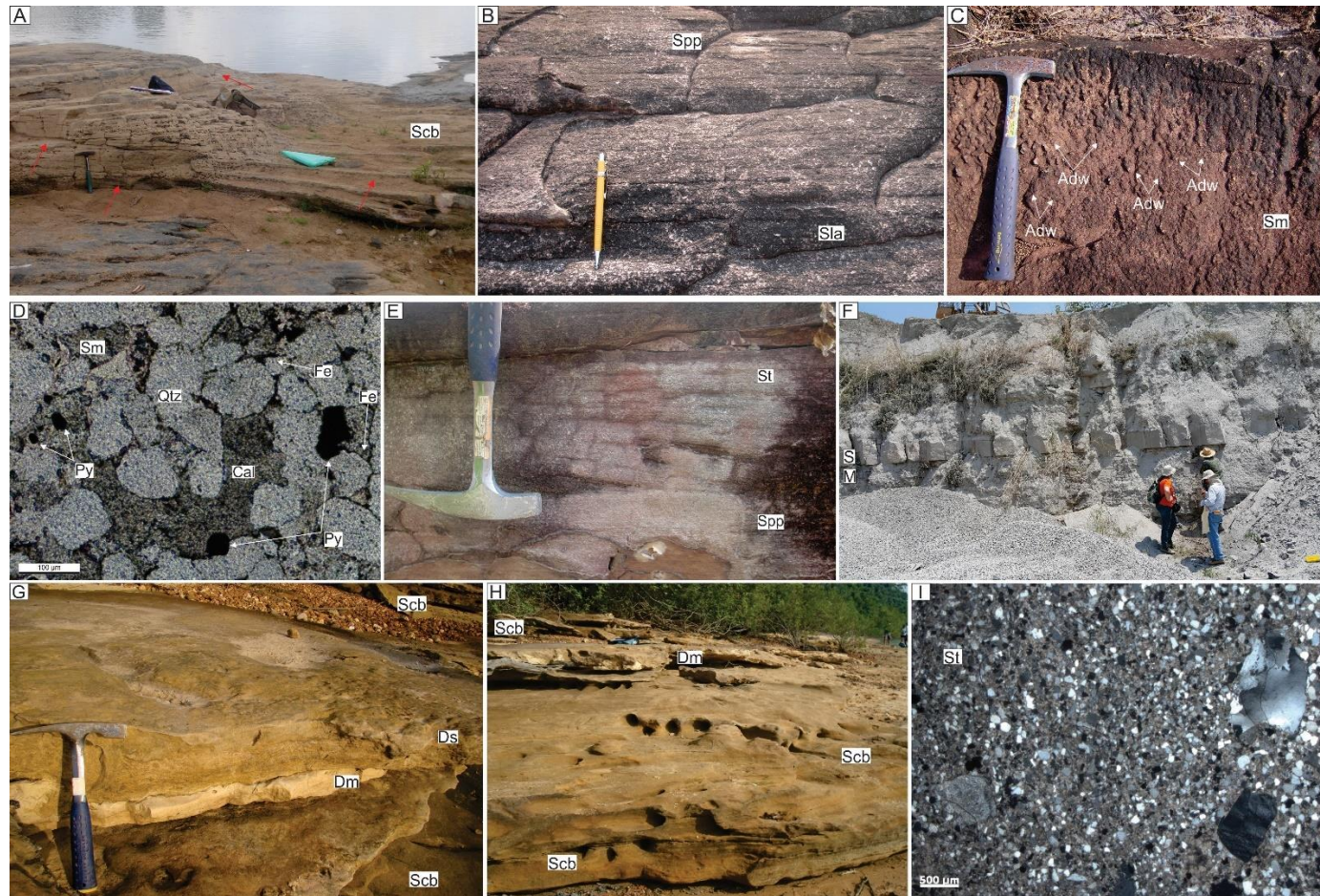
Figure 3- Coastal desert facies association. A - Sandstone facies with medium-scale trough cross-bedding (Scb), Monte Alegre region. B- Sandstone facies with low-angle cross-bedding (Sla) and sandstone with even-parallel bedding (Sep). C- Massive sandstone (Sm) with adhesion warts (Adw). D- Photomicrography of Sm showing pyrite (Py), calcite cement (Ca) and iron oxides and hydroxide (Fe). E- Sandstone facies with tangential cross-bedding (St) in contact with sandstone showing even-parallel bedding (Sep). F-. Smc facies showing alternating beds of sandstone (S) and mudstone (M). G- microfacies Dm e Ds in contact with Scb, the basal facies represent the dolomitized part of the dune field. H- General view of exposures along the Tapajós River with facies Scb and Dm with gradational contacts. I- Photomicrography of St facies, showing fine to coarse grained siliciclastic grains.

Palaeophycus is seen as slightly curved cylindrical tubes having a smooth surface. The tubes are brown in colour and lie horizontally in beds of the Ds facies (Figure 4a), when seen in plain view in outcrops. These trace fossils do not have branches and vary in size from 5 to 13 cm in length and up to 5 cm in diameter. They are filled with very fine sediment. *Lockeia* occurs as bodies horizontal to the bedding. They are elliptical to oval in shape, and vary from 5 cm to a maximum of 10 cm in size. They possess a smooth surface with convex hypo-relief (Figure 4a). They are filled with silty material on a carbonate substrate. Meniscate trace fossils form tubes displayed longitudinally to the bedding (Figure 4b). The menisci features have a maximum length of 9 cm and thickness of 5 cm. The menisci are regularly spaced with an average thickness of 5 mm. The *Thalassinoides* are `Y´- shaped vertical tubes from about 10 to 50 cm long and up to 8 cm in diameter (Figure 4.c). `T´- shaped forms are observed, locally. These are smooth forms, and are filled with very fine-grained particles. *Rosselia* occurs vertically to the carbonate bedding, and reaches a maximum length of 10 cm, and 9 cm in diameter. These are inclined, slightly curved and funnelled towards the base of the bed (Figure 4d).

Interpretation

The Scb, Sla, Sep, Sm, St, Smc, Dm and Ds facies correspond to a complex association of coastal desert facies. This facies association is found along both the northern and southern margins of the Amazonas Basin. One observes the transition of an aeolian system with detrital deposition to a humid system under direct coastal influence. This system corresponds to a siliciclastic-carbonate succession represented by the transition between the Monte Alegre and Itaituba formations.

The siliciclastic part comprises Scb, Sla, Sep, Sm, St and Smc facies. Generally, these facies consist of sediments having the grain-size of very fine to fine sand, except in the case of St facies, which is coarse-grained. The Sc facies is the most representative of this aeolian environment. The sediments are bimodal and medium-scale trough cross-bedding is observed. It was formed by the alternation of processes involving the fall-out and the flux of grains in the dunes, in other words, the intercalation of sediments transported by the cloud of sediments with sediments formed by the avalanche of grains at the crest of the dune. (Hunter 1977). The beds attain a thickness of 8 m, and in this way may be differentiated from large dune field deposits because it has a coastal influence in the sedimentation.
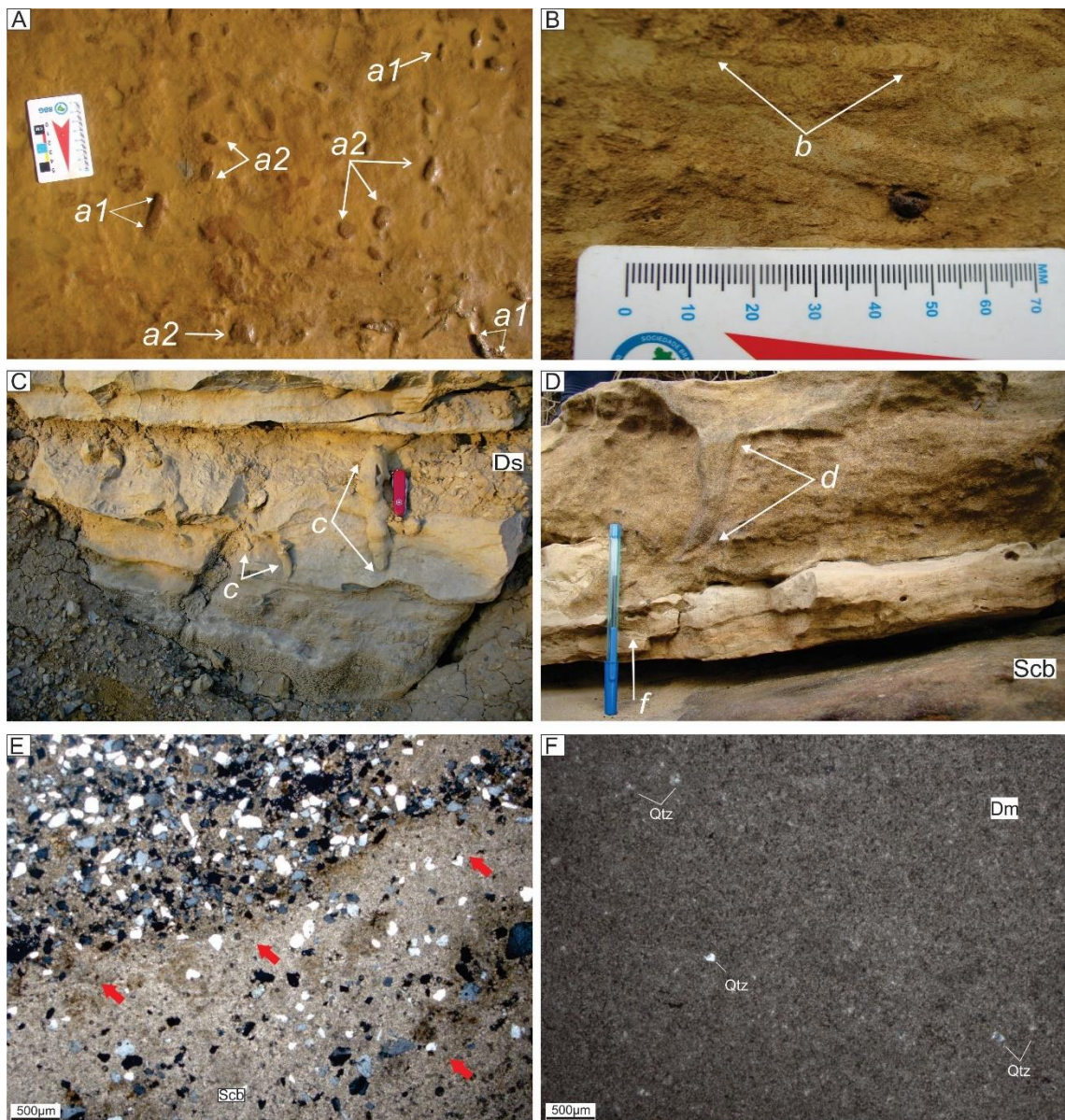
Figure 4- Ichnofossils of the desert-coastal facies association. The ichnofossils are concentrated in the dolomitic facies containing terrigenous material, which in turn is intercalated with facies Scb. A- ichnofossil *palaeophycus* (*d1*) and ichnofossil *lockeia* (*d2*); B- meniscate trace fossil; *(b)*. C– ichnofossil *Thalassinoides* (*c*). D– ichnofossil *Rosselia* in transverse view (d). E– dolomitization of facies Scb in contact with facies Ds, alternance of grains with different size mark the lamination (red arrows). F– microfacies Ds with a fine-grained matrix and quartz grains (Qtz) disseminated in the matrix.

The Sep and Sla facies are originated from the high velocity and aeolian influence incidence on a planar surface, or even low-angle, grain transport occurred by saltation and suspension (Mountney 2006, Brokfield and Silvestro 2010, Hunter 1977). This high velocity may have been obtained during sandstorms, with velocities too high for the formation of wind ripples (Fryberg *et al.* 1979, Brookfield 1992). Generally, the grains are sub-rounded to rounded, which is attributed to grain abrasion, differentiating planar deposits formed by subaqueous currents not related to the low flow regime due to the viscosity limit of the bed (Brookfield and Silvestro 2010). These types of structures are directly related to extensive flat-

lying areas (Hunter 1977), which due to the wind velocity, or even the humidity coming from the water table prevented the formation of dunes (*sensu stricto*) resulting in the sand beds (Hummel and Kocurek 1984, Kocurek and Nielson 1986).

The Sm facies is very fine to fine sand-size, and have adhesion warts on the tops of beds, these marks have a low-relief and small elevations, which grow by adhesion due to wind action on a damp surface under the influence of the water table closest to the surface, thus suffering migration against the wind (Mountney 2006, Olsen *et al.* 1989). These are preserved on the surfaces of beds and form wrinkled and wavy sheets (Hummel and Kocurek 1984). This type of structure is quite common in low-lying areas in interdunes and flanking dunes (Hummel and Kocurek 1984, Ahlbrandt and Fryberg 1982, Gleannie 1970). The occurrence and preservations of adhesion ripples suggests the presence of a local humid source, not only in function of the environment, but also the level of the water table. Lima (2010) described root marks associated with the top of this facies in the Monte Alegre region, which may suggest plant colonialization in a humid interdune system

The St facies originated by the migration of straight crest bed forms in the low flow regime over a plane surface (Harms *et al.* 1982). The unidirectional nature of the flow regime is probably related to channelling. The alternating sedimentary pattern of the aeolian sedimentation over an extensive flat area with sporadic subaqueous deposition suggests the occurrence of ephemeral streams cutting planar deposits (Ahlbrandt and Fryberger 1982, Mountney 2006). The coarse-grain size and the absence of mud suggest high energy transport in these channels, probably originating from sudden floods during times of high rainfall in a desert environment (Mountney 2006).

The Smc facies is composed of intercalated sandstone and mudstone, and represents an alternation of traction and suspension. The sandstone beds originated from the ripple migration, and the deceleration of material from currents and suspension forming climbing cross-laminations. The predominance of decantation processes is observed by the preservation of crests, which are characteristic of supercritical climbing ripple lamination (Tucker 2013). The laminated mudstone originated from the decantation of sporadic traction influx of silt and very fine sand forming planar laminations (Allen 1982, Lindholm 1987). These processes are probably associated with current deceleration and the settling of material in suspension in a body of water (Lindholm 1987, Bridge and Demicco 2008). This is likely to have been a lagoon in which the sedimentation was predominantly muddy, but with a probable marine connection,

or channels flowing into small lakes or lagoons dominated by mud, which graded into marine carbonate beds.

The carbonate part of this rocky succession corresponds to microfacies Da and Ds. These micro-facies are locally intercalated with facies Scb, suggesting a local variation in the predominantly tractive and siliciclastic sedimentation to a biochemical and carbonate one. In the Tapajós River, the dolomitic beds are intercalated with massive mudstone. The Dm contains terrigenous material disseminate in the matrix, whereas the Da shows, in addition to the carbonate matrix, rare terrigenous grains, pyrite and bioturbated fragments. Of these the most important are *Palaeophycus*, *Lockeia*, *Thalassionoides*, *Rosselia* and meniscate trace fossils. The carbonate precipitation and the ichnofossils assemblage suggest a marine connection for the carbonate facies, colonized by invertebrates and subsequently dolomitized, this process is supported by the fact that the crystals of the matrix are larger than 10 µm, and by the dissolution features observed on the terrigenous grains indicating substitution of calcite by dolomite.

The ichnofossil assemblage are related to habitation, locomotion, and feeding habits, and according to MacEachern *et al.* (2010) have characteristics that place them in the *Cruziana* ichnofacies. The bioturbations are contained within the carbonate substrate, probably corresponds to the soft ground substrate where organisms protected by shells, were easy of both horizontal and vertical locomotion. This is corroborated by the filling of those possessing the same composition of the carbonate matrix, by the non-ornamentation of the tubes and by the variety of the organisms responsible for the bioturbation. Terrigenous grains are concentrated only in the matrix Carbonate precipitation and the large variety of bioturbation attributed to marine invertebrate organisms, as well as the intercalation of these sediments with those related to the dune fields suggests that this aeolian system was connected to the sea. This is similar to Recent aeolian coastal systems (Clemmensen *et al.* 2001, Rodríguez-López *et al.* 2014).

4.1.2 Mixed tidal flat facies association (FA2)

The FA2 consists of an intricate facies association interpreted as a mixed tidal flat, consisting of the facies and microfacies: massive dolostone (Dm), dolostone with terrigenous (Dt), silicified dolostone with terrigenous (Dts), massive sandstone (Sm), dolomitic breccia (Bd), massive conglomerate (Cm), sandstone with wavy cross-lamination (Sw), sandstone with tidal bundle (Stb), sandstone with trough cross-bedding (St), sandstone with swash cross-bedding (Ssw), siltstone with cross-lamination (Scl), sandstone with sigmoidal cross-bedding (Ss), marl with climbing cross-lamination (Mcr), sandstone with climbing cross-lamination

(Scr), massive mudstone (Mm), massive siltstone (Sim), massive shale (Shm), massive lime mudstone (Lm), wackstone with terrigenous (Wt) and floatstone with brachiopods (Fb).

The Dm microfacies is found in all outcrops and cores in the study area (Figure 5a). It is brown in colour, 80 cm thick and consists of a dolomitic matrix that amounts to 91% of the rock and it possesses a dirty cloud texture. The microfacies contains monocrystalline quartz (5%) with silt-sized and sub angular to angular in shape. Subhedral pyrite amounts to 4%, and the crystals reach a maximum of 20 µm in size.

The Dt microfacies was found throughout the study area. It has a massive texture, and is up to 45 cm thick (Figure 5h). It has a fine-grained dolomitic matrix (90%) and is dark grey in colour. The grains are of microcrystalline quartz (8%). These are subangular to sub-rounded in shape and vary in size from silt-size to fine sand. They display corroded margins. Subhedral pyrite crystals (2%) are dispersed in the matrix with a maximum size of 30 µm.

The microfacies Dts occurs in the regions of Uruará and Aveiro, it has a centimetric thickness with grey-green colour. It is intercalated with microquartz, sheets of detrital quartz and clay (Figure 5a). Petrographically, the facies form horizontal to sub-horizontal sheets, cut by micro faults forming micro convolutions. The intercalations represent the alternation of traction, suspension, dolomization and silicification. The terrigenous grains consist of monocrystalline quartz, and the particles are very fine to fine sand-sized. The dolomite is brown in colour. The microquartz laminae follows the dolomite crystals and generally exhibit corroded contact. The clay occurs as a thin undulating sheet, dark brown in colour and covered by silicified beds. Euhedral pyrite crystals up to 90 µm follow the same orientation.

The Sm facies was observed in all areas covered in this study. This facies is dark grey in colour and up to 65 cm thick. The grain-size is very fine to fine (Figure 5b). The minerals are monocrystalline quartz, polycrystalline quartz, plagioclase, microcline, fragments of chert, fragments of metamorphic rocks, fragments of muddy rocks and pyrite, all cemented by calcite, silica and iron oxide and hydroxide. In general, the grains are subangular to sub-rounded and poorly sorted. There are euhedral to subhedral crystals of pyrite amounting to about 8% of the rock. These crystals have a maximum size of 80 µm.

The Bd facies occurs in all the regions coved by this study. It has a maximum of 50 cm thick. It is grey in colour and has a fine-grained dolomitic matrix (Figure 5b). This facies consists of subangular to angular clasts of laminated dolostone, which vary in size from 180

µm to 2900 µm, and grains of monocrystalline quartz the size of which is that of fine sand in addition of clay minerals disseminated in the matrix.

The Cm facies is exposed only along the Tapajós river. It is only centimetres thick. It has a fine-grained silty matrix and is brown in colour. The texture is massive, and clasts float in the matrix. The clasts are quartz, generally subangular to sub-rounded, and vary in size from 600 µm to a maximum of 4900 µm. The matrix is composed of monocrystalline quartz and clay mineral.

The Sw facies is observed in the regions of Uruará and Monte Alegre. It is about 70 cm thick, and is whitish in colour. It consists of very fine to fine grained sand with wavy cross-lamination (Figure 5c). The laminations are covered by clay. Microscopically, the rock is seen to consist of monocrystalline quartz, polycrystalline quartz, plagioclase, fragments of muddy rock, chert fragments and calcite cement, iron oxide and hydroxide and syntaxial overgrowths of silica in addition to anhedral pyrite attaining a maximum size of 25 µm.

The Scl facies may be observed along the Tapajós river as well as in the regions of Monte Alegre and Uruará. It is 40 cm thick (Figure 5e), grey in colour, and consists of an argillaceous matrix and iron oxide and hydroxide, with silt-sized terrigenous grains and rare very fine sand-sized grains. Low angle cross-lamination and locally small convolutions are observed.

The Mcr facies is found in the Uruará and Monte Algre regions. It is 50 cm thick and green in colour. It consists of an argillaceous-carbonate matrix with supercritical climbing cross lamination (Figure 5f), with evidence for the alternation of traction and suspension currents with the preservation of forms. The minerals consist of monocrystalline quartz, plagioclase, pyrite, muscovite, muddy rock fragments and chert, all floating in an argillaceous-calcitic matrix.

The Stb facies is observed along the margins of the Tapajós river as well as in the regions of Monte Alegre and Uruará. It is brown in colour and 85 cm thick. It consists of very fine to fine grained sandstone with marine cross-bedding (Figure 5d). The minerals consist of monocrystalline quartz, polycrystalline quartz, plagioclase, microcline, muscovite, fragments of muddy rock, chert fragments, and clay covering the bedding. The cement is carbonate, iron oxide and hydroxide and silica.

The St facies is observed along the banks of Tapajós River as well as in the regions of Monte Alegre and Uruará. It has a maximum thickness of 1 m, and is brown in colour. It consists of very fine to fine grained sand and displays channel cross bedding (Figure 6b). The grains consist of monocrystalline and polycrystalline quartz, plagioclase, microcline, fragments of muddy rock, carbonate fragments, chert fragments and pyrite. The cements are silica and iron oxide and hydroxide/clay minerals. Generally, the grains are subangular to sub-rounded. In the region of Monte Alegre, the St facies is intercalated with the Mm facies.

The Ssw facies was observed only in the Monte Alegre region. It is up to 70 cm thick, and consists of very fine to fine-grained sand; whitish in colour and displaying swash cross-bedding (Figure 6a). The minerals consist of monocrystalline quartz, polycrystalline quartz, plagioclase, chert fragments and cements consisting of iron oxide and hydroxide and silica.

The Scr facies is described along the Tapajós River, Monte Alegre and Uruará. It is 40 cm thick, yellow in colour, and composed of very fine to fine grained sandstone (Figure 6d). The climbing cross-lamination is supercritical and there is evidence for the alternation of traction currents and decantation with the preservation of form.

The Ss facies is described only in the Tapajós River region. It is 1 m thick, white in colour, and composed of very fine to fine-grained sandstone displaying a typical sigmoid geometry (Figure 6c). The sediments show evidence for rapid current deceleration in the presence of very fine to fine-grained particles. The minerals consist of monocrystalline quartz, polycrystalline quartz, plagioclase, microcline, chert fragments, microcline fragments of muddy rock, and cements that include iron oxide and hydroxide, silica and carbonate.

The Mm facies is found along the Tapajós River and in the localities of Monte Alegre and Uruará. It is 50 cm thick and grey in colour (Figure 5d). The minerals consist of clay minerals and rare quartz grains in an argillaceous matrix.

The Sim facies is found in the regions of Monte Alegre and Uruará. It is red in colour, massive, and has a maximum thickness of 2 m (Figure 5f). In thin section it is observed to have a matrix consisting of iron oxide and hydroxide and clay minerals in which occur angular to subangular grains of monocrystalline quartz and chert fragments.

The Shm facies is found at Mont Alegre and at Uruará. It is 45 cm thick and is black in colour (Figure 5h). It consists of clay minerals and yellow pyrite, disseminated throughout the bed.

The Lm micro-facies may be observed in all sections. It is 60 cm thick (Figure 5d), grey in colour and of massive texture (Figure 5g). The matrix is micrite (93%) and composed of magnesian calcite, grains of silt-sized monocrystalline quartz (4%) and pyrite (3%). The pyrite is subhedral to euhedral and disseminated in the matrix.

The microfacies Wt is observed along the Tapajós River, at Monte Alegre, Uruará and Aveiro. It is 50 cm thick, grey in colour, massive, and has a micrite matrix (78%) composed of magnesian calcite, terrigenous material (10%), bioclasts (8%) and pyrite (4%) (Figure 6f). The terrigenous grains consist of monocrystalline quartz varying in size from silt to very fine sand-sized particles. The bioclasts are fragments of brachiopod shells, brachiopod spines, and echinoderm spines. These are mainly composed of calcite and some are partially silicified.

The Microfacies Fb is found in the regions of Uruará. It is 50 cm thick, grey in colour and has pseudo laminations (Figure 6e). The matrix is micrite (70%) and the bioclasts consists of brachiopod shells (7%), brachiopod spines (10%) and echinoderm spines (8%). These bioclasts ate larger than 2000 µm, and may be silicified, locally. Pyrite (5%) is disseminated in the carbonate matrix with. euhedral and subhedral crystals. They have a maximum size of 40 µm.
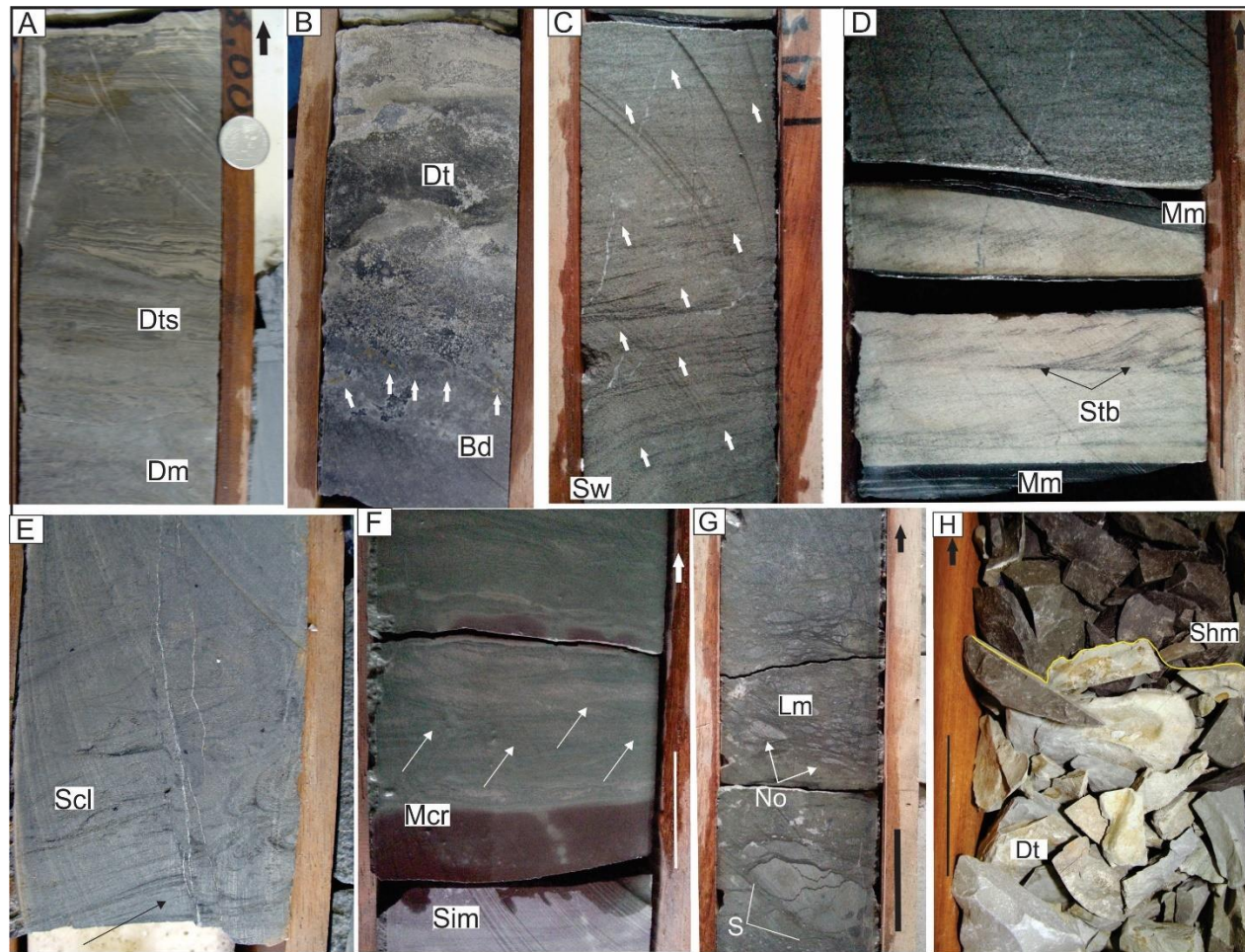
Figure 5: Tidal flat facies association in dill core. A-Massive dolostone micro-facies (Dm), silicified dolostone with terrigenous (Dts). B-Massive sandstone facies (Sm) and pyrite (arrows) of dolomitic breccia (Bd). C- Sandstone with wavy cross laminations (Sw), showing a muddy covering (arrows). D- Sandstone with tidal bundle (Stb), in contact with massive mudstone (Mm). E- Siltstone with cross-lamination (Scl), in detail convolutions (arrows). F- Massive siltstone (Sim) in contact with the facies marl with climbing ripple cross-lamination (Mcr), cross-laminations (arrows). G- Massive lime mudstone (Lm) with diagenetic nodules (No) and stylolites (S). H- Dolostone with terrigenous (Dt) in contact with massive shale (Shm) with pyrite.

Interpretation

This grouping of facies corresponds to the interaction of a mixed tidal flat depositional system with detrital and carbonate rocks. This association corresponds to a system dominated by marine action with the development of tidal flats and channels, which flow in the form of lobes characteristic of marine deltas into lagoons bringing fine grained siliciclastic sediments. These lagoons containing siliciclastic sediments grade laterally into carbonate lagoons. The association could be divided into supratidal, tidal channels, marine deltas, beach and lagoon.

The supratidal deposits correspond to microfacies Dm, Dt, Bd, Dts and Sm. Their characteristic is their mixed dolomitic and siliciclastic composition. They were deposited on that part of the tidal flat subject to subaerial exposure (Shinn 1983, Tucker and Wright 1990, Longhitano *et al.* 2012). Mud cracks are typically associated with subaerial exposure, and these are found in association with the Bd facies, where solar exposure breaks and fragments forming typical polygonal-shaped fragments. Under certain circumstances, the supratidal environment may be flooded by storm waters or even by the action of spring tides (Shinn 1983, Longhitano 2010), which partially inundated the area forming ponds or depressions filled with sea water.

It was in these ponds formed in depressions that carbonate precipitated, which was subsequently dolomitized during diagenesis. Likewise, these ponds were the sites of the precipitation of evaporite minerals that were altered to silica during diagenesis (Morrow 1990a, Warren 2000, Tucker 1992, Warren 2010). The dolomite is secondary, and this process occurs following the initial precipitation of carbonate, whether be this in the form of calcite or aragonite during eodiagenesis. At this time the mixture of marine and meteoric waters and the intense evaporation concentrated the solutions precipitating them in like manner to that which generated the dolomitic micro-facies (Morrow 1990b, Warren 2000).
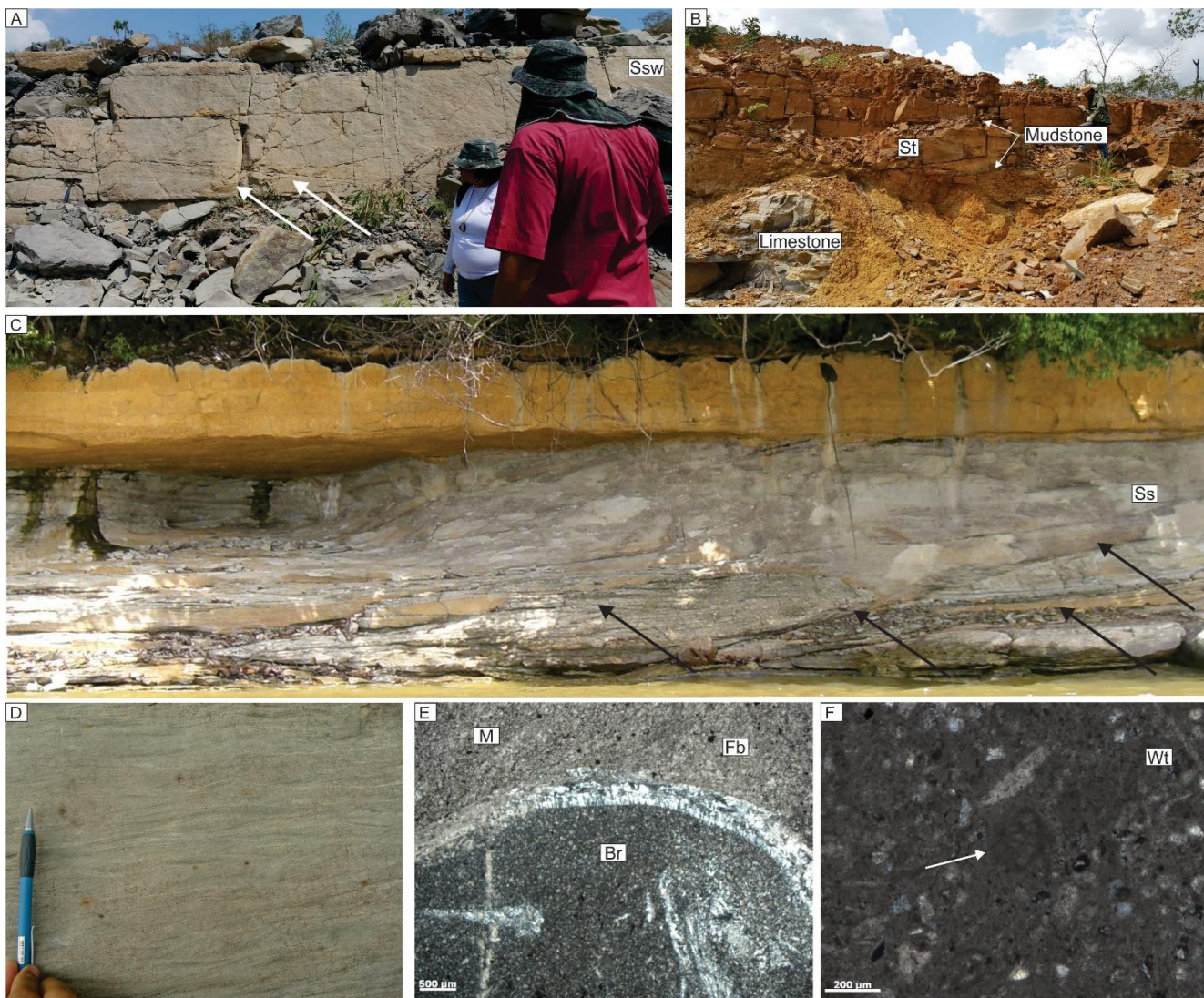
Figure 6- Facies association of the mixed tidal flat as seen in exposures and in photomicrographs of the carbonate sections. A- Ssw facies seen on the N border of the basin. The arrows point to the swash cross-bedding; B- marine channels (St) with a muddy cover underlying shelf carbonate sediments (limestone); C- Sigmoidal cross-bedding sets (facies Ss) separated by climbing surfaces (arrows) (M); D- facies sandstone with climbing cross lamination (Scr). E- Fb microfacies having a calcitic matrix and bioclasts of brachiopods (Br). F- Wt microfacies, showing the micritic matrix and disseminated bioclasts and indication of a probable fusulinid (arrow).

The Dts microfacies shows the dolomitization and partial silicification of the fabric, by microquartz and chalcedony. This process is quite intense, and locally may corrode the edges of the dolomite crystals, inhibiting their development (Dietrich *et al.* 1963). In this context the silicification originates from the substitution of the evaporite mineral by silica, identified by the presence of microquartz and quartzine (Tucker 1992), the provenance of the silica being the siliceous material derived from the continent. The terrigenous material is originated by aeolian action, probably due a grain-size. The transport of these grains is attributed to wind-driven clouds of grains dependent on the wind velocity. The transport of terrigenous material by wind action is a common phenomenon of mixed tidal flat and coastal environments (Mountney 2006). The particles were derived directly from the sand of the interdunes and that of the dune fields (Kocurek 1996, Mountney 2006).

The Sm facies is associated with the rapid deposition and probable fluidification at the supratidal-intertidal interface, the accumulation of pyrite and the formation of iron oxide and hydroxide is related to the concentration and maturation of organic matter, presumably generated by flooding of the channels in the intertidal zone or by the direct action of larger bodies of water. This explains the large amounts of siliciclastic material of variable composition such as quartz, plagioclase, clay minerals and pyrite. The channels cut the tidal flats carrying very fine to fine-grained sediments, behaving as meandering channels (Shinn 1983, Longhitano *et al.* 2012).

The facies Cm, St, Sw and Stb are attributed to the tidal channels and represent high-energy facies. Cm originated by the action of unidirectional flow, responsible for the intense reworking of the sand and clay that resulted in the formation of the matrix and differentiated clasts (Visser 1980, Longhitano 2010). The St facies is attributed to the migration of subaqueous bed forms of sinuous crests in the lower flow regime, carrying sediments up to medium sand-size particles. The St facies may be intercalated with the Mm facies, signifying a change in the sedimentation from traction to suspension suggesting the direct influence of the sea (Dalrymple and Choi 2007, Hughes 2012). The Sw and Stb facies have equal amounts of sand and clay, covering the bed form. This interaction of processes corresponds to the intercalation of marine processes with intertidal ones.

The tidal channels are controlled by processes of traction and suspension originating from tidal action (D'Alpaos *et al.* 2005, Hughes 2012). These channels cut the intertidal zone. They are sinuous in like manner to the meandering continental deposits, with the development

of muddy intertidal flats, probably containing carboniferous coastal vegetation as described by Lima (2010). The channels branch and discharge in the form of lobes in lagoons initially silty, grading into carbonate deposits. The lobes correspond to tidal deltas, and are represented by the facies Ss, Scr Scl and Mcr.

The tidal deltas are defined by their sigmoidal and lobed geometry of the Ss and Scr facies, as well as by the deposition of sediments in suspension in a body of water (Goodbred and Saito 2012). These facies are an integrated system formed by processes of migration of bed forms having straight crests by unidirectional flow due to current deceleration which generates lobes in suspension. Locally, Scr is intercalated with Mm facies. The lobes flow into a lagoon dominated by fine-grained siliciclastic sediments, marl and lime mudstone.

The lagoon containing siliciclastic sediments (Mm, Sim and Shm) is the most proximal part of the system and subject to the action of the tidal deltas. The dominant sedimentary process is the decantation of particles representing all three facies. The Mm and Sim facies correspond to the shallowest parts having the largest amounts of terrigenous grains and subject to oxidation processes. The Shm facies represents a slightly deeper subaqueous part due to the concentration of organic matter, reflected in the precipitation of pyrite of centimetric size and the absence of evidence of traction currents. The lagoons contain fine-grained siliciclastic sediments deposited by decantation (Weimer *et al.* 1982, Dalrymple 1992).

The part of the lagoon containing carbonate present micrite, bioclasts, pyrite, quartz, terrigenous grains and authigenic silica. The micrite is originated due to the presence of organic matter (Flügel 2004). The bioclasts are of brachiopods and echinoderms with size over 2000 µm in the Fb microfacies, correspond to fragments and spines of these organisms. Pyrite may have its origin from the maturation of organic matter. The terrigenous quartz is attributed to the sporadic aeolian influx. The silica is attributed to the diagenetic precipitation of material that substituted the bioclasts. The occurrence of brachiopods and echinoderms supports a marine connection. However, the low diversity of the marine organisms and the low terrigenous content of the sediments suggest that the lagoon was to some extent isolated by a barrier (Shinn 1983, Tucker and Wright 1990, Haas 2004).

The low diversity of the organisms of the tidal flats may be associated with the sedimentary contribution from the channels that discharged into these aqueous bodies as well as the aeolian contribution. The lagoons are surrounded by a system of depressions or even carbonate and/or sand bars (Tucker and Wright 1990), causing confinement with restricted

connection to the sea resulting in that the variety of organisms was very much more restricted as compared as to what would be expected on a marine shelf (Figueiras 1983, Matsuda 2002, Moutinho 2006).

4.1.3. Epicontinental carbonate shelf facies associations (FA3)

The FA3 facies consists of bioclastic ooliic grainstone (Gbo), bioclastic grainstone with terrigenous (Gbt), carbonate sandstone with cross-lamination (Scc), marl with cross-lamination (Mcl), bioclastic wackestone (Wb), bioclastic wackestone with terrigenous grains (Wbt), bioclastic packstone (Pb), bioclastic packstone with terrigenous (Pbt), bioclastic lime mudstone (Lb) and massive lime mudstone (Lm). This facies association is marked by the large quantity of bioclasts, which are summarized in accordance with the associated microfacies, composition, size and description on Table 3. These microfacies are founded in the Uruará, Monte Alegre and Aveiro regions.

The Gbo microfacies is grey in colour and has a massive texture (Figure 7a). Petrographically it consists of ooids, bioclasts of brachiopods, echinoderms and bivalves. The ooids (60%) are rounded to sub-rounded and have a maximum size of 900 µm. The brachiopods (15%) occur as shells, the echinoderms (12%) as angular to subangular fragments. The bivalves (8%) are shell fragments. All these components are cemented by equant magnesian calcite (4%), with a maximum of 30 µm in size. Subordinately, anhedral to subhedral crystals of pyrite up to 30µm (1%) are observed to be disseminated in the rock.

The Gbt microfacies is grey in colour, has a massive texture, and displays diagenetic structures such as stylolites and druses. Microscopically, the rock is seen to consist of shells (10%) and spines (5%) of brachiopods, echinoderms (10%), bryozoans (7%), gastropods (5%), algae (3%), trilobites (6%), ostracods (5%) and foraminifers (9%) (Figure 7b). The terrigenous grains consist of monocrystalline quartz (15%) and plagioclase (5%). These grains are subangular to sub-rounded and vary from silt to fine sand-sized particles. They are described as pyrite (6%), and pelloids (4%), all cemented by equant magnesian calcite (10%), and the echinoderms display syntaxial overgrowths. Generally, the echinoderms attain a size of 3100 µm. They are composed of calcite, and are partially silicified, locally, by authigenic quartz and microquartz.

The Scc microfacies is grey in colour, and is composed of very fine to fine grained sandstone with cross-lamination. Microscopically, the facies is seen to consist of

monocrystalline quartz (26%) polycrystalline quartz (15%, plagioclase (21%), chert fragments (8%) and fragments of metamorphic rocks (4%), fragments of brachiopod shells (5%), fragments of carbonate rock (7%), calcite cement (5%) and quartz (4%), in addition to pyrite (3%) and subordinate muscovite (2%).

The Mcl microfacies is grey green in colour. It consists of silt-sized particles with calcite and clay minerals as a matrix. The climbing ripple cross-lamination is supercritical. The grains are silt-sized, and consist of monocrystalline quartz. These are subangular to angular and are set in a matrix consisting of clay minerals and calcite. Subhedral crystals of pyrite up to 30 µm occur, subordinately.

The Wb microfacies is dark grey in colour. It has a massive texture and dissolution seams. It has a micritic matrix composed of ferroan calcite (40%), and is locally, peloidal due to the dissolution features. It consists of bioclasts of brachiopods (14%), echinoderms (9%) algae (4%), bivalves (6%), ostracods (5%), trilobites (5%), and foraminifera (12%). Subhedral to euhedral pyrite is observed to be disseminated in the matrix (5%), and reaches a maximum size of 40 µm. The bioclasts vary from 30 µm to 4900 µm and correspond to a few fragments whereas other are well-preserved. They are angular to rounded and composed of calcite (Figure 7f).

The Wbt microfacies is grey in colour. It consists of a micrite matrix (42%), brachiopod bioclasts (14%), echinoderms (11%), bivalves (6%), foraminifera (8%) and trilobites (4%), monocrystalline quartz (8%), plagioclase (4%) and pyrite (3%) (Figure 7e). The grain size varies from silt to fine sand-sized particles, and the grains are angular to subangular. In general, the bioclasts vary in size from 60µm to 4100 µm. These are angular to subangular. However, the remains of spines and foraminifera are rounded in shape.

The Pb microfacies is grey in colour and is massive. The matrix is micrite (25%) and supports bioclasts, consisting of brachiopods (14%), echinoderms (12%), foraminifera (10%), corals (5%), gastropods (4%), bryozoan fragments (5%) and bivalves (9%). Iron oxide and hydroxide (7%), and pyrite (9%) are disseminated in the rock. The pyrite forms subhedral to euhedral crystals up to 30 µm in size. The bioclasts vary in size from 10 to 2600 µm. These are composed of calcite and are angular to rounded in shape (Figure 7c).

The Pbt microfacies is grey in colour with irregular pseudo-laminations. The matrix is micrite and composed of magnesian calcite (21%). The rock consists of brachiopod bioclasts

(14%), brachiopod spines (6%), echinoderms (15%), trilobites (7%), bryozoans (4%), bivalves (5%), foraminifera (11%), corals (4%), and ostracods (7%) in addition to monocrystalline quartz (6%). These particles are subangular to sub-rounded in shape and vary in size from silt to fine sand. The brachiopods vary in size from 400 to 2100 µm. These fragments are angular to rounded in shape, and are composed of calcite (Figure 7d).

The Lb micro-facies is grey in colour. The matrix consists of micrite (91%). Dissolution seams are disseminated in the matrix. The bioclastic constituents consist of brachiopod shells (2%), echinoderms (1%) and monosserial foraminifera (2%). In general, the bioclasts vary from 20 µm to 180 µm in size. Subhedral to euhedral pyrite (4%) are observed in the matrix and have a maximum size of 30 µm.

The Lm microfacies is light grey in colour. It is massive and has a micrite matrix consisting of calcite (97%). Pyrite crystals in the matrix have a maximum size of 40 µm, and these are subhedral to euhedral (3%).

Interpretation

This facies association comprises microfacies Gbo, Gbt, Pb, Pbt, Wb, Wbt, Lb and Lm, which correspond to an epicontinental carbonate shelf association. This shelf system has at its margin in its proximal part a set of bioclastic bars, which are periodically cut by tidal inlets (Scc and Mcl). These bars transition to the carbonate shelf with a gradual increase in mud having a larger amount of bioclasts, which is noted by the facies variation from grainstone to packstone and from packstone to wackestone/lime mudstone.

The bioclastic bars separate the shelf of lagoons, and represent the action of tidal currents, waves or even storms, which reworked the sediments and deposited these in mounds adjacent to the lagoon (Enos 1983, Tucker and Wright 1990). Ooids and similar carbonate particles characteristic of high energy were not observed in lagoons deposits, suggests that conditions of deposition were relatively calm, without the constant occurrence of major events such as storms affecting the adjacent shelf (Tucker 1992, Flügel 2004). These evidences suggest predominance of quite shallow environments (Pomar 2002). The tidal inlets were responsible for the reworking of terrigenous material and carbonate particles deposited in the proximal zone of the shelf. These are very fine to fine-grained sediments, suggesting a shallow channel with low energy.

The part of the shelf is represented by the intense carbonate sedimentation with the deposition of abundant bioclasts of algae, bivalves, brachiopods, bryozoans, corals, echinoderms, foraminifera, gastropods, ostracods and trilobites. The diminution of terrigenous material towards the top of the succession until there is a complete absence of terrigenous material in the sediments, which coincides with the larger diversification of organisms with autochthonous characteristics. The shelf has low energy as its characteristic, with the sedimentation of carbonate mud and the proliferation of marine invertebrates in a shallow water environment.

The shallow marine environment of the Itaituba Formation is best defined as an epicontinental carbonate shelf, having the characteristics of pure carbonate shelfs (Kiessiling *et al* 2003) such as: *i*) the abundance of benthic foraminifera besides abundant brachiopods, and echinoderms; and *ii*) at the time the area lay geographically near the equator. Taking these items into consideration it may be concluded that the Itaituba Formation was deposited in a shallow body of water under the influence of the open sea. Mixed sedimentation occurred on the borders, whereas in the centre of the basin the sedimentation was typical of that associated with shallow carbonate shelfs with the proliferation of a biota typical of Pennsylvanian benthic organisms.

The large and differentiated variety of organisms suggest a benthic assemblage of Pennsylvanian age (Osleger 1991, Anelli 1999, Moutinho *et al* 2016b). Besides the diversity of the organisms, the carbonate precipitation, marine cements and the paucity of terrigenous sediments restricted to the tidal channels and sporadic aeolian influx, suggest a depositional environment with little wave action or even tidal action. These are the characteristics of Palaeozoic epicontinental seas (Ross and Ross 1985).

This model for epicontinental seas is differentiated from the classical model proposed by Irwin (1965) for the carbonate deposits of the North American mid-continent, due to the fact that the sedimentation was dominated by tidal deposits at the margins of the basin, generating a mixed succession (Caputo 1984, Figueiras and Truckenbrodt 1987, Lima 2010, Silva *et al*. 2015), very similar to the model stressing tidal influences proposed by Pratt and James (1986).

5. AGE CONSTRAINS

The Bashkirian-Moscovian interval for the upper part of the Monte Alegre Formation is based in the description and interpretation of conodonts in the basis of the species *Idiognathoides incurvus* and *Neognathodus symmetricus*, described from carbonate rocks in the region the Tapajós River (Scomazzon *et al.* 2016, Moutinho *et al.* 2016a). Lima (2010), placed the succession of the northern margin of the Amazonas Basin in the contact between the Monte Alegre and Itaituba formations, following the proposal of Matsuda (2002) for the southern margin in the interval Morrowan-Atokan interval, representing the present Bashkirian-Moscovian interval. Our study concentrated in the Uruará region, situated on the southern border of the Amazonas Basin, where samples corresponding to the epicontinental shelf carbonates is inserted in a system of bioclastic bars developed in carbonate shelfs.

Bioclasts	Epicontinental carbonate shelf			
	Microfacies	*Size (μm)*	*Composition*	*Description*
Alga	Gbo, Gbt, Pbt e Pb;	50 - 150	Calcite;	Micrite locally substituting the internal structure with the preservation of talus. They are reworked, brownish, undulatory extinction and internal radial form;
Bivalve	Gbo, Gbt, Wb, Wbt, Pbt e Pb;	30 - 950	Calcite;	Shell fragments, and unbroken shells, occur totally substituted by calcite, without internal structures. However, some show planar structures. High interference colours. Locally micritized;
Brachiopod	Gbo, Gbt, Wb, Wbt, Pbt, Mb e Pb;	40 - 5100	Calcite e silica;	Show *punctae*, which are locally silicified by microquartz and radial chalcedony. Shell fragments show undulatory extinction and low interference colours. Locally, identified as the genus *Composita sp.*;
Bryozoan	Gbo, Gbt, Wb, Wbt, Pbt e Pb;	110 - 3400	Calcite;	Corresponds to fragments. The zooecia are filed with fine-grained calcite. Terrigenous grains observed locally. Internal filaments observed in some thin sections;
Coral	Gbo, Gbt, Wb, e Pb;	90 - 400	Calcite;	Correspond to isolated and colonial zooecia forms. The isolated forms occur as transverse fragments and show undulatory extinction, micritized borders and interiors filled with fine to medium grained calcite. The colonial forms have septa filled with calcite. These are whitish in colour and microcrystalline calcite is observed at their margins;
Echinoderm	Gbo, Gbt, Wb, Wbt, Pbt, Mb, e Pb;	75 - 4200	Calcite e silica;	Have a sieve texture, undulatory extinction, high interference colours, and are composed of both reworked fragments and fragments that have not been reworked. Rarely silicified, but when they are the silicification is local and consists of microquartz;
Brachiopod spine	Gbo, Gbt, Pb, Pbt e Mb;	70 - 800	Calcite e silica;	These are rounded to sub-rounded. Locally, they may be partially silicified. Due to their micritic composition they do not show undulatory extinction and have a hollow nucleus;
Echinoderm spine	Gbo e Gbt;	90 - 500	Calcite e silica;	Have a sieve texture, and the spines do not have a defined nucleus. They display undulatory extinction. Transverse sections with internal radial structures. Locally, the spines may be partially silicified by quartz;
Foraminifera	Gbo, Gbt, Wb, Wbt, Pbt, Pb Mb;	50 -	Calcite;	Spiral and biserial forms are easily recognized. Fusilinid and miliolid foraminifera are easily recognized. They are composed of black microcrystalline calcite. The chambers are composed of fine calcite, whitish in colour. Completely round forms (calcispheres) are also observed;
Gastropod	Gbo, Gbt, Wb, Wbt, Pbt e Pb;	200 - 3600	Calcite;	Show undulatory extinction and low interference colours. The chambers may be filled with spathic calcite. Spiral and fragmented forms are observed;
Ostracode	Gbo, Wb, Wbt, Pbt e Pb;	80 - 600	Calcite;	Occur in the form of shells with the characteristic `v` junction of the valves. Show undulatory extinction, and do not show signs of reworking. Some of the valves are seen to be disarticulated;
Trilobite	Gbo, Gbt, Wb, e Pb;	80 - 4100	Calcite;	Correspond to disarticulated fragments of thoracic segments. The borders are frequently observed to be micritized. Have a calcite composition. Show undulatory extinction. Locally, showing high interference colours.

Table 2- Bioclasts of the epicontinental shelf facies found in the area under study, showing their respective sizes, microfacies, composition and brief description.
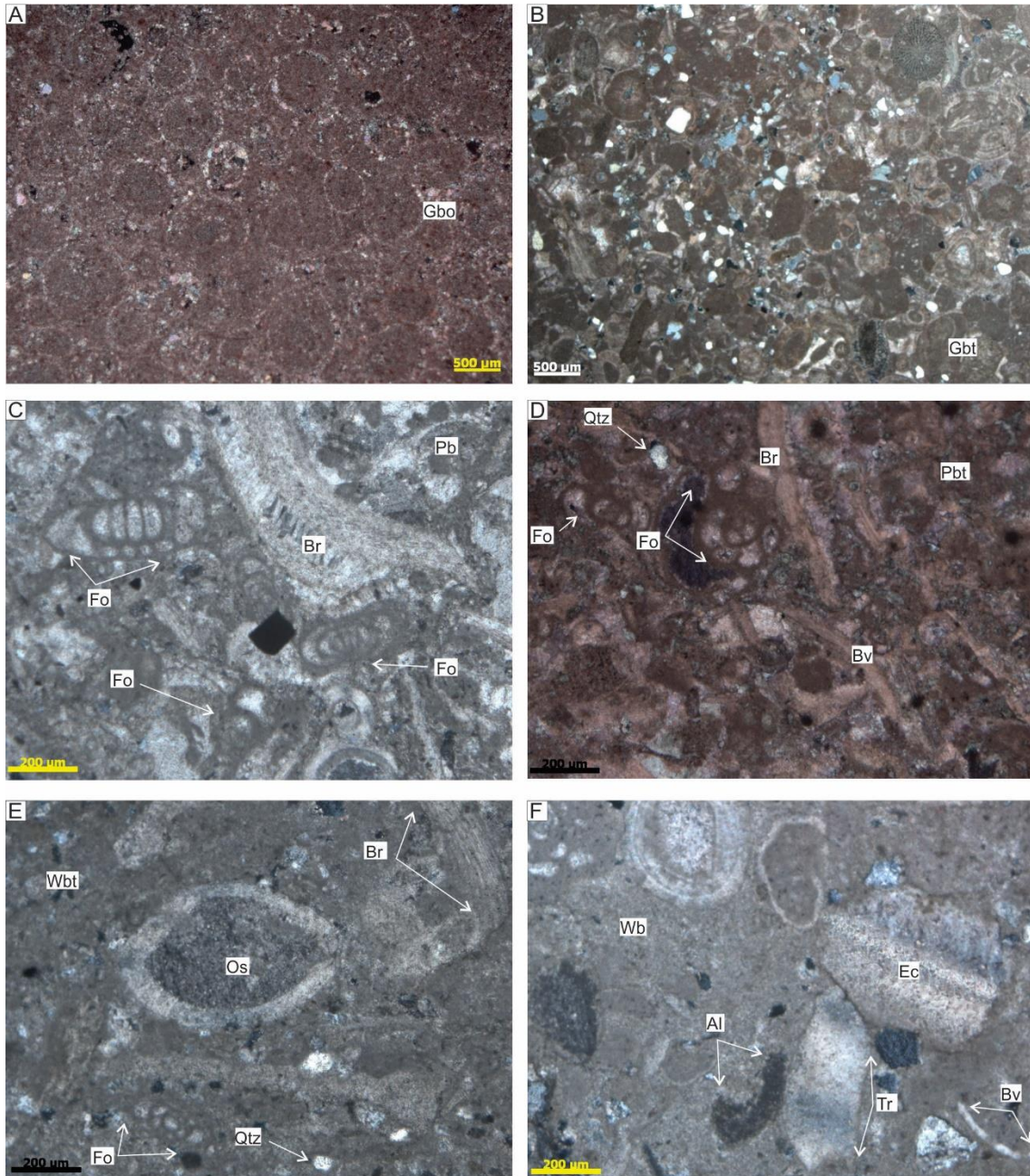
Figure 7- Microfacies representative of the epicontinental carbonate Shelf facies association. A- Gbo micro-facies, mostly composed of ooids; B- Gbt microfacies, consisting of terrigenous material, bioclasts and allochems; C- Pb microfacies where the grains support the muddy matrix, composed mainly of brachiopod fossils (Br) and foraminifera (Fo); D- Pbt microfacies, showing the calcite matrix with bioclasts of brachiopods (Br), bivalves (Bv) and foraminifera (Fo), in addition to grains of terrigenous quartz (Qtz);. E- Wbt micro-facies having a calcite matrix with bioclasts of ostracods (Os), brachiopods (Br) and foraminifera (Fo) with terrigenous quartz (Qtz) disseminated in the matrix; F- Wb micro-facies with a micrite matrix containing some bioclasts of echinoderms (Ec), bivalves (Bv), algae (Al) and trilobites (Tr).

About 20 samples were collected from drill cores it was possible to identify three distinct species of conodont, represented by *Ellisonia sp., Neognathodus symmetricus* e *Streptognathodus sp*. *Ellisonia sp* shows a central recurved cusp, a reverted basal cavity, cracks of a large denticule, besides the central cusp (Figure 8 a, b, g, h). *Neognathodus symmetricus* shows six denticules of which the shelf is observed to be in an average position, continuing as a central carena to the later final (Figure 8 c, d, e, f). *Streptognathodus sp*. *Streptognathodus sp*. Is seen in thin section as a robust shelf and backward final pointed, in addition to possessing in the later part ornamented by transverse ribs, a long basal cavity, deeper to the center is asymmetric (Figure 8 i, j).

The fauna associated with the conodonts consists essentially of fragments of sponge spicules, bryozoans and rarely foraminifera, fish teeth and fragments of bivalves (Figure 9) in addition to echinoderms and bryozoans. In thin section fossils characteristic of epicontinental carbonate shelfs are observed and described in FA3.

Interpretation

The presence of conodonts *Ellisonia sp., Neognathodus symmetricus* and *Streptognathodus sp*., suggest a Bashkirian-Moscovian age for the deposits of the epicontinental shelf in the region of Uruará. These species are found in the contact between the Monte Alegre and Itaituba formations, in the basal part of the Itaituba Formation in the region of the Tapajós river (Matsuda 2002, Scomazzon *et al* 2016), as well as in drill core from the southern border of the Amazonas Basin.

The conodonts belonging to the genera *Neognathodus* and *Streptognathodus* were here identified in the carbonates of the shelf system, whereas the genus *Ellisonia*is identified in the rocks the carbonate shelf. *Neognathodus* is typical of normal marine and intertidal/infratidal environments. *Streptognathodus* is a pelagic genus, more characteristic of shelf environments, here represented by the FA3 facies. According to Merrill and von Bitter (1984), conodonts of the genus *Ellisonia*are are characteristic of restricted environments and low salinity. In North America these are found in shallow water biofacies.
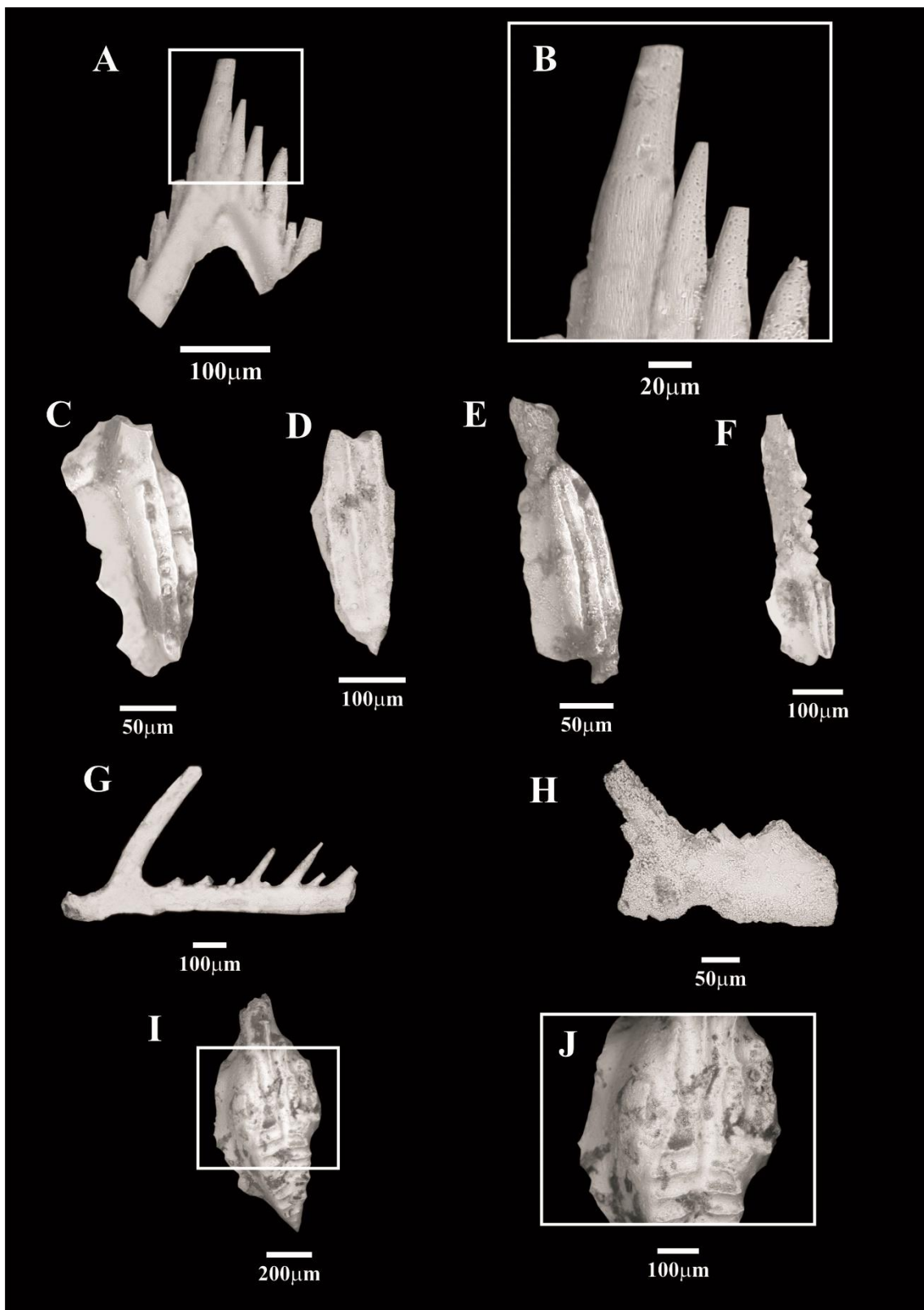
Figure 8- Conodonts identified from the epicontinental carbonate shelf succession of the Itaituba Formation in the region of Uruará. A. G. H - *Ellisonia sp.* B- detail of *Ellisonia sp.* C.D.E.F- *Neognathodus symmetricus.* I- *Streptognathodus sp.* J- detail of *Streptognathodus sp.*
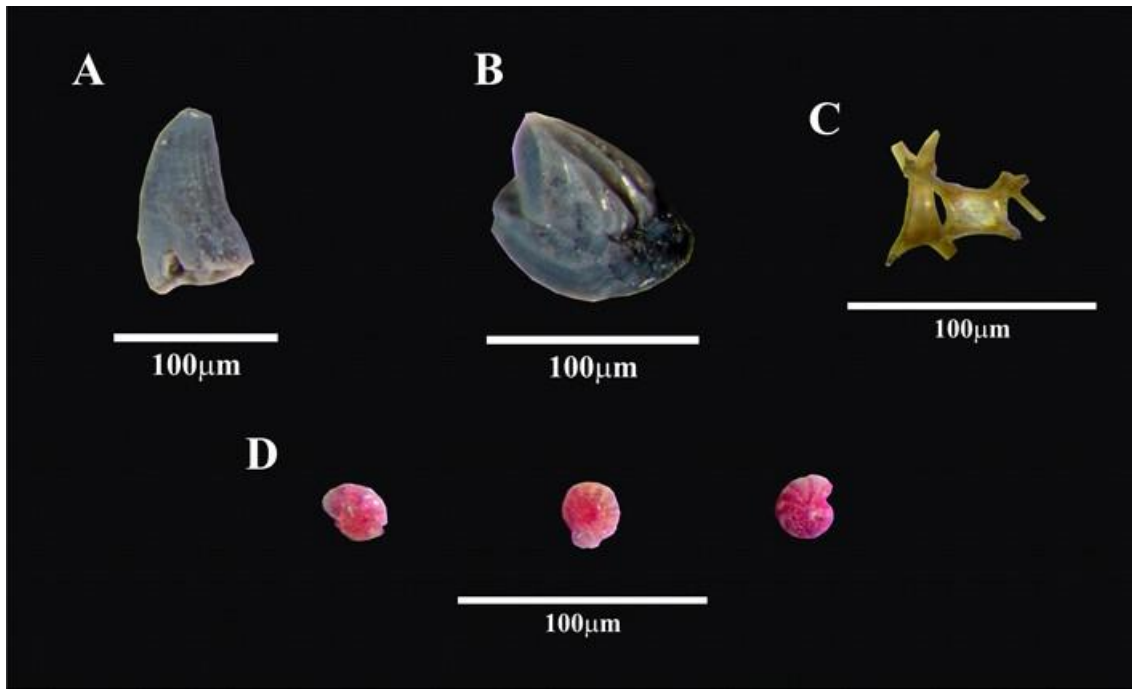
Figure 9- Fauna associated with the conodonts found in the epicontinental shelf of the Itaituba Formation, Uruará region. A- Fragment of a fish tooth. B- Fish scale. C- Sponge spicules. D- Foraminifera.

The occurrence of *Neognathodus*, *Ellisonia and Streptognathodus* togther suggest a deposit typical of a shallow marine environment under conditions of low salinity and moderate energy, as is the case of the upper subtidal and shelf. The fossiliferous assemblage associated with the conodonts suggests the presence of both fixed benthic, vagrant and nektonic organisms, which inhabited the warm shallow waters of the Itaituba Sea (Anelli 1999).

6. DEPOSITIONAL MODEL-DISCUSSION

The depositional model proposed for the area includes the three facies associations: coastal desert, mixed tidal flat and epicontinental carbonate shelf (Figure 10), which occur along the northern and southern margins of the Amazon Basin. The coastal desert system includes an association of dune fields, humid interdunes, sand sheets and fluvial channels (FA1). These aeolian deposits may had covered hundreds of kilometres along the basin wedging out in the direction of the current region of the Gurupá Arch or can have reached the east most regions inland to central Gondwana such as Parnaiba Basin (Caputo 1984, Medeiros *et al.* 2019).

This aeolian sandy plain installed on the margins of epicontinental sea was gradually flooded by an expressive post-glacial transgression and gradually replaced by carbonate shelf deposition. This event was linked to the global sea-level rise after the retreat of the ice cap related to the glacial II stage occurred in the Early Bashkhirian (cf. (Ross and Ross 1987,

Davydov *et al.* 2012). The continuity of marine influence amplified the tidal processes propitiating the installation of extensive tidal flats (FA2) with the interaction of both siliciclastic and carbonate sedimentation (Figure 10). The tidal flats covered an area with predominance of subaerial processes and periodic ebb-flood tides. Tidal channels incised in the plain were the site of tidal delta with siliciclastic deltaic lobe indicating riverine influence. Carbonate precipitation in the more distal settings including lagoon and ponds. The organisms were restricted to the carbonate lagoons and are represented by species that tolerated turbid waters (Harries 2011). These tidal deposits had low amplitude filling reduced accommodation space in the interior shallow sea (Witzke 1987). The tidal action in this epicontinental sea would be much less than compared with a coastal oceanic basin, but its amplification will be directly related to the increase of oceanic connection, in this case, the invasion of the Panthalassa Ocean to west of the Gondwana (Harrington 1962, Lockzy 1966, Ross and Ross 1985, Osleger 1991, Vasconcellos 2000, Matsuda 2002, Almeida and Carneiro 2004, Cunha *et al.* 2007). (Figure 10).

The epicontinental sea had bioclastic bars at its margin that separate the lagoon environment from the marine shelf setting. The lagoon mixed siliciclastic-carbonate sediments grade to bioclast carbonate with terrigenous until exclusively carbonate shelf deposits (FA3) containing abundant Pennsylvanian benthic fossil assemblage (Figure 10). Locally, tidal inlets and tidal channels that sporadically spread the influx of terrigenous material onto the shelf setting. Fine-grained siliciclastics are abundant in all microfacies were provided by eolian inflow on peritidal and shelf settings. It does not discard the storm-generated suspension siliciclastic clouds in shelf environment. In addition, these regular pulses of siliciclastic basinward suggest a basin surrounded by continental mass compatible with epicontinental sea (Figure 10). The Pennsylvanian flooding come from to the Panthalassa Ocean promoted an expressive carbonate record in all sedimentary basins of the Western Gondwana (Figure 11a). The marine carbonate sequences overlying continental deposits similar those found in the Amazonas Basin, can be correlated with the Gondwana coastal basins (current subandean basins) and Acre, Solimões and Parnaíba basins in the West Gondwana (Millani and Thomaz Filho 2000, Cunha 2007, Cunha *et al.* 2007, Vaz *et al.* 2007, Wanderley Filho *et al.* 2007) (Figure 11b and 11 c).

A

PANTHALASSA · SIBÉRIA · laurússia · CHINA · PALEO THETYS · AMÉRICA DO SUL · ÁFRICA · GONDWANA

N

Eolian Coastal

Lockeia · *Palaeophycus*

Thalassinoides

Shallow marine

Fluvial Channel

Sandy sheet

Dune field

B

PANTHALASSA · SIBÉRIA · laurússia · CHINA · PALEO THETYS · AMÉRICA DO SUL · ÁFRICA · GONDWANA

Brachiopds *Bivalves* *Echinoderm* *Gastropods* *Conodonts* *Foraminifers*

Algaes *Corals* *Ostracods* *Bryozoans* *Trilobites* *Fishes*

N

Epicontinental Shelf

Shelf

Bioclastic bar

Brachiopds *Echinoderm* *Foraminifers*

Lagoon

Brachiopds spine *Echinoderm spine*

Mixed Tidal Flat

Intertidal

Supratidal

52

Figure 10- The evolution of the Carboniferous Monte Alegre-Itaituba succession in the Epicontinental Sea of the Western Gondwana. A. The continent was covered by aeolian dune fields with humid interdune zones forming a coastal desert with fluvial channels cut the extensive sand sheets. These aeolian sandy plain installed on the margins of epicontinental sea was gradually flooded in the beginning of the marine transgression with deposition of the first beds of dolostone in ponds and lagoons. B- With the establishment of the Itaituba epicontinental sea the margin was strongly influenced by tidal processes generating widespread mixed tidal flats. Periods of subaerial exposition are indicated by mud cracks and brecciated dolostone layers characteristic of the supratidal zone. Tidal channels carrying siliciclastic sediments flowing over mixed flats in the intertidal zone. These tidal channels flow until lagoons forming tidal deltas. These lagoons initially were the sites of siliciclastic sedimentation deposited from lobes carrying terrigenous grains. The reduction of terrigenous input and the increase of transgressive movement coming from Panthalassa favoured the biological activity with establishment of carbonate fabric and flourishment of benthic assemblage typical of epicontinental carbonate shelfs.
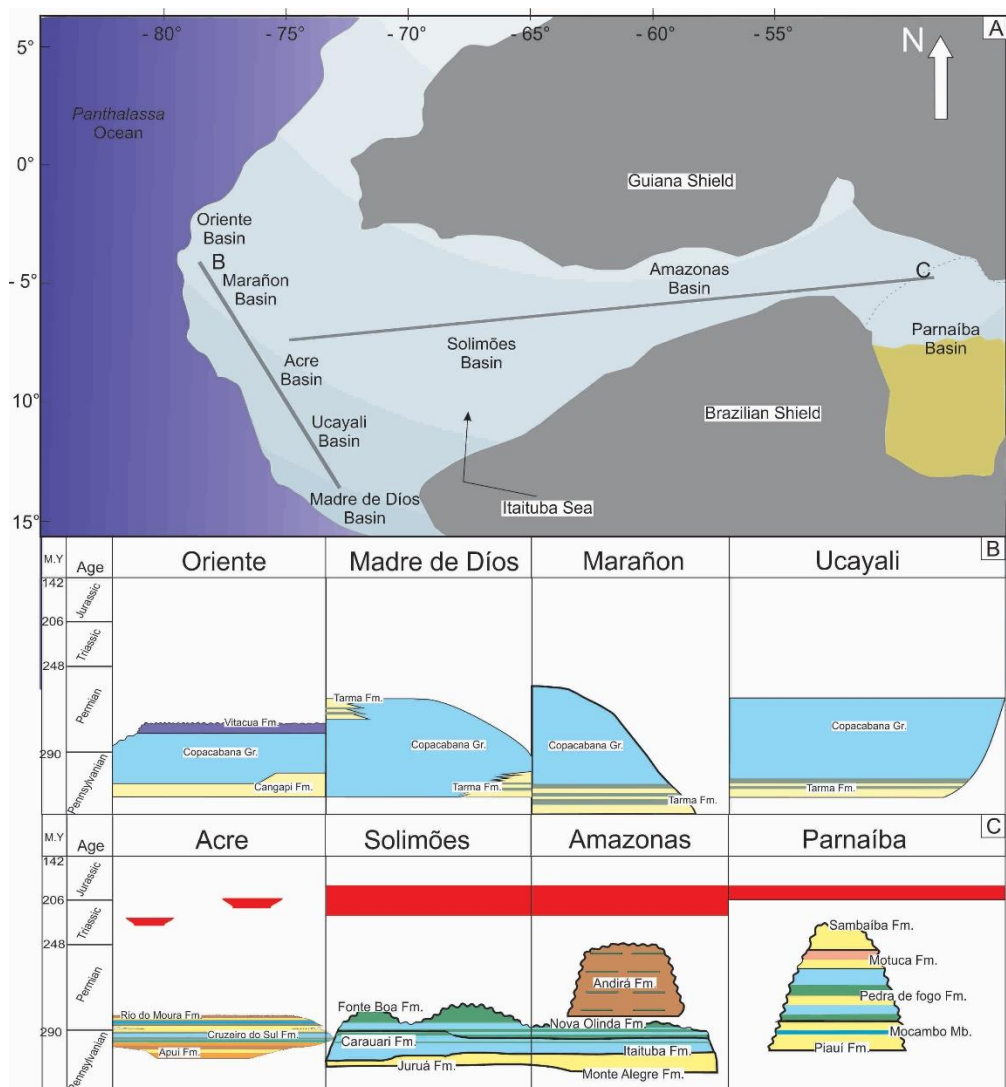
Figure 11- Pennsylvanian paleogeography and sedimentary basins of the Western Gondwana. A- Proposed configuration for the Itaituba epicontinental sea with indications of the cross sections of the basins with units correlated to the Itaituba Formation showed in the figure 11B and C. B- Stratigraphic chart showing the subandean basins with Copacabana Group. C- Stratigraphic chart of Northern Brazilian basins with Cruzeiro do Sul, Carauari and Piauí (Mocambo member) formations. Modified from Millani and Thomaz Filho (2000), Vaz *et al.* (2007), Cunha *et al.* (2007), Wanderley Filho *et al.* (2007), Cunha (2007), Caputo *et al.* (2013), Hurtado *et al* (2019) and Medeiros et al. (2019). Colour of lithologies = yellow, sandstone, orange, conglomerate, blue, limestone, green, evaporite, brown, siltstone, rose, mudstone, purple, dolostone, red, volcanic rocks.

7. CONCLUSIONS

The facies and stratigraphic analysis combined with petrography data and chronostratigraphic framework based on conodont and foraminifera paleontology was possible propose a robust paleoenvironmental and stratigraphic model for the Monte Alegre-Itaituba succession exposed in the Central Amazonas Basin. This model considers data from 34 facies/microfacies and three distinct but interrelated facies associations. The interpreted paleoenvironments were coastal aeolian system (FA1), mixed tidal flat (FA2) and open epicontinental shelf (FA3). The large vertical facies variation since continental to coastal environment grading to marine carbonate shelf define a retrogradational trend that record expressive transgression event occurred in the Amazonas Basin during the Pennsylvanian. This event is attributed to the interglacial period after the retreat of ice caps, reflecting a post-glacial transgression.

The age of the Monte Alegre-Itaituba succession is considered as Bashkirian-Moscovian based on the occurrence of the conodont species *Neognathodus symmetricus, Streptognathodus sp. e Ellisonia sp*. which form a biozone correlated worldwide. *Neognathodus* is a genus typical of neritic environments, whereas *Streptognathodus*is is a pelagic genus, corroborating the proximity and connection to the shallow shelf settings interpreted to the Monte Alegre-Itaituba succession. In the same way, the genus *Ellisonia* is associated with shallow environments with low salinity. This leads us to consider the carbonate shelf deposits described here as marine, of low salinity and moderate energy with a fossiliferous assemblage of fixed benthic, vagrant, and nektonic organism representatives of an epicontinental sea implanted in the Wester Gondwana during Pennsylvanian. The Monte Alegre-Itaituba siliciclastic-carbonate succession can be correlated with the Gondwana coastal basins and Acre, Solimões and Parnaíba basins in the West Gondwana. Ongoing stratigraphic studies in the Amazon Basin to the same detail of those reported here for the Monte Alegre-Itaituba succession will hopefully give a more complete picture of the epicontinental sea sedimentary record of the Western Gondwana during Late Mississippian to Early Pennsylvanian.

Acknowledgements

This work is part of the PhD dissertation of the first author with technical support of the PPGG (Programa de Pós -Graduação em Geologia e Geoquímica) of the University Federal of Para (UFPA). We thank to CNPq (National Council for Scientific and Technological Development) and the CAPES (Coordination for the Improvement of Higher Education Personnel; financial code 001) as the funding agency of Brazil to the concession of fellowship research to the first author. This work had finnancial support by the research projects "Rochas calcárias da Bacia do Amazonas e Plataforma Bragantina: Avaliação de áreas potenciais para insumos agrícolas do Estado do Pará, regiões de Santarém-Uruará e do Salgado" (ICCAF: 111/2014 FAPESPA) coordinated by Afonso Nogueira, and "Estudo das ocorrências de minerais industriais–carbonatos, fosfatos e evaporitos – na região de Santarém–Itaituba (PA), Carbonífero da Bacia do Amazonas" (MCT/CT -Mineral/ CNPq N 44/2010) coordinated by Moacir Macambira.

CAPÍTULO 4 DIAGÊNESE DOS ARENITOS E CARBONATOS DA SUCESSÃO MARINHA MISTA CARBONÁTICA–SILICICLÁSTICA DO PENSILVANIANO DA BACIA DO AMAZONAS

Pedro Augusto S. Silva[1]; Afonso C. Rodrigues Nogueira[1]; Joelson Lima Soares[1]; José Bandeira[1]; Isabele Barros Souza[1]

[1]Programa de Pós-Graduação em Geologia e Geoquímica - PPGG, Instituto de Geociências, Universidade Federal do Pará – UFPA, Rua Augusto Corrêa, s/n, CEP 66075-110, Belém, Pará, Brasil (pedrogeologia8@hotmail.com ; anogueira@ufpa.br; jlsoares@ufpa.br; jotabandeira@gmail.com; isabelebarros7@gmail.com)

Resumo

Rochas siliciclásticas e carbonáticas são os principais litotipos encontrados nas unidades Pensilvanianas da Bacia do Amazonas, estas rochas correspondem as formações Monte Alegre e Itaituba, interpretadas como um sistema desértico costeiro a plataformal, associados a pulsos transgressivos do Carbonífero. Os arenitos são intensamente afetados por processos diagenéticos, tais como: compactação física, porosidade, cimentação de calcita equigranular, cimentação de sílica, dolomitização, piritização formação de óxidos e hidróxidos de ferro e a alteração mineral. Enquanto que a diagênese observada nas rochas carbonáticas compreende os processos de micritização, nemorfismo, compactação física, porosidade, cimento de calcita fibrosa, cimento de calcita em bladed, cimento de calcita equigranular, cimento de calcita espática, cimento de sílica, a dolomitização, piritização, compactação química e silicificação. Tanto os arenitos quanto os carbonatos mostram eventos diagenéticos associados a diagênese a processos rasos e precoces ocorridos logo após o soterramento dos sedimentos. A porosidade dos arenitos da Formação Monte Alegre varia de 0% a 20%, são representados por poros intergranulares e móldicos Enquanto que os arenitos da Formação Itaituba variam de 0% a 11%, com poros intergranulares, móldicos, agigantados e intragranulares . A redução da porosidade é observada na passagem da Formação Monte Alegre, dominada por uma sedimentação eólica, para a Formação Itaituba, com uma sedimentação carbonática-mista, em que os arenitos se restringem aos ambientes de maré. Para os carbonatos a porosidade diferencia-se de 0% a 5% e são compostos por interpartícula, *vug,* móldico, fratura, intercristal e intracristal. Os poros carbonáticos encontram-se parcialmente a totalmente preenchidos por cimento. O predomínio dos processos eodiagenéticos fazem com que os carbonatos das duas unidades apresentem uma baixa porosidade e permeabilidade, o que contrasta diretamente com a ampla porosidade observada nos arenitos, esta mudança está diretamente relacionada a sedimentação carbonática e a característica e possivelmente com uma característica de selante que a Formação Itaituba apresenta.

Palavras-chave: Diagênese de arenitos e carbonatos; Processos Eodiagenéticos; Pensilvaniano, Bacia do Amazonas

1. INTRODUÇÃO

Os processos diagenéticos influem de forma diferente de acordo com o tipo de rocha, a temperatura e a profundidade, gerando diferentes tipos de texturas e feições características (Boggs Jr. 2006). Dentre estas principais feições, destacam–se os processos de geração e redução de porosidade que sãos os responsáveis diretos por tornar uma unidade porosa e permeável para a acumulação de petróleo e gás, ou mesmo tornar a unidade selante, que confina e impede a migração do óleo. Estes processos são de fundamental importância na determinação de sistemas petrolíferos exploráveis, como o caso do sistema petrolífero Barreirinha–Itaituba registrado na bacia do Amazonas (Millani e Zálan 1999).

O sistema petrolífero Barreirinhas–Nova Olinda é constituído pela Formação Barreirinhas, de idade Devoniana e interpretada como a rocha geradora do óleo encontrado na bacia, com valor de COT de 11% (Millani e Zálan 1999). A rocha reservatório seria os arenitos eólicos da Formação Monte Alegre, que em sua porção basal alcançaria valores de porosidade da ordem de 22% e de permeabilidade de 1400md. A rocha selante seria os carbonatos e evaporitos da Formação Nova Olinda com migração por falhas e trapas anticlinais. Apesar disso muito se especula sobre o papel da Formação Itaituba e também da porção de topo da Formação Monte Alegre, já que as camadas de carbonatos e evaporitos da Formação Itaituba também poderiam funcionar como selantes para o sistema petrolífero. (Millani e Zálan 1999)

Por meio deste trabalho procurou–se investigar os processos diagenéticos atuantes nas porções de topo da Formação Monte Alegre e base da Formação Itaituba, nas regiões de Monte Alegre, Uruará, Itaituba e Aveiro (figura 1b, c e d), com o objetivo de interpretar os processos inibidores e geradores de porosidade.

2. GEOLOGIA REGIONAL

A bacia intracratônica do Amazonas localizada no Norte do Brasil (Figura 1a), engloba os estados do Pará e Amazonas. É limitada a Norte pelo Escudo das Guianas, a Sul pelo Escudo Brasileiro, a Leste pelo Arco de Gurupá e a Oeste pelo Arco de Purus (Cunha *et al.* 1994). Possui uma área de cerca de 500.000 Km^2 com uma pilha sedimentar e vulcano–sedimentar de 6 km de profundidade em seu depocentro. O preenchimento sedimentar é composto por duas sequências de primeira de ordem, a Paleozoica e a Mesozoica–Cenozoica. A sequência Paleozoica é dividida em quatro sequências de segunda ordem: Ordovício–Devoniana, Devoniana–Tournasiana, Neoviseana e Pensilvaniano–Permiano (Cunha *et al.* 2007). A sequência Pensilvaniana–Permiana é responsável pela deposição das unidades estudas, as formações Monte Alegre e Itaituba, que juntamente com as formações Nova Olinda e Andirá correspondem ao Grupo Tapajós, que representa a variação completa de um ciclo transgressivo–regressivo (Matsuda *et al.* 2004).

A Formação Monte Alegre é interpretada como um ambiente eólico com campos de dunas, áreas de interdunas e extensos lençóis de areia eventualmente cortados por canais de *wadi* (Matsuda 2002, Lima 2010) de idade Bashkiriana (Moutinho *et al.* 2016b, Scomazzon *et al.* 2016). O contato entre o topo da Formação Monte Alegre e porção basal da Formação Itaituba as unidades é gradacional com a intercalação de dolomitos e arenitos e o predomínio de carbonatos fossilífero para o topo da sucessão. A Formação Itaituba é interpretada como uma sucessão carbonática corresponde a depósitos de planície de maré mista e plataforma carbonática (Matsuda 2002; Lima 2010, Silva *et al.* 2015) com fósseis de invertebrados marinhos bentônicos (Moutinho *et al.* 2016a). A idade com base em conodontes e foraminíferos posicionam a unidade no intervalo Bashikiriano–Moscoviano (Scomazzon *et al.* 2016, Moutinho *et al.* 2016b).
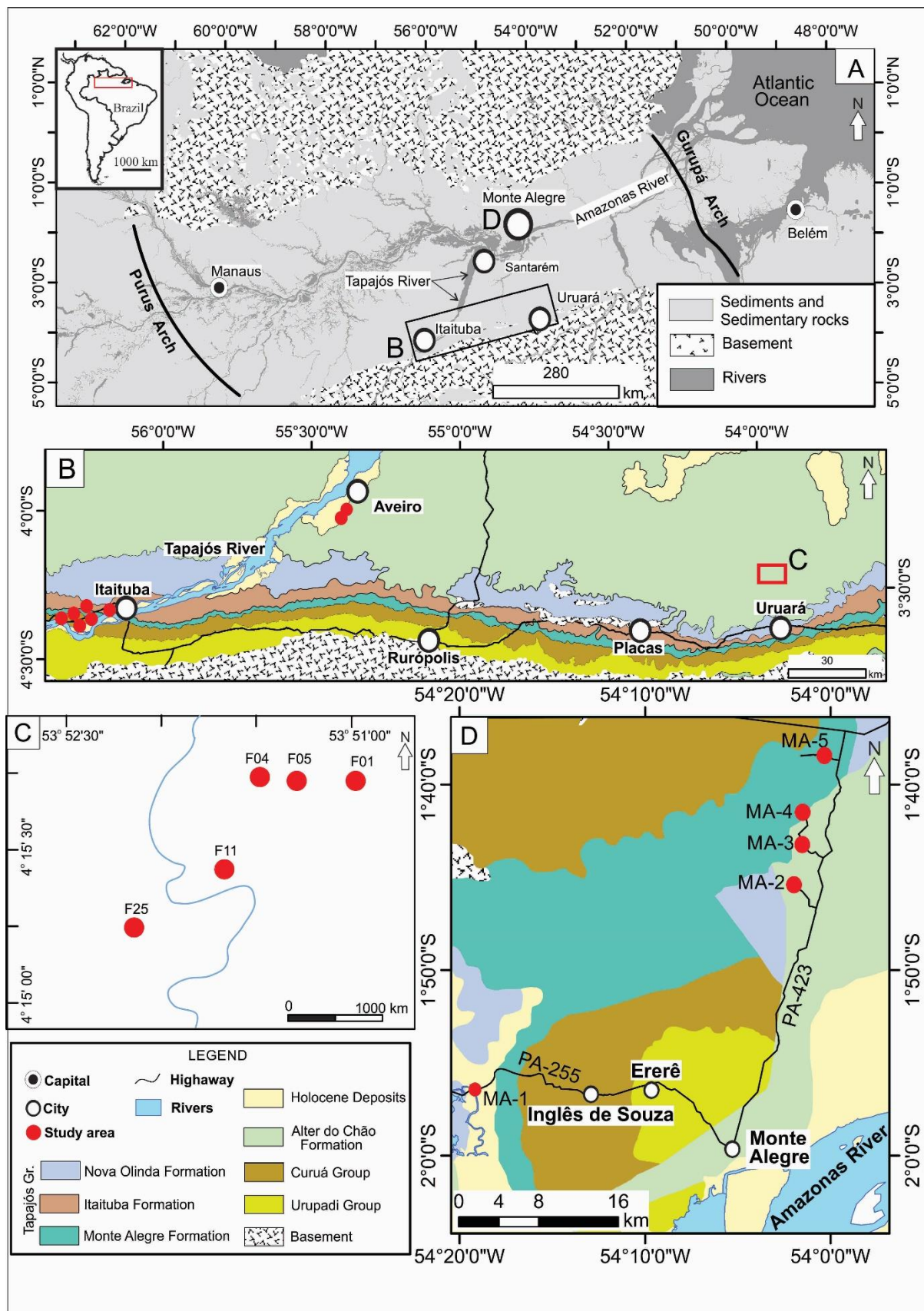
Figura 1- Mapa de Localização dos perfis estratigráficos estudados. A– As três áreas de estudos, nos municípios de Monte Alegre, Itaituba e Uruará. B– Afloramentos das formações Monte Alegre e Itaituba a beira do Rio Tapajós, além de testemunho de sondagem da região de Aveiro, borda Sul da bacia. C– Testemunhos de sondagem da Formação Itaituba, região de Uruará, borda Sul da bacia. D– Afloramentos e pedreiras das duas unidades, região de Monte Alegre, borda Norte da bacia do Amazonas.

3. METODOLOGIA

As análises diagenética foram realizadas em 228 amostras de arenitos e carbonatos, de afloramentos e testemunhos de sondagem das três regiões estudadas (figura 1), onde 20 amostras correspondem a arenitos, 9 da Formação Monte Alegre e 11 da Formação Itaituba, e 200 amostras de carbonatos. Sendo 12 da Formação Monte Alegre e o restante da Formação Itaituba, as demais amostras são representadas por siltitos e margas da Formação Itaituba.

As técnicas analíticas empregadas foram a descrição de lâminas delgadas, microscopia eletrônica de varredura (MEV), espectroscopia por energia dispersa (EDS) e catodoluminescência. A análise petrográfica semiquantitativa consistiu na contagem de 300 pontos em lâminas delgadas com espaçamento de 1mm. As rochas com conteúdo carbonático foram tingidas com Alizarina vermelho S para a distinção mineralógica entre calcita e dolomita, além do tingimento de ferrocianeto de potássio para distinção de calcita ferrosa e calcita não ferrosa (Dickson 1966). As rochas carbonáticas foram classificadas conforme Dunham (1962) e Embry e Klovan (1971), enquanto que as rochas siliciclásticas seguiram a proposta de Folk (1974). A análise mineralógica por MEV/EDS foi realizada no equipamento modelo LEO 1430, sendo as condições de análise para as imagens de elétrons secundários: corrente do feixe de elétron=90 μA, voltagem de aceleração constante=20kv e a distância de trabalho 10 mm.

A análise de catodoluminescência indicou informações das diferentes fases minerais que afetaram a porosidade inicial das rochas carbonáticas, bem como a sua condição de formação, permitindo individualizar as diferentes gerações e composições do cimento. As imagens foram feitas em lâminas delgadas polidas, submetidas à luminescência gerada pelo impacto de elétrons energéticos, revelando as estruturas que são invisíveis à luz natural branca ou polarizada. O equipamento é composto de microscópio ótico Leica modelo DM 4500 P LED acoplado ao aparelho Optical cathodoluminescence CL 8200 MK5-2. As amostras de carbonato foram submetidas as condições de kv variando de 11,2 a 15,0 e o tempo de exposição variando de 9 segundos a 28 segundos.

4. SUCESSÃO MISTA CARBONÁTICA-SILICICLÁSTICA

O paleoambiente foi determinado através da análise de fácies/microfácies sedimentares propostos no capítulo 2, interpretados como três grandes associações de fácies: deserto costeiro, planície de maré e plataforma epicontinental (figura 2).

4.1 Eólico costeiro

Esta associação de fácies é encontrada em perfis na região de Monte Alegre, Itaituba e em um testemunho em Aveiro. Compõem um complexo sistema composto por arenitos com estratificação cruzada acanalada de médio porte, arenitos com estratificação plano paralela, arenitos com estratificação cruzada de baixo ângulo, arenito com estratificação cruzada tangencial, arenitos maciços, arenito/pelito com laminação cruzada cavalgante, dolomitos maciços e bioturbados. Todas essas fácies são agrupadas em uma associação composta de um campo de dunas eólico, lençol de areia, interdunas, canal fluvial e porção costeira carbonática.

4.2 Planície de maré mista

A planície de maré mista é encontrada em todas as regiões estudadas e são constituídas por: dolomito maciço, dolomito com terrígenos, arenito maciço, brecha dolomítica, conglomerado maciço, dolomito silicificado com terrígenos, arenito com estratificação cruzada *wavy*, arenito com bandamento de maré, arenito com estratificação cruzada acanalada, arenito com estratificação cruzada *swash*, siltito com laminação cruzada, arenito com estratificação cruzada sigmoidal, marga com laminação cruzada cavalgante, arenito com laminação cruzada cavalgante, *mudstone* maciço, siltito maciço, folhelho maciço, *wackestone* com terrígenos, *mudstone* maciço e *floatstone* com braquiópodes. Todas estas fácies/microfácies representam uma intricada interação de supramaré, canais de maré, delta de maré, laguna siliciclástica e laguna carbonática.

4.3 Plataforma epicontinental

A plataforma carbonática epicontinental é composta predominantemente por microfácies carbonáticas, como: *grainstone* bioclástico oolítico, *grainstone* bioclástico com terrígenos, *wackestone* bioclático, *wackestone* bioclástico com terrígenos, *packstone* bioclástico com terrígenos, *mudstone* bioclástico e *mudstone* maciço, além de arenito carbonático com laminação cruzada e marga com laminação cruzada. Estas fácies e microfácies compõem um sistema de barras bioclásticas que grada para a plataforma carbonática epicontinental colonizada por uma assembleia de organismos marinhos, tais como: algas, braquiópodes, bivalves, briozoários, corais, equinodermas, foraminíferos, gastrópodes, ostracodes e trilobitas.

5. DIAGÊNESE

Nota–se que em diferentes ambientes ocorrem os mesmos processos diagenéticos, evidenciando que a diagênese não depende diretamente do processo sedimentar de deposição, e sim das condições de soterramento, pressão, temperatura, tipo de rocha e a ação de diferentes fluidos nas rochas (James e Choquette 1990, Worden e Burlen 2003). Baseado nas descrições petrográficas pôde–se identificar os principais processos diagenéticos encontradas para os arenitos: compactação física, cimentação, dolomitização, piritização, alteração de grãos e geração e redução de porosidade. Os principais processos diagenéticos encontrados nos carbonatos são: micritização, cimentação, dolomitização, compactação química, silicificação dos bioclastos, piritização, alteração de grãos e redução de porosidade.

5.1 Diagênese dos Arenitos

A diagênese dos arenitos foi observada nos depósitos de rochas característicos das associações de fácies de deserto costeiro e da associação de planície de maré mista, de forma geral os arenitos variam em granulometria de muito fina a média, com grãos angulosos a arredondados e moderadamente selecionados a bem selecionados. Quanto aos processos diagenéticos, são observadas a compactação física, cimentação, dolomitização, piritização, a porosidade e alteração de grãos.

5.1.1. Compactação Física

A única evidência de compactação física nos arenitos inclui a deformação de grãos dúcteis, tais como as micas (figura 3b). As micas podem alcançar até 250 μm e apresentam-se contorcidas ou levemente curvadas. Este processo pode ocorrer nos estágios de eodiagênese e no limite com a mesodiagênese. Em ambos o processo de deformação dos grãos dúcteis se dá pela pressão litoestática exercida nos grãos, a grande pilha sedimentar faz com que grãos mais susceptíveis a pressão, como as micas, deforme-se mostrando feições recurvadas e contorcidas (Boggs Jr. 2006).
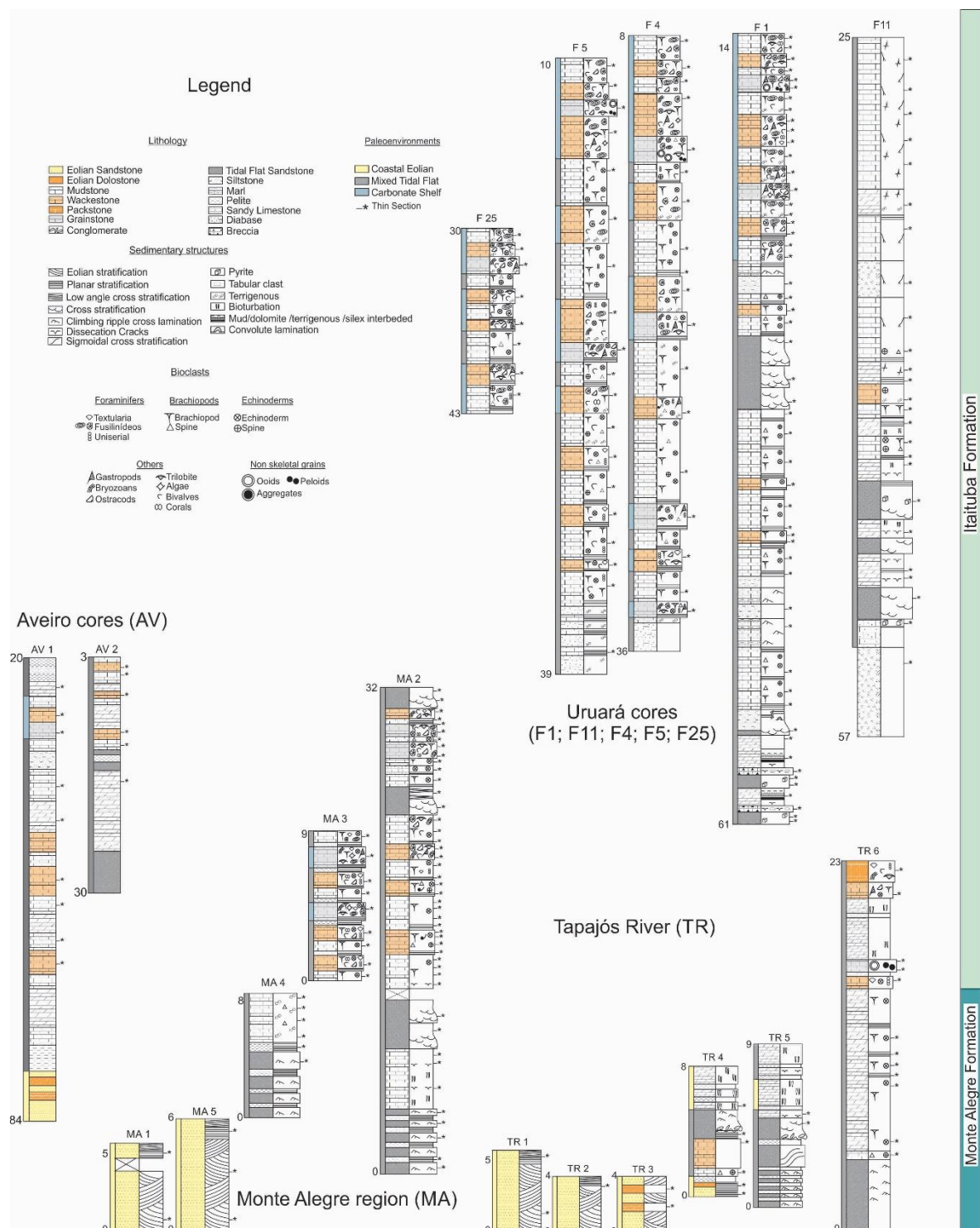
Figura 2- Perfis estratigráficos de afloramentos e pedreiras das localidades de Monte Alegre e Itaituba (Rio Tapajós), além dos testemunhos de sondagem de Aveiro e Uruará. Foram agrupadas 34 fácies, distribuídas em 18 perfis estratigráficos representativos dos paleoambientes desértico costeiro, planície de maré mista e plataforma carbonática epicontinental.

5.1.2. Cimentação

Os principais tipos de cimentos encontrados nos arenitos são de sílica, calcita e óxido/hidróxido de ferro que preenchem poros ou fraturas. O cimento de sílica ocorre na forma de sobrecrescimento sintaxial em grãos detríticos de quartzo monocristalino, podendo ser

observados pela linha de sujeira ou contatos retos de compromisso (Figura 3c). Sílica também ocorre, localmente, preenchendo fraturas. Este tipo de cimento, quando associado a depósitos eólicos, pode ter como fonte de sílica a poeira derivada da abrasão de grãos (Sharma 1965, Waugh 1970). Contudo, a ausência de evidências de compactação química nas rochas estudadas não descarta a possibilidade da fonte de sílica provir de dissolução por pressão de grãos de quartzo (Tucker 1992, McBride 1989).

A cimentação carbonática é bastante comum nos arenitos de planície de maré mista e ocorre preenchendo poros e fraturas. Este cimento é composto por cristais de calcita que se dispõe em formas equigranulares com textura poiquilotópica, englobando grãos de quartzo, feldspato e plagioclásio. No contato com o cimento de calcita intersticial os grãos de quartzo exibem as bordas corroídas (figura 3d e 3e). A origem da cimentação carbonática nestes arenitos pode estar relacionada a reações orgânicas como a redução bacteriana de sulfatos e a oxidação que tendem a aumentar a concentração de CO_2 causando primeiramente dissolução. Enquanto que a precipitação só pode ocorrer devido a oxidação ou a redução de sulfato, gerando uma reação que consume o íon H^+ conduzindo a formação de pirita e a concentração de bicarbonato nos poros e dependendo da concentração dos íons pode formar dolomita ou mesmo calcita magnesiana (Curtis e Coleman 1986, Tucker 1992, Morad 1998).

O cimento de óxido-hidróxido de ferro é caracterizado por formar envelopes muito finos ao redor dos grãos (figura 3f). A gênese deste cimento está relacionada provavelmente a processos eodiagenéticos aditivos, representada pelas películas muito finas de óxidos e hidróxidos de ferro no contato entre os grãos e a telodiagênese alterando grãos de minerais opacos, formando óxidos e hidróxidos de ferro associados à cimentação e disseminados no arcabouço da rocha.

5.1.3. Dolomitização

A dolomitização nos arenitos é característica da associação de fácies deserto costeiro, onde os campos de dunas se intercalam com as microfácies dolomíticas marinhas bioturbadas. As dolomitas substituem o arcabouço dos arenitos parcialmente, onde ainda consegue-se distinguir os grãos e o acamamento cruzado dos estratos (figura 3g). De forma geral as dolomitas variam de muito finas a finas (acima de 4 μm), apresentam formas romboedrais, subédricas a anédricas, aspecto sujo ("*dirty cloud*") e por vezes exibem alta cor de interferência. No contato com os grãos terrígenos é possível discernir as bordas corroídas (figura 3h).
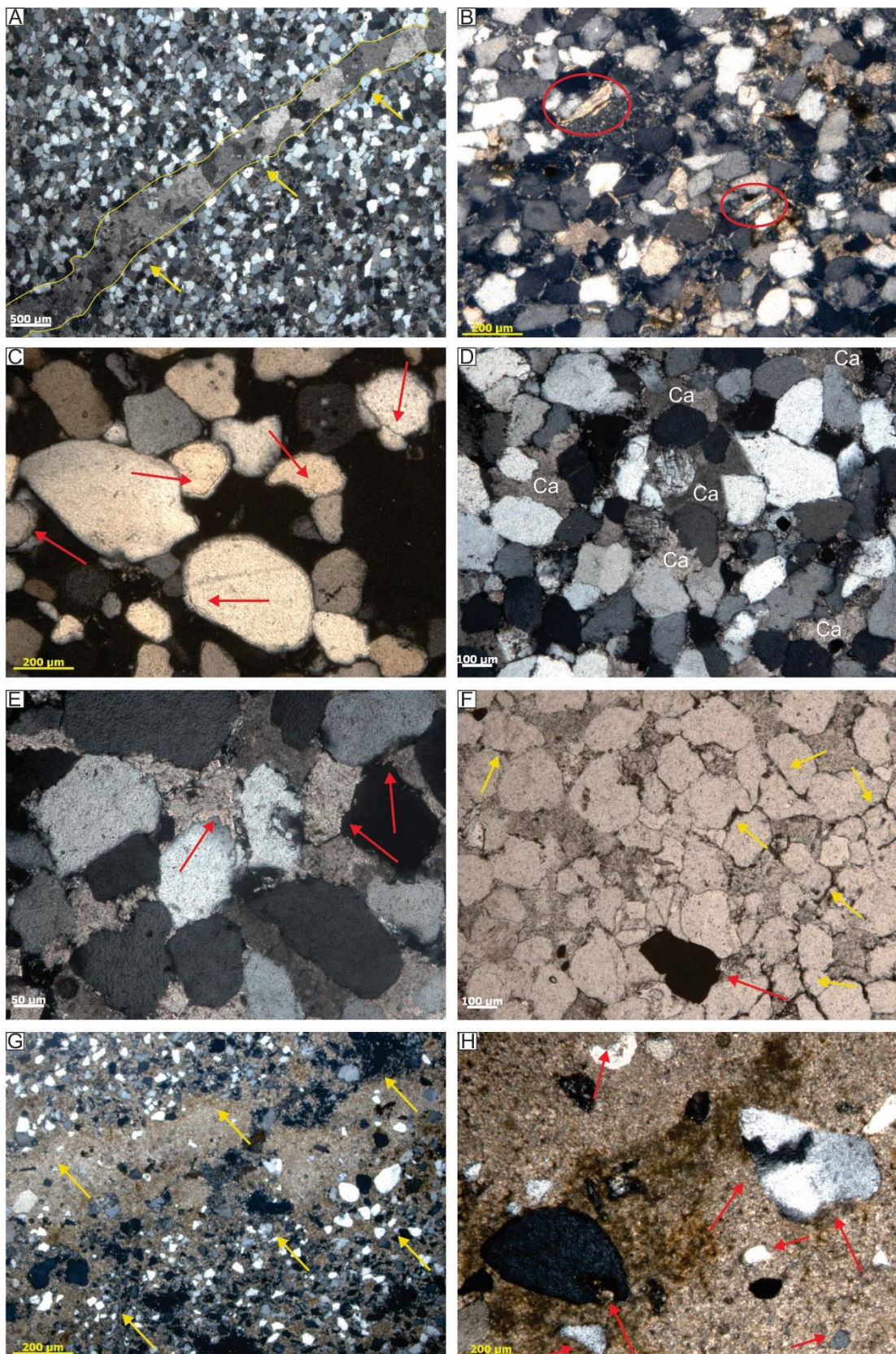
Figura 3- fotomicrografia das feições diagenéticas encontradas nos arenitos. A-fratura preenchida por cimento de calcita. B- mica detrítica deformada com extinção ondulante (círculos vermelhos). C-sobrecrescimento sintaxial de sílica (setas). D- cimento de Calcita (Ca). E- borda de grão terrígeno corroída pela ação do cimento calcítico. F- cimento de óxido e hidróxido de ferro (setas amarelas) e pirita alterada (seta vermelha). G- arenito dolomitizado, mostrando a direção da estratificação (setas amarelas). H- bordas dos grãos terrígenos corroídas pela dolomitização.

O processo de dolomitização foi observado principalmente no contato dos arenitos da Formação Monte Alegre e dos dolomitos da Formação Itaituba. O contato com os arenitos eólicos e porosos faz com que os fluidos contidos nos dolomitos da Formação Itaituba percolem pelos poros do arenito e precipite na forma de dolomita, o continuo processo acaba por substituir parcialmente o arcabouço da rocha. Este processo provavelmente se deu ainda na eodiagênese, onde os carbonatos inicialmente compostos por calcita ou aragonita foram dolomitizados pela mistura de águas meteóricas e marinhas (Morad *et al* 1992) provavelmente em ambiente com alta evaporação (Warren 2000).

5.1.4. Porosidade

Nos arenitos a porosidade é composta por poros intergranular, móldico, agigantado e raros poros intragranulares (figura 4 a, b, c). Nota-se que na Formação Monte Alegre os arenitos variam em porosidade de 0% a 20% enquanto que a porosidade nos arenitos da Formação Itaituba varia de 0% a 11%.

Os poros da Formação Monte Alegre são representados por poros intergranulares possuem diminutos tamanhos, da ordem de poucas micras até 50 µm. Os poros móldicos alcançam até 450 µm de tamanho, apresentam formas que lembram o formato de um grão detrítico. Os poros agigantados são raros, ocorrendo apenas nas fácies de planície de maré, com forma irregular e tamanhos alcançando até 600 µm.

A porosidade nos arenitos da Formação Itaituba é composta por poros intergranulares, móldicos, agigantados e intragranulares. Os poros intergranulares correspondem a maioria dos poros da unidade, são encontrados nas fácies de canais de maré e quanto ao tamanho variam de 16 µm a 100 µm. Os poros móldicos mostram formas irregulares subangulosas e alcançam até 125 µm de tamanho. Os poros intragranulares são raros e correspondem a dissolução parcial de grãos terrígenos de feldspatos, não ultrapassam 20 µm.

As unidades exibem distinções quanto a quantidade e os tipos de poros, a Formação Monte Alegre evidencia uma maior variedade e quantidade de poros, encontrados em sua maioria nas fácies de campo de dunas e lençóis de areia, apesar disso nas fácies em contato com as porções dolomíticas apresentam o menor conteúdo de poros chegando até zero, com isso constata-se que os processos de dolomitização e de cimentação inibem a preservação dos poros.

A Formação Itaituba ostenta uma menor quantidade de poros nos arenitos, concentrando-se nas fácies de canais de maré, essa diminuição se dá provavelmente devido a

precipitação de diferentes tipos de cimento como os de calcita, sílica, óxidos e hidróxidos de ferro, além da presença de lama nas fácies arenito com estratificação cruzada *wavy* e arenito com bandamento de maré.

5.1.5. Alteração mineral

É observado nos grãos de plagioclásio e feldspato pequenos minerais placóides, com extinção reta picotada correspondentes a argilominerais (figura 4d), há também a alteração dos minerais opacos para óxidos e hidróxidos de ferro, que se precipitam sob a forma de cimentos e disseminam-se pela rocha, dando um aspecto "sujo" a rocha (figura 3f). Ambos os processos pertencem a telodiagênese, quando as rochas são expostas à superfície. No primeiro caso a modificação mineral se dá por reações de hidrólise e já no segundo caso reações de oxidação derivadas de águas meteóricas dissolvem os minerais opacos precipitando-os na forma de cimento ou disseminado na rocha (Berner 1983, Boggs Jr. 2006).
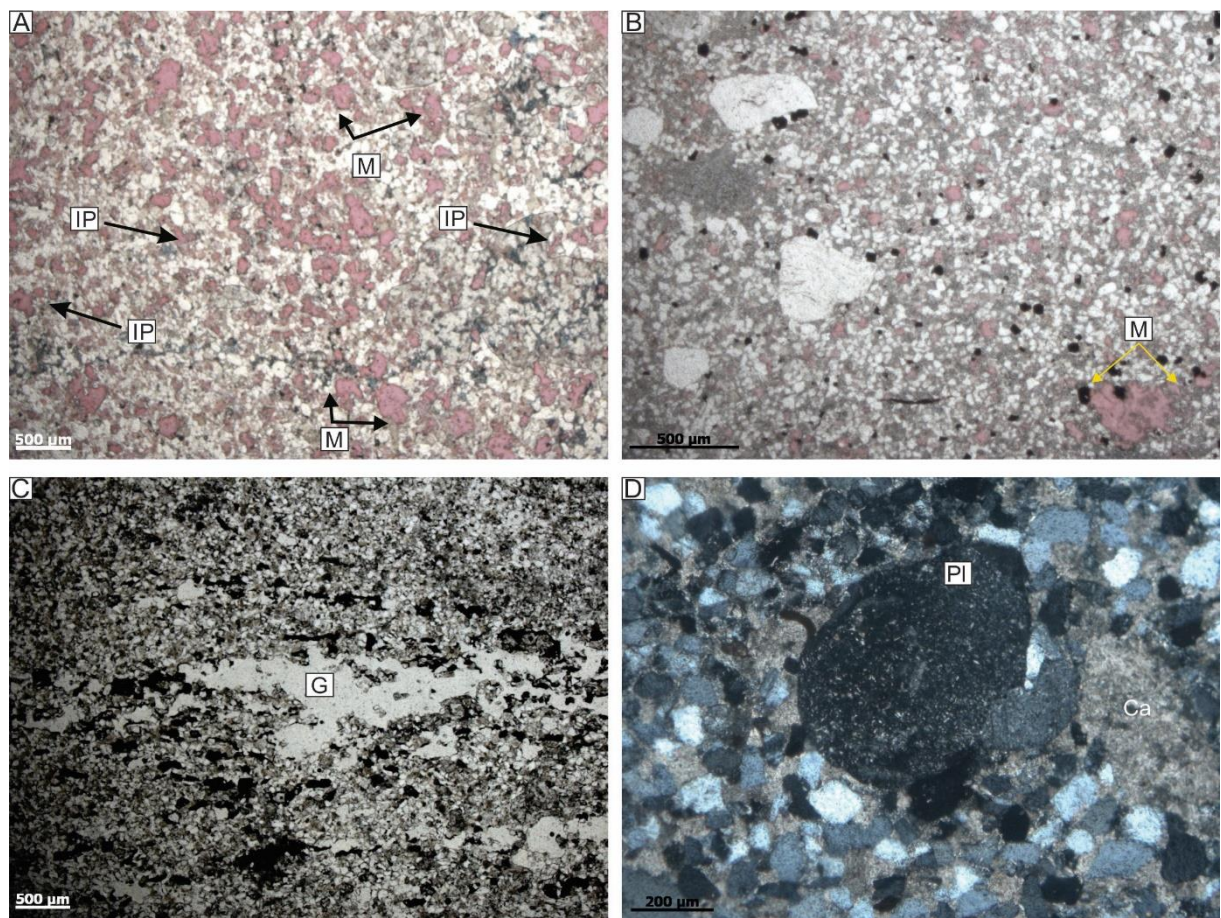
Figura 4- Poros nos arenitos das formações Monte Alegre e Itaituba. A- poros intergranulares nos arenitos das fácies de campo de dunas (IP) e poros móldicos (M). B- poro móldico nas fácies de canais de maré (M). C- poro agigantado (G) nas fácies de canais de maré. D- alteração para argilominerais em grão de plagioclásio (Pl).

5.2. Diagênese dos Carbonatos

A diagênese nos carbonatos envolve os processos de micritização, neomorfismo, compactação física, porosidade, cimentação, dolomitização, compactação química, precipitação de Pirita, formação de óxido/hidróxido de ferro e silicificação.

5.2.1. Micritização

Formam um envelope de coloração marrom escura ao redor das carapaças dos bioclastos de algas, braquiópodes, bivalves, equinodermas, gastrópodes, trilobitas e ostracodes (figura 5 a) e ocorre nas microfácies de *wackestones* e *grainstones*. A micritização é resultado da ação de bactérias e fungos endolíticos que perfuram as carapaças dos bioclastos resultando em um denso envelope micrítico na parte externa da carapaça dos fósseis (Bathurst 1971; Tucker & Wright 1990). Este processo é característico de eodiagênese indicando deposição na zona fótica, associando este processo a uma batimetria de até 200 m (Tucker 1992).

5.2.2. Neomorfismo

Este processo é registrado nas microfácies *wackestone* com terrígenos e, *lime mudstone* maciço correspondentes a planície de maré mista, além de *lime mudstone* maciço e *lime mudstone* bioclástico de plataforma epicontinental. Ocorrem tanto na matriz micrítca quanto substituindo bioclasto de bivalve. No primeiro caso os cristais são subeudrais a euedrais, exibem aspecto límpido esbranquiçado, composição calcítica não ferrosa e os cristais apresentam granulação fina a média (figura 5c). No segundo caso, cristais de calcita substituem bioclastos de bivalve (figura 5b), estes cristais são irregulares, variam em granulação de finos a médios, aspecto límpido e alta cor de interferência. O neomorfismo da matriz está diretamente associado a eodiagênese e representa um aumento no tamanho dos cristais da matriz micrítica, ambos possuem a composição calcítica, sua gênese está relacionada a reações em estado sólido por fluidos meteóricos ou mesmo marinhos. Já a substituição em carapaças de bivalves é oriunda da ação de fluidos eodiagenéticos que dissolvem parcialmente a carapaça de bioclasto, fazendo com que o fluido infiltre e percole, precipitando a calcita com granulação maior (Boggs Jr. 2006, Tucker 1992).

5.2.3. Compactação Física

Este processo inicia-se no estágio eodiagenético e envolve a redução da porosidade inicial (Athy 1930, Boggs Jr. 1992), são representadas por falhas e fraturas nas microfácies *mudstone* maciço e dolomito silicificado com terrígenos, ambas de planície de maré. As fraturas são escassas, irregulares, alcançam até 300 μm e são descontínuas, geralmente encontram-se preenchidas por calcita. As microfalhas são encontradas apenas na microfácies dolomito silicificado com terrígenos, são descontinuas e deslocam as camadas associadas a está fácies. Ambos os processos estão relacionados a compactação física eodiagenética, onde a pilha sedimentar gera pressão suficiente para o rompimento na forma de fraturas e o deslocamento na forma de microfalhas.
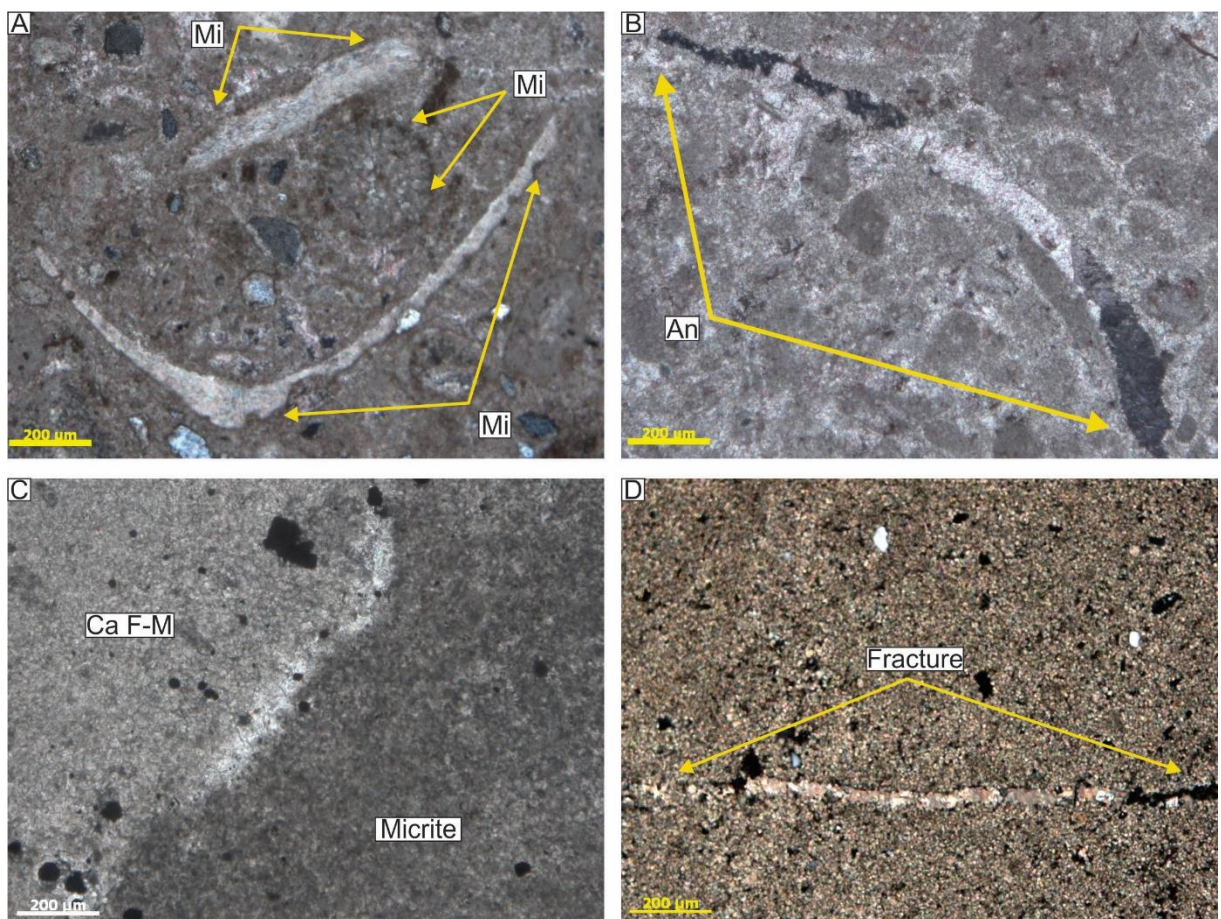
Figura 5- fotomicrografias das feições diagenéticas de micirtização, neomorfismo e compactação física dos carbonatos da Formação Itaituba. A- micritização (Mi) nas carapaças de bioclastos nas microfácies *lime mudstone* maciço de plataforma epicontinental. B- neomorfismo agradacional em carapaça de biválvio nas microfácies *wackestone* bioclástico com terrígenos de plataforma epicontinental. C- neomorfismo na matriz de microfácies de planície de maré, onde a matriz micrítica (micrite) passa a calcita de granulação fina a média (Ca F-M). D- fratura (seta amarela) associada a compactação física com posterior precipitação de cimentos de calcita nas bordas.

5.2.4. Cimentação

A cimentação é um dos principais processos responsáveis pela perda de porosidade em rochas carbonáticas, tomando o espaço poroso com fluido supersaturado na fase mineral (Bathurst 1971, Tucker & Wright 1990, Tucker 1992). Os cimentos ocorrem em praticamente todas as microfácies exceção à algumas de plataforma epicontinental, como *packstone* bioclástico com terrígeno e *wackestone* bioclástico. O cimento possui composição calcítica, preenche poros do tipo *vug,* fraturas (figura 6 a e 6 b), interpartículas, intercristais e mólidicos. Quanto à forma os cimentos são equigranulares (figura 6 c), espáticos (figura 6 f), fibras aciculares (figura 6 d), *bladed* (figura 6 e) e sobrecrescimento sintaxial em equinodermas (figura 6 g). Além dos cimentos calcíticos foram observado a precipitação de dolomita (figura 6 h) e de sílica (figura 6 f).

Observa-se na fase de cimentação calcítica até quatro gerações de cimentos carbonáticos, a primeira é formada por cristais muito finos a finos que bordejam os poros sob formas fibrosas de provável composição aragonítica, estas fibras são anisópacas, com extinção ondulante, comprimento de até 140 μm e espessura menor que 5μm. Esta geração de cimento se forma em eodiagênese e é representada pela substituição de aragonita por calcita não ferrosa. A segunda geração de cimento corresponde ao cimento equigranular, no qual seus cristais apresentam granulação fina a média, com formas subeudrais a euedrais, aspecto límpido, alta cor de interferência e por vezes direção de clivagem preservada, sua procedência é na eodiagênese formada pela percolação de fluidos ricos em calcita não ferrosa em zona marinha vadosa.

A terceira geração de cimento calcítico é constituída por cimento *bladed* que possui extinção ondulante, cristais de granulação média a grossa, com espessura máxima de até 50 μm e comprimento de até 80 μm e sua gênese é a direta precipitação de calcita magnesiana em zonas marinhas rasas. A quarta geração de cimentação é observada pelos cimentos de calcita espática e de sobrecrescimento sintaxial em equinodermas. O cimento espático apresenta granulação média a grossa, aspecto límpido esbranquiçado, extinção ondulante, alta cor de interferência e até duas direções de clivagem nítidas. A precipitação deste cimento é comum em zonas marinhas freáticas pela direta precipitação de cimento calcítico não ferroso. Já o sobrecrescimento sintaxial de calcita em equinodermas ocorre nos bioclastos das fácies de *grainstone* bioclástico oolítico e *grainstone* bioclático com terrígenos da associação de plataforma. Os cristais deste cimento mostram granulação média a por vezes grossas, extinção

ondulante e alta cor de interferência. É formado em zonas marinhas vadosas a freáticas também relacionadas a diagênese em baixa subsuperfície rasa.

As dolomitas são amarronzadas com granulações finas a grossas, extinções ondulantes e a cor de interferência é cinza de baixa ordem, além disso os cristais são recurvados nas bordas apresentando a textura em "sela" característica (figura 6 h). O processo de geração destas dolomitas compreende o soterramento profundo em mesodiagênese com temperaturas de pelo menos 60°C e pressões suficientes para causar singelas deformações nas arestas dos cristais (Morrow 1982, Gawthorpe 1987, Warren 2000, Scholle & Scholle 2003, Flügel 2004). A coloração amarronzada das dolomitas é típica de sua associação com ferro de origem mesodiagenética ou mesmo com a interação com possíveis atividades hidrotermais (Barale *et al.* 2013). A cimentação por sílica ocorre juntamente com a cimentação por calcita espática, o quartzo possui cristais subeudrais a anedrais, baixa cor de interferência amarela a laranja, extinção ondulante e se concentra na borda dos poros preenchidos. Sua origem pode estar relacionada com a influência hidrotermal do Diabásio Penatecaua na área de estudo.

5.2.5. Dolomitização

Este processo ocorre nas associações de fácies de deserto costeiro e de planície de maré. Em geral, quando substitui a matriz corrói a borda dos grãos de quartzo terrígenos ou mesmo forma frentes de dolomitização como ocorre na microfácies *lime mudstone* maciço. Os cristais de dolomita em geral são muito finos a finos (figura 7 a), apresentam aspecto límpido, cristais são xenotópicos e possuem extinção ondulante quando nítido. Já as dolomitas em selas, possuem granulações grossas, textura hipidiotópica, extinção ondulante, textura *"dirty cloud"*, pelo menos uma direção de clivagem e as bordas recurvadas.

A formação da Dolomita necessita de pelo menos três fatores essenciais, a fonte de magnésio, um mecanismo para mover os volumes de fluidos e a redução termodinâmica para conter as inibições à precipitação do mineral (Morrow 1990b, Tucker 1992, Warren 2000). Na área de estudo as dolomitas de deserto costeiro e de planície de maré mista podem ser explicadas pelo refluxo de percolação (*seepage reflux*) e o modelo de águas mistas (*mixing water model* ou *Dorag model*) (Tucker 1992).
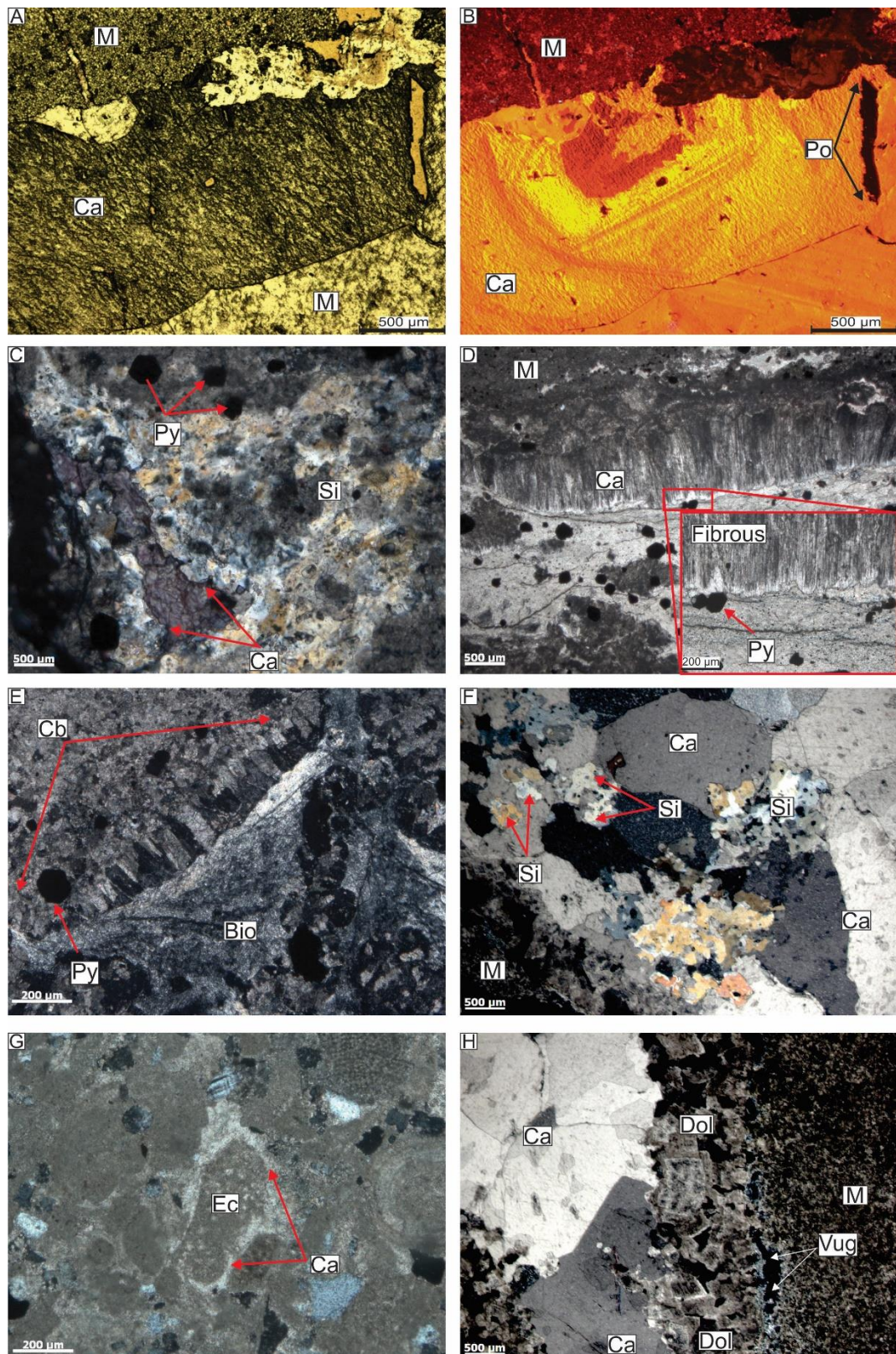
Figura 6- fotomicrografia dos cimentos encontrados nas associações de fácies da área de estudo A- cimento de calcita (Ca) espática preenchendo a matriz (M) fraturada. B- catodoluminescência em cimento calcítco espático mostrando as duas gerações preenchendo a fratura (1º amarela e a 2º vermelha). C- cimentação equigranular de calcita (Ca) com cimentação de sílica (Si) e pirita disseminada (Py). D- cimentação de calcita fibrosa, em detalhe as fibras em matriz calcítica com cristais de pirita (Py). E- cimento de calcite em *bladed* (Cb) em bioclasto calcitizado (Bio) com piritas disseminadas na matriz (Py). F- cimentação residual de sílica em fratura preenchida por calcita espática (Ca). G- cimento de sobrecrescimento sintaxial de calcita em equinoderma. H- dolomita em sela (dol) em contato com a cimentação de calcita espática em matriz calcitica com poros em *vug*.

O primeiro modelo explica a precipitação de dolomita nas microfácies dolomito silicificado com terrígenos, características de supramaré/intermaré, onde as dolomitas possuem uma granulação de muito fina a média, localmente formando lâminas contínuas, intercaladas com sílica microcristalina, esta sílica microcristalina está diretamente associada aos processos de evaporação (Matsuda 2002). Nas demais microfácies de deserto costeiro as dolomitas podem estar associadas à zona mista, com mistura de águas meteóricas e marinhas, diretamente ligada ao modelo de Dorag que se baseia no comportamento não linear das curvas de solubilidade quando soluções com concentrações diferentes de eletrólitos são misturadas (Warren 2000). Outro tipo de dolomita encontrado na área de estudo é a dolomita em sela, que se restringem a forma de cimentos que se dispõe de granulações médias a grossas, de coloração amarronzada com as bordas curvas pelos processos mesodiagenéticos de soterramento (Qing e Mountjoy 1994, Warren 2000).

5.2.6. Compactação Química

A compactação química corresponde a ação da dissolução por pressão nos carbonatos gerando *dissolutions seams* e estilólitos (figura 7 b e figura 7 c). Estas feições são características de soterramento em mesodiagênese (Flügel 2004). Os *dissolution seams* ocorrem nas fácies lagunares carbonáticas, onde são subparalelos, descontínuos e impregnados por óxidos e hidróxidos de ferro (figura 7 b). Os estilólitos são vistos tanto macroscopicamente quanto em lâminas, formam superfícies serrilhadas preenchidas por óxidos/hidróxidos de ferro, quartzo e argilas e por vezes podem formar feições nodulares (figura 7 d).

A compactação química é oriunda da dissolução por pressão causada pela carga sedimentar e em alguns casos pelo estresse tectônico (Flügel 2004), no caso da área de estudo o principal causador é a própria pilha sedimentar, onde os processos de dissolução se dão como resultado do estresse de compressão dentro dos limites partícula a partícula, resultando na dissolução ou subcotação (Rutter 1983, Tada e Siever 1989).

5.2.7. Piritização

As piritas correspondem a cristais hexagonais, apresentando formas subeudrais a euedrais, com tamanhos de até 300 µm (figura 7 e), apresentam-se disseminadas nas rochas e são encontradas em carbonatos, arenitos e até folhelhos da associação de fácies de planície de

maré mista, além de observadas na petrografia as análises de EDS confirmam a presença de cristais dispersos na matriz calcitíca (figura 7 f). A pirita se forma em ambientes com bastante conteúdo de matéria orgânica e sulfatos, como em estuários e planícies de maré. Pode se dispor de forma cúbica disseminada ou mesmo substituindo bioclastos (Fisher 1986, Tucker 1992). Os sedimentos calcários quando não se apresentam em contato com camadas argilosas ou siltosas, não possuem uma proporção adequada de íons de ferro fazendo com que a formação de pirita seja ausente ou escassa. Apesar de ter uma alta concentração de matéria orgânica e abundante H_2S, se o sedimento dominante é $CaCO_3$, a precipitação de pirita é baixa (Berner 1983, Berner & Raiswell 1984).

Constata-se que as piritas encontradas na área de estudo podem estar relacionadas a duas prováveis origens: a primeira relaciona-se a acumulação de matéria orgânica em lagunas siliciclásticas e também carbonáticas, onde este conteúdo pode advir de um influxo continental, ou mesmo, associado a proliferação de organismos invertebrados nas porções carbonáticas de planície de maré mista. Outra situação observada corresponde ao contato das camadas de carbonato com a fácies siltito maciço avermelhado, que forneceria H_2S e Fe^{+2} em uma zona euxínica lagunar, onde bactérias são envolvidas na redução de sulfato (sulfobactérias) para sulfetos e o Fe^{3+} oriundo de óxidos/hidróxidos, é reduzido para Fe^{2+} (Fisher 1986, Berner 1983).

5.2.8. Silicificação

A silicificação encontrada na área de estudo aparece substituindo a matriz nas microfácies de planície de maré mista (figura 7 g) e substituindo os bioclastos nas fácies lagunares (figura 7 h). A sílica que substituí a matriz é composta por microquartzo e escassa quantidade de calcedônia que alcançam até 60 µm de tamanho. Já a sílica encontrada nos bioclastos de braquiópodes e alguns bioclastos de equinodermas é composta por quartzo autigênico, com faces subeudrais a euedrais e extinção ondulante.

O processo de silicificação é característico de mesodiagênese (Tucker 1992), onde a sílica microcristalina ou autigênica substitui a matriz e os bioclastos mais susceptíveis a essa ocorrência, como é o caso dos braquiópodes e dos equinodermas. A substituição da matriz pode estar relacionada a substituição da dolomita por microquartzo ou mesmo por possíveis evaporitos associados a dolomita (Hesse 1990). Apesar disso, nota-se que a precipitação da sílica inibe o crescimento da dolomita, que apresenta seus cristais parcialmente dissolvidos pela sílica, semelhante ao descrito por Dietrich *et al.* (1963). A sílica autigênica que substitui os bioclastos origina-se de soluções que se precipitam por filmes finos nas carapaças de

organismo, fazendo com que a sílica dissolva o carbonato e se precipite (Maliva & Siever 1988). A provável origem da sílica está relacionada à dissolução de quartzo detrítico durante a redução de sulfatos para a posterior precipitação.

5.2.9. Porosidade

A porosidade dos carbonatos da área de estudo varia de 0% a 5% sendo compostos por poros interpartícula, *vug,* móldicos, fratura, intercristal e intracristal. Em sua maior parte, os poros estão preenchidos por cimento, não apresentam uma interconexão e configuram baixa permeabilidade.

Os poros interpartículas variam de 60 µm a 180 µm de tamanho, sem interconexão, ocorrem normalmente nas fácies de planície de maré mista. Os poros *vugs* ocorrem nas fácies de planície de maré mista e em plataforma carbonática, encontram-se parcialmente preenchidos por cimento, são vistos em formas macroscópicas de até 2 cm (figura 8 a) e vistos em lâmina também (figura 8 g e 6 h).

Os poros móldicos, variam em tamanho de 20 µm a 100 µm, e sua distribuição é homogênea (figura 8 b e 8 d), apresentam formas de grãos do arcabouço. Os poros de fratura variam de 200 µm a 5000 µm, encontram-se parcialmente ou totalmente preenchidos por calcita espática de granulação média (figura 8 c). Os poros intercristal alcançam até 50 µm, são heterogêneos, apresentam-se de forma caótica disseminados nas rochas. A porosidade intracristalina é rara e ocorre apenas em cristais de pirita, em raros cristais de clacita da matriz neomorfisada, sua forma é angulosa e apresentam até 60 µm.

A baixa porosidade dos carbonatos da Formação Itaituba pode estar diretamente relacionada a precipitação de carbonatos com grande conteúdo de matriz e aos diferentes processos de cimentação que limitam a ocorrência da porosidade nesta unidade. Até mesmo quando processos de dissolução associados tanto a compactação física e química, responsáveis por gerar poros, são observados, há precipitação de cimento preenchendo parcialmente ou totalmente esses poros.
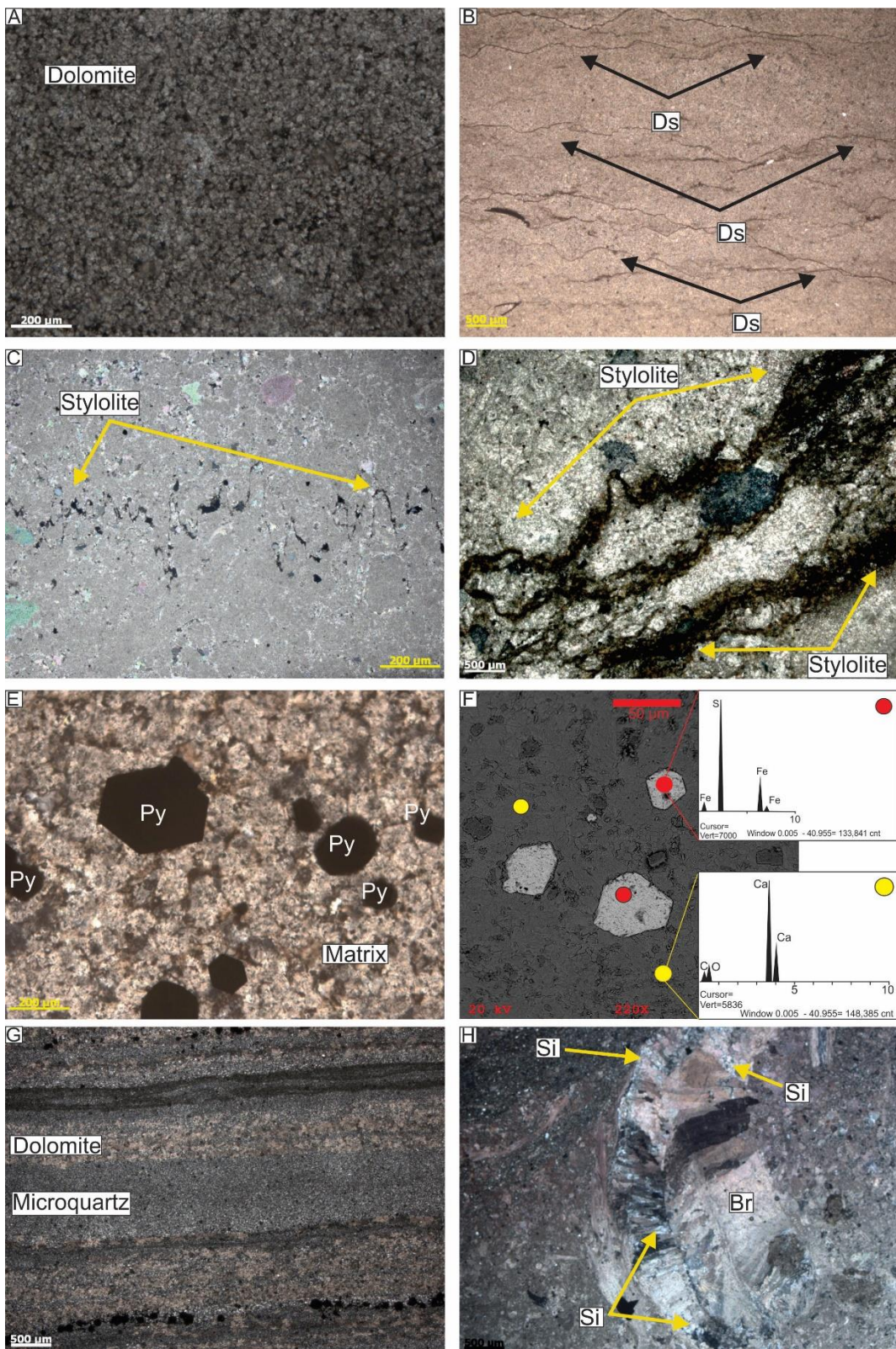
Figura 7- Fotomicrografias dos processos diagenéticos de dolomitização, compactação química, formação de piritas e silicificação. A- dolomitização total do arcabouço nas microfácies dolomíticas de planície de maré mista. B- feições de *dissolution seams* subparalelas a paralelas em matriz carbonática das fácies lagunares. C- estilólito irregular nas microfácies de plataforma carbonática. D- estilólitos irregulares formando pseudolaminações com textura nodular. E- cristais de pirita em matriz calcita nas microfácies de planície de maré. F- análise de MEV-EDS em matriz carbonática lagunar, revelando cristais de pirita menores que 50 µm com forma subeudral. G- silicificação parcial da matriz dolomítica em microfácies de planície de maré mista. H- bioclasto de braquiópodes (Br) parcialmente silicificado por quartzo autigênico (Si).

6. DISCUSSÕES E INTERPRETAÇÕES

Os processos diagenéticos nos arenitos e carbonatos das formações Monte Alegre e Itaituba causaram modificações mineralógicas, geração e redução de porosidade e a precipitação de novos minerais no arcabouço. Com isso é observado que grande parte dos processos diagenéticos atuantes na área de estudo possuem características de ambiente eodiagenético, enquanto que a ocorrência de ambientes diagenéticos mais profundas fica restrito a dissolução e compactação. Para isso uma sequência de eventos diagenética é proposta tanto dos arenitos quanto dos carbonatos de ambas as unidades (tabela 1). Os arenitos em eodiagênese referem-se a diagênese rasa em subsuperfície, é representada pelos processos de compactação física, cimentação, dolomitização e porosidade. Estes processos são responsáveis pela redução inicial da porosidade logo após o começo do soterramento.
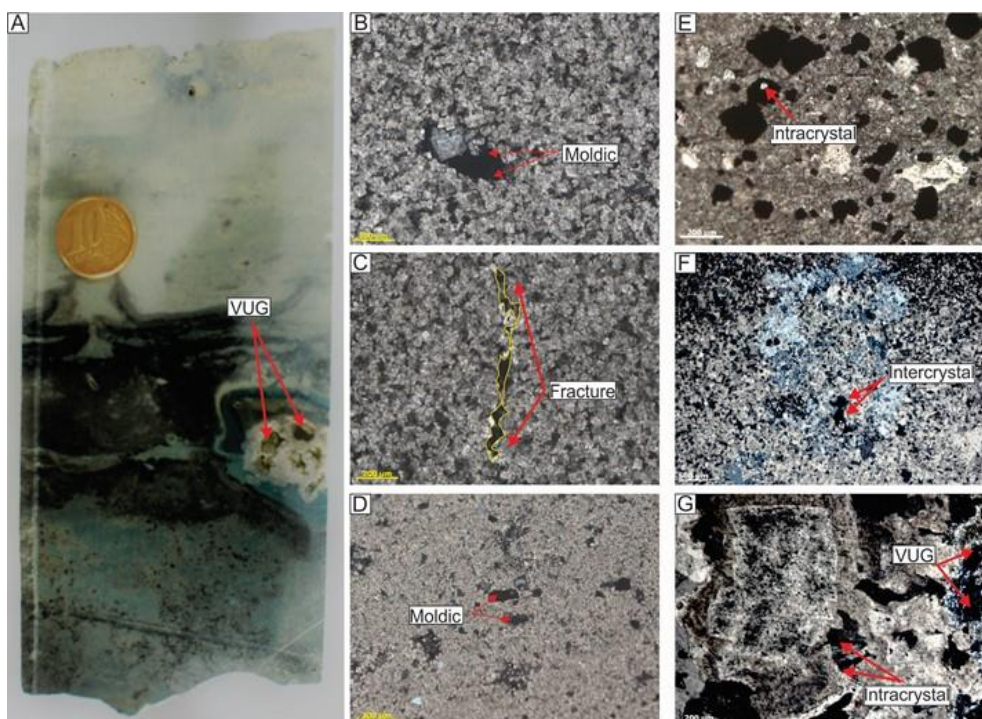
Figura 8- Porosidade nos carbonatos das formações Monte Alegre e Itaituba. A- poros macroscópicos do tipo *vug* em testemunhos de sondagem da Formação Itaituba. B- poros móldicos em matriz dolomíticas naas microfácies de deserto costeiro. C- porosidade em fratura, parcialmente preenchida por cimento calcítico espático, encontrada em dolomitos da microfácies de planície de maré mista. D- poros móldicos em grãos de terrígenos em matriz calcítica, das fácies de planície de maré mista. E- poros intracristalinos em cristais de piritas das fácies carbonáticas de laguna. F- poros intercristal das microfácies de planície de maré mista, onde a matriz encontra-se parcialmente silicificada mas com preservação do poro. G- porosidade em *vug* e intracristal nas fácies dolomíticas de planície de maré associadas a dolomitas e dolomitas em sela.

Neste ambiente diagenético é observado reações típicas da ação de diagênese rasa, com processos meteóricos e marinhos como a dissolução dos grãos instáveis e reações de redução bacteriana para gerar as fontes da cimentação calcítica, apesar de serem processos caracterizados como redutores da porosidade inicial, nota-se que os arenitos são os mais porosos

da área de estudo com até 20% na Formação Monte Alegre e no máximo 11% na Formação Itaituba. Os processos de cimentação por óxido hidróxido de ferro, calcita equigranular, cimentação por sílica e a dolomitização fazem com que a porosidade observada na Formação Monte Alegre, seja bastante reduzida quando comparada com os arenitos da Formação Itaituba. A precipitação de piritas evidencia reações redutoras de sulfato e da maturação da matéria orgânica em ambientes de planície de maré. A precipitação de óxidos e hidróxidos de ferro juntamente com a alteração mineral se forma em telodiagênese a partir da exposição da rocha aos processos intempéricos. O ambiente de soterramento é observado nos arenitos pelas reações de dissolução por pressão dos grãos devido aos contatos côncavo-convexos dos grãos quartzos derivados da maior pressão e temperatura.

A sequência de eventos diagenéticos nos carbonatos revela assim como nos arenitos um predomínio dos processos eodiagenéticos, sendo representados pela micritização, neomorfismo, compactação física, porosidade, cimentos de calcita fibrosa, de calcita *bladed,* de calcita equigranular e calcita espática, além da piritização e dolomitização, enquanto que os processos mesodiagenéticos detectados são compostos por precipitação de dolomita em sela, compactação química e silicificação, sendo que a telodiagênese se restringe a óxidos e hidróxidos de ferro disseminados na rocha. Percebe-se que nos carbonatos a geração de porosidade se restringe as zonas de eodiagênese, com porcentagens que variam de 0% a 5%, apesar disso valores que variam de 0% a 2% são observados nos carbonatos afetados pela mesodiagênese representados pela dissolução por pressão e formação de porosidade secundária. Assim como nos arenitos os carbonatos apresentam uma gama de cimentação que impede o maior desenvolvimento de porosidade e da permeabilidade.

Rochas	Rochas	EVENTOS	EODIAGÊNESE	MESODIAGÊNESE	TELODIAGÊNESE
AF1	Arenitos	Compactação Física	---------- ----------		
		Porosidade	------------		
		Cimentação de Calcita equigranular	--------------		
		Cimentação de Sílica	------------------		
		Dolomitização	---------------		
		Piritização	------------------		
		Óxidos e Hidróxidos de Fe			------------------
		Alteração Mineral			--------------------
AF2 e AF3	Carbonatos	Micritização	--------------		
		Neomorfismo	---------------		
		Compactação física	---------------		
		Porosidade	---------------- --------------		
		Cimentação de Calcita fibrosa	---------------------		
		Cimentação de Calcita *bladed*	------------------------		
		Cimentação de Calcita equigranular	---------------------------		
		Cimentação de Calcita espática	--------------------------------------		
		Cimentação de Sílica		-------------	
		Dolomitização	---------------	-----------------------	
		Compactação química		--------------------	
		Piritização	------------------		
		Silicificação		------------------------	
		Óxidos e Hidróxidos de Fe			-------------------

Tabela 1- Sequência de eventos diagenéticos para os arenitos e carbonatos das formações Monte Alegre e Itaituba com seus respectivos processos e seus ambientes diagenéticos como a eodiagênese, a mesodiagênese e a telodiagênese.

Figueiras e Truckenbrodt (1987), Matsuda (2002) e Lima (2010) apontam também que os processos eodiagenéticos foram dominantes nas microfácies estudadas tanto em afloramentos quanto em testemunhos de sondagem da calha central da bacia e da região de Aveiro. Nota-se que a diagênese de soterramento foi restrita a formação de piritas, a uma segunda geração de dolomitização e a fluoritização (Figueiras 1983). Lima (2010) em análises de afloramentos na região de Monte Alegre descreve uma média de até 4% dos carbonatos da Formação Itaituba enquanto que Matsuda (2002) encontra até cerca de 6% de porosidade em *vug,* apesar de notar algumas diferenças nas sequências de eventos diagenéticos destes autores, pode-se concluir que a efetiva diagênese na área de estudo se concentra no ambiente eodiagenético apresentando influências tanto marinhas quanto meteóricas.

7. CONCLUSÃO

A análise dos dados diagenéticos revelou que os arenitos das formações Monte Alegre e Itaituba foram submetidos aos processos de compactação física, porosidade, cimentação de calcita equigranular, cimentação de sílica, dolomitização, piritização, formação de óxidos e hidróxidos de ferro e a alteração mineral. Esta sequência de eventos diagenéticos associa a diagênese a processos rasos e precoces ocorridos logo após o soterramento dos sedimentos. Os processos mesodiagenéticos se restringem apenas aos contatos côncavo-convexos dos grãos nos arenitos.

Assim como os arenitos, os carbonatos das duas unidades apresentam uma sequência de eventos com predomínio de eodiagênese. Estes processos correspondem a micritização, nemorfismo, compactação física, porosidade, cimento de calcita fibrosa, cimento de calcita em *bladed*, cimento de calcita equigranular, cimento de calcita espática, cimento de sílica, a dolomitização e a piritização. Os processos mesodiagenéticos são associados a compactação química e a silicificação. Esta sequência de eventos diagenéticos e ampla precipitação de cimentos, fazem com que os carbonatos das duas unidades apresentem uma baixa porosidade e permeabilidade corroborando com o descrito por Matsuda (2002) e Millani e Zálan (1999), que associam essa baixa porosidade e permeabilidade, a ampla precipitação de carbonatos, sem a ocorrência dos processos de dissolução, a uma provável rocha selante. Estes dados dão suporte ao observado nos valores de isótopos de C e O, indicando que houve pouca alteração diagenética, significando que o sinal isotópico de δ^{13} C é primário.

Agradecimentos

CAPÍTULO 5 DEPOSITIONAL CONTROLS ON MIXED SILICICLASTIC-CARBONATE CYCLES IN THE LATE MISSISSIPIAN-PENNSYLVANIAN EPICONTINENTAL SEA DEPOSITS OF THE WESTERN GONDWANA

Pedro Augusto Santos da Silva[1], Afonso César Rodrigues Nogueira[1], José Bandeira[1], Gulherme Rafaelli Romero[1] Lucieth Cruz Vieira[2]

[1]Programa de Pós-Graduação em Geologia e Geoquímica - PPGG, Instituto de Geociências, Universidade Federal do Pará – UFPA, Rua Augusto Corrêa, s/n, 66075-110, Belém, Pará, Brazil (pedrogeologia8@hotmail.com; anogueira@ufpa.br; jotabandeira@gmail.com; graffaeli@gmail.com)

[2]Laboratório de Estudos Geocronológicos, Geodinâmicos e Ambientais, Universidade de Brasilia, Instituto de Geociências, Asa Norte, 70910-900, Brasília, Distrito Federal, Brazil (lucieth@gmail.com).

Abstract

Mixed-carbonate-siliciclastic systems organized in centimeter to meter-scale cycles form the main pattern to recognize the factors controlling deposition in Paleozoic carbonate shelf in the Gondwana. This cyclicity trend is examined here in detail using core and outcrop-based facies and stratigraphic analysis of 50 m-thick Pennsylvanian mixed-carbonate-siliciclastic succession. This succession includes coastal desertic, tidal flat and marine shelf deposits called here of Itaituba epicontinental sea record, exposed in the central portion of the Amazonas Basin, Brazil. The primary carbonate accumulation was induced by microbial, algae activity and euphotic-controlled benthic organisms. Five types of shallowing upward cycles are described: I) alternance of dolostone and sandstone; II) interbedded of sandstone-mudstone and sandstone-lime mudstone-floatstone rhythmites; III) dolostone interbedded with sandstone; IV) rhythmite formed by wackestone/lime mudstone couplets; and V) consist of asymmetric cycles ABC formed by alternance of grainstone, wackestone and mudstone passing upsection for BC asymmetric cycles composed by wackestone and lime mudstone with high diversity of fossils. The stacking of 53 cycles with average thickness of 1,1 m, combined with Fisher plot diagram, indicated an aggradational to retrogradational stacking pattern of succession recorded a lowstand to early system tract (Cycles I-III) passing upsection to late transgressive system tract (Cycles IV and V). Individual cycles accumulated in an approximately 0.25 my and thus represent fourth order cycles related to high-frequency fluctuations of relative sea level. The succession exhibit $\delta^{13}C$ curve with strong enriched trend upward ranging from ~+0.58 to ~+5.28‰, interpreted as representative of Pennsylvanian epicontinental seawater with high organic productivity in the Amazonas Basin. The facies succession presents the following $\delta^{13}C$ values: 1) peritidal in coastal desertic siliciclastic deposits ranging from -1.5 to +0.3‰; 2) tidal

flat and lagoon deposits ranging from +3,98‰ to +4, 62‰; and 3) shelf deposits ranging from +3,65‰ a +5,28‰. This $\delta^{13}C$ curve combined with high frequency cycles analysis are correlated to global $\delta^{13}C$ and sea-level curves that allowed the adjustment of previously Bashkirian to Moscovian age for Late Serpukhovian to Early Moscovian of this Pensylvanian succession. This new age adjusts for studied succession coadunate with an interglacial interval influenced by pulses of a post-glacial transgression combined with slow subsidence of the basin to generation of allogenic cycles (I, IV and V). This work characterizes, for the first time, the cyclicity signature of a Pennsylvanian epicontinental sea of the Western Gondwana in South American.

Key words: High frequency cycles, Monte Alegre-Itaituba succession, Mississippian-Pennsylvanian, Amazonas Basin

1. INTRODUCTION

Epicontinental seas were the dominant geomorphic features of the Carboniferous paleogeography of West Gondwana (Scotese & Mckerrow 1991, Davydov *et al*. 2012, Saltzman & Thomas, 2012). The inland seas developed in the Amazonia were connected to the Panthalassa Ocean with open aperture to the west of South American continent (Scotese & Mckerrow 1991, Davydov *et al*. 2012, Saltzman & Thomas, 2012). The Carboniferous was a period between 358.9 ± 0.4 Ma and 298.9 ± 0.2 Ma strongly influenced by the formation of the supercontinent Pangea. This agglomeration of crustal blocks caused major palaeoceanographic changes, increase of the continental weathering rates, waxing and waning of Gondwanan glaciers accompanied of expressive oscillations of global sea-level and deposition of cyclic marine successions (Smith & Read 2000, Isbell *et al*. 2003; Menning *et al*. 2006; Davydov *et al*., 2012, Saltzman & Thomas 2012). The high bio provincialism contrasts with extinction or decline event of biota, with rapid diversification of reptiles, amphibians, land plants, wingless insects, brachiopods, crinoids, rugose corals, radiolaria, ammonoids, mollusks, benthic foraminifera, sharks and conodonts. Conodonts and foraminifera are commonly used for Carboniferous chronostratigraphy propitiating regional and global correlation of successions worldwide. Additionally, this period records the Earth's first episode of widespread, massive coal formation and CO_2 fluctuations, as well as, an expressive glacial maximum of Paleozoic Era (Crowley *et al.* 1996).

The Carboniferous system include two subsystems, the Mississippian and the Pennsylvanian. The end of Mississippian and the entire Pennsylvanian are marked by typical high frequency cyclicity that reflects factors that control the deposition in the marine carbonate shelfs (Heckel 1986, Boardman II & Heckel 1989, Mazzullo *et al.* 2007, Haq & Schutter, 2008). During the Pennsylvanian shallowing upward and deepening upward cycles are recorded in shallow marine deposits with the best examples in carbonate succession of North America (Smith & Read, 2000, Isbell *et al*. 2003, Menning *et al*. 2006, Davydov *et al.* 2012). These cycles record complete variations of transgressive - regressive cycles and reflect a predominantly carbonate sedimentation with tidal influence (Einsele *et al.* 1991). The origin of the cycles has been related to the variation of the sea level, with high potential of preservation during progradational events (Strasser 19991, James 1984, Pratt & James. 1986). In the Carboniferous other external factors have caused the cyclical patterns are the tectonic and glacial-eustatic events reflected in the global sea level variation. All these causes are interpreted mainly for open continental seas, while inland seas with limited oceanic connection are still few studied. In addition, the lack of cyclostratigraphic studies in the Carboniferous deposits of the Amazonia has hindered the better understanding of the recurrent sedimentary processes and its correlation with the global events occurred in the Western Gondwana.

The record of the Pennsylvanian epicontinental seas developed in the central portion of West Gondwana is found mainly in the Amazon Basin, exposed in excellent outcrops in fluvial scarps of the Amazon River and some of its tributaries in Amazonia (Figure 1). This record has been studied mainly using only lithostratigraphic criteria, which did not allow a more complete appraisal based on sea level changes and cyclostratigraphy. Even though the sedimentological data available to date (Matsuda 2002, Lima 2010, Scomazzon *et al.* 2016) evoke some components of the depositional systems and a preliminary inference of the cyclicity, they have not yet been adequately integrated into a paleoenvironmental and stratigraphic framework. In addition, the scarcity of continuous outcrops due to the dense vegetation associated with the high degree of weathering of the Amazon region makes it difficult for the precise recognition of the depositional systems and sequences. In this work, a detailed study on sedimentary microfacies carried out in outcrops and cores combined with carbon and oxygen isotopic data allowed recognize a cyclicity pattern for the Carboniferous succession exposed in the Amazon Basin, Northern Brazil (Figure 1). These high-resolution analyses aiming the understanding of the cyclicity controls and, as well as, its global correlation with the sea-level (eustatic and glacio-eustatic) and paleoceanographic changes occurred during the Late Mississippian (?) to

Early Pennsylvanian. Finally, this study also provides an excellent opportunity to characterize, for the first time, the high frequency cyclicity and carbon isotopic signatures related to the Carboniferous epicontinental seas of the West Gondwana.
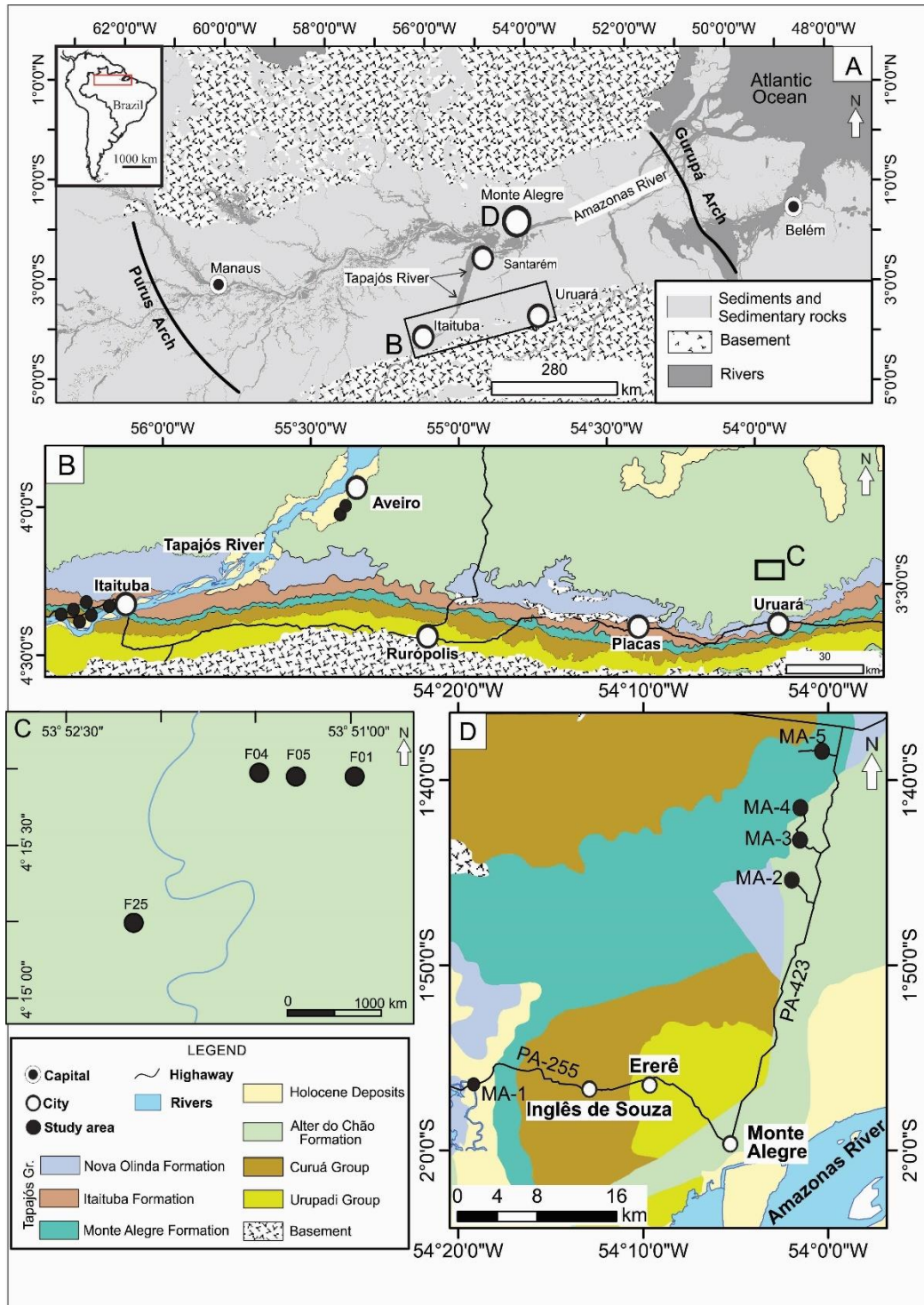
Figure 1- The Central Amazonia, Northern Brazil. A) Geological map showing the structural limits (Arches and Cratonic shields) of the Amazon Basin with indication of studied areas near to Itaituba, Uruará and Monte Alegre cities. B) Detailed geological map of the Itaituba-Uruará region where the classical outcrops occur in fluvial scarps of the Tapajós River. C) Location of drill cores sites (F1-F25) in the Uruará region. D) Location of studied outcrops in road cuts (MA1-MA 5) and quarries (MA 3 and MA 4) in the Monte Alegre region.

2. GEOLOGIC SETTING

The Amazonas Basin is an enormous depression originating as an intracratonic basin on the Amazon Craton situated within the north of the Brazilian territory, particularly in the Central Amazonia (Cordani *et al.* 1984). The basin has well defined limits in its more than 500,000 km^2 of area, it is bordered to the north by the Guiana Shield and to the south by the Brazilian Shield. It is separated to the west by the Solimões Basin and the Purus Arch and to the east is limited by the Gurupá Arch (Figure 1). The 6 km-thick of sedimentary and igneous rocks in its depocenter are dated from the Ordovician to the Cenozoic. The sedimentation is predominantly siliciclastic with carbonate deposition in the Late Carboniferous. Volcanic rocks, mainly diabase, reveal magmatic events occurred during Jurassic and Triassic (Cunha *et al.* 2007). The sedimentary filling is composed of two first-order sequences, the Paleozoic and Mesozoic–Cenozoic sequences (Cunha *et al.* 2007). The Paleozoic sequence is divided into four second order-sequences: Ordovician-Devonian, Devonian-Tournasian, Late Visean and Pennsylvanian-Permian; and two Mesozoic-Cenozoic tectonic sequences that include Cretaceous and Tertiary succession. The igneous rocks form dikes and sills and are related to the extensional events linked to the opening of the Atlantic Ocean.

The interval analyzed in the current study comprises the Pennsylvanian-Permian sequence that include the deposition of the Tapajós Group, which represents a transgressive-regressive megacycle in the Amazon Basin. This group is composed from the base to the top by the Monte Alegre, Itaituba, Nova Olinda and Andirá formations (Matsuda *et al* 2004). The Monte Alegre and Itaituba formations are the object of this work and represent the basal portion of the Tapajós Group. The Monte Alegre Formation consists of sandstone and mudstone interpreted as a desertic depositional system composed of dune field, interdune, fluvial and sand sheets deposits (Matsuda 2002, Lima 2010). The contact between the Monte Alegre and Itaituba formations is gradational with the intercalation of sandstone and dolostone and, upsection, predominate fossiliferous carbonates.

The Itaituba Formation is composed of limestone, dolostone, sandstone, shale, marl and siltstone interpreted as mixed tidal plain and carbonate shelf deposits (Matsuda 2002, Lima 2010, Silva *et al.* 2015). This formation contains an abundant and diversified fossils assemblage with predominance of normal marine benthic invertebrates, including, fish remains, foraminifers, brachiopods, echinoderm, gastropods, bryozoans, trilobites, corals, ostracods, scolecodonts, sponges and conodonts all of them typical Pennsylvanian age (Scomazzon & Lemos, 2005, Moutinho *et al.* 2016a). Palynomorphs analyzes suggest a mid-Morrowano age

(Playford & Dino 2000) while ages based on conodonts and foraminifera, considered more precise, revealed the Lower to mid- Pennsylvanian age (Scomazzon *et al.* 2016, Moutinho *et al.* 2016b). Conodonts are widely distributed in the Itaituba deposits predominating the genera *Rhachistognathus*, *Neognathodus*, *Idiognathodus* and *Diplognathodus* considered as the most important for age calibration. The occurrence of *Diplognathodus coloradoensis*, *D. orphanus*, and the first appearance of *D. ellesmerensis* in the Itaituba Formation, corroborate the Atokano age. Morrowan and Atokan refers a North American nomenclature correlate to the Bashkirian-Moscovian interval (323 to 307 Ma). This age was extrapolated to the underlain Monte Alegre deposits.

3. METHODS

The description and characterization of sedimentary facies followed Walker (1992), which comprises: i) the recognition and individualization of sedimentary facies, its geometry, lithology, sedimentary structures, paleontological content and paleocurrent patterns; ii) understanding the origin and sedimentary processes that form the structures; iii) grouping of genetic and contemporaneous facies in facies associations and thus to reconstruct the different paleoenvironments and depositional system. The facies were represented in stratigraphic profiles and analyzed according to vertical and lateral variations. Microfacies study considered the determination of constituents and classification of limestone and dolostone rocks using Dunham (1962) and Warren (2000). The constituents, such as allochemicals, bioclasts, terrigenous and cements, were based on Flügel (2004), Barthrust (1971) and Tucker (1992). For the distinction between calcite and dolomite, solutions of alizarin red S were applied in thin sections and for the distinction of magnesium or ferrous composition was used the solution of potassium Ferrocyanide. The microfacies were included into of the facies associations contributing with paleoenvironment interpretations.

The sedimentary cycles analysis of Pennsylvanian deposits of the Amazonas Basin was based on the propositions of Posamentier & James (1993) and Strasser *et al.* (2006) for the basic concepts of cyclicity and their identification. The term "cycle" adopted here is that proposed by Kerans & Tinker (1997) which considers a sequence of 4ª and 5ª order with duration of 10^4 to 10^3 years (high frequency cycles) usually observed in outcrop scale and inserted in third order sequences of 0.5 to 3 million years. Small-scale cycles ranging from 0.5 to 10 m-thick are typical of open carbonate shelf/ramp, lagoon and tidal flats settings (Tucker 1991). The cycle patterns evaluation considers facies/microfacies changes, shallowing upward tendency, thickness variations and cycle frequencies and patterns (progradational, aggradational and

retrogradational), as well as, the identification of key surfaces such as maximum flooding surfaces, parasequence and sequence limits (Strasser 1991, Schwarzacher 1993, Perlmutter & Azambuja Filho 2005, Cateneanu 2006, Tucker & Harland 2010). Fischer plots graphic was used to better evaluate the sea-level fluctuations related to peritidal carbonate cycles (Fischer 1964; Sadler *et al* 1993, Bosence *et al* 2009). The plots cumulative graph departure obtained from mean thickness against cycle number modelling the accommodation space rate and their correlation with the sea level changes, characterizing the system tracts (Goldhammer 1987, Goldhammer *et al.*1991; Kerans & Tinker 1997; Bosence *et al.* 2009). The fisher plots scheme was constructed using the Fischer plot excel program (Husinec *et al*. 2008). The analysis of the cyclicity in Pennsylvanian carbonates favors the reconstruction of the sedimentation control processes, as well as the causes for the continuous repetition of the layers couplets and their relationship with autogenic and/or allogenic origin.

Carbon and oxygen isotope signature were obtained from samples after reacting with 100% H_3PO_4 at 25°C for at least 1 hour. Isotopic composition of the released CO_2 was determined by using a Finnigan DELTA Plus Advantage mass spectrometer at the Geochronos Laboratory, University of Brasília. Measurements were made with PDB standards for $\delta^{13}C$ and $\delta^{18}O$. Analytical reproducibility of $\delta^{13}C$ and $\delta^{18}O$ values, based on replicas of NBS-18 and NBS-19 standards, was better than ±0.1‰. The results are reported in conventional notation per mil (‰) relative to the VPDB (Vienna Pee Dee Belemnite) standard. VPDB is a scale recognized by the National Institute for Standards and Technology (NIST) that is used for reporting relative abundances of $\delta^{13}C$ or $\delta^{18}O$ via the delta notation.

4.PALEOENVIRONMENT

The mixed siliciclastic-carbonate deposits of the Monte Alegre-Itaituba succession were previously described by Matsuda (2002) based on classical outcrops of the southern and northern border of the Amazonas Basin. We revisited these outcrops and the facies and stratigraphic studies were complemented by high frequency stratigraphic analysis. The mixed siliciclastic-carbonate deposits of the Monte Alegre-Itaituba succession were subdivided into three facies associations of coastal desert, tidal flat and carbonate shelf (Figure 2).

The coastal desert deposits consist in dune field, sand sheet, interdune, fluvial channel and dolomitic lagoon deposits. The dune field deposits consist of fine- to medium-grained sandstone with small to medium-scale low angle and cross-bedding and translatent climbing-ripple cross lamination. Root marks occur in the top of sandstone generally presenting a whiteness halo and indicate stabilization phases of dunes. These facies reaching up to 8m-thick

and are laterally continuous for hundreds of meters. The sand sheets are characterized by tabular packages of fine-grained sandstone with even parallel and low angle laminations interbedded with fine- to medium-grained sandstone with tangential cross stratification interpreted with fluvial deposits. Lenses of dolostone is locally interbedded with dune field deposits (Figure 2b). The fine dolostone is bioturbated by *Palaeophycus*, *Lockeia*, *Thalassionoides*, *Rosselia* and meniscate trace fossils, indicating a softground substrate inhabited by shallow waters marine organism.

The mixed tidal flat association is classified as: supratidal, tidal channels, tidal delta, siliciclastic and carbonate lagoon (Figure 2c). The supratidal deposits is composed of laminated to massive fine dolostone with desiccation cracks indicating precipitation and episodic emergence. Laminae of silicified dolostone suggests replacement of evaporites. Trough cross-bedded fine- to medium-grained sandstone forming sets of 50cm-thick interbedded is interpreted as tidal channels (Figure 2d). Mud drapes occur in the inclined strata and topsets of of cross-bedding (tidal bundles) characterizing suspension process during slack waters. This deposit is interbedded with sandstone/mudstone (tidal) rhythmite. Fine-grained sandstone with low angle stratification and ripple marks were formed by swash and backwash wave flow associated a foreshore zone. Sigmoidal cross-stratified fine-grained sandstone alternate with sandstone layers of supercritical climbing ripple-cross lamination between 5m-thick siltstone and marls layers represent tidal ebb-flood delta deposits on siliciclastic lagoon. The siliciclastic lagoons correspond to the more proximal portion of this tidal system while limestone rich in brachiopods, echinoderms and scarce monosserial foraminifera, indicating a more confined setting of central lagoon.

The shallow shelf carbonate deposits are associated with complex of bioclastic bars sediments with abundant benthic fossils, allochemical and terrigenous grains (Figure 2 c). Medium- to coarse-grained grainstone constitute the bioclastic bar deposits which is separated of lagoon carbonate facies from the shelf carbonate deposits (Figure 2e). The shelf deposits consist in wackestone and lime mudstone with abundant fossils of algae, brachiopod, bivalve, bryozoan, coral, echinoderm, foraminifera, gastropod, ostracod and trilobite, as well as, conodonts and fish fragments (Figure 2f). They differ from the tidal flat association because present a greater fossil diversity of benthic organisms colonizing the carbonate substrate. The low content of terrigenous is observed only in limestone beds laterally in contact with inlet channel deposits of tidal flat association.

Figure 2- Main characteristics of the facies associations of the study area. A - association of coastal desert with fine- to medium grained sandstone with low angle cross stratification. B – Fine dolostone with *Lockeia* (a) and *Palaeophycus* (b) trace fossils representative of lagoon deposits. C – Contact between marls of lagoon deposits, bioclastic grainstone interpreted as bars in contact with lime mudstone rich in benthic fossils. D - tidal channel deposit, presenting sandstones with cross-stratified fine sandstone with sets separated by centimeter layers of mudstone and/or mud drape (negative profile in outcrop). E - Photomicrograph representative of bioclastic bar facies (grainstone) showing abundant bioclasts and allochemical particles, as well as, terrigenous grains. F - Photomicrography characteristic of shelf deposits, composed of carbonate matrix with abundant foraminifera and ostracod bioclast.

5. CYCLICITY

The cyclicity of the Pennsylvanian deposits of the Amazonas Basin are observed in all three facies associations of the Monte Alegre-Itaituba succession and consists of five types of sedimentary cycles (I-V) of carbonate, siliciclastic and mixed composition (Figure 3). Individual cycles show a shallowing upward tendency, and the 50m-thick vertical succession has a general deepening upward trend with predominance of limestone shelf facies in the top (Figure 3).

5.1. Cycle I - Sandstone / dolostone

Cycle I correspond to the intercalation of the sandstones with the initially massive dolostone, which to the top are bioturbated by *Palaeophycus*, *Lockeia*, *Thalassionoides, Rosselia* and meniscate trace fossils. Root marks are found in the top of sandstone. Cycle I was observed in two profiles in the region of Tapajós River and in core succession of the Aveiro region (Figure 1 and 3). This intercalation represents the transition zone between Monte Alegre and Itaituba formations (Figure 4b). The cross-bedded sandstone exhibits a thinning upward trend concomitant with thickness upward of massive and bioturbated layers of dolostone. Although this type of cycle has a very thin thickness, reaching up to 65 cm, this type of cycle presents a great lateral continuity. This centimetric intercalation is recurrent up to three times along the succession, have tabular geometry. This cycle marks the beginning of an expressive flooding (transgressive) zone laterally continuous for hundreds of meters and possibly correlated along of the basin.

The Cycle I was generated during the lateral migration of eolian dunes and lagoon deposits inserted on coastal plain in the margin of epicontinental sea. At the beginning of Pennsylvanian, a significant glacial cover was developed in the southern portion of Gondwana, causing a drop in the global level of the oceans more significative than those inferred for the Late Bashkirian (Veevers and Powell 1987). This drop-in sea level led to the establishment of large desert areas along the North of Gondwana, with record in the Solimões, Amazonas and Parnaíba basins, as well as, the fluvial deposits in the Acre Basin (Wanderley Filho *et al.* 2010). The cycle marks the limit between the finish of icehouse condition and the beginning of Bashkirian interglacial period succeeded by the progressive establishment of an expressive carbonate shelf in the Amazonas Basin. These allogenic processes led the definitive installation of the epicontinental sea in the Western Gondwana.
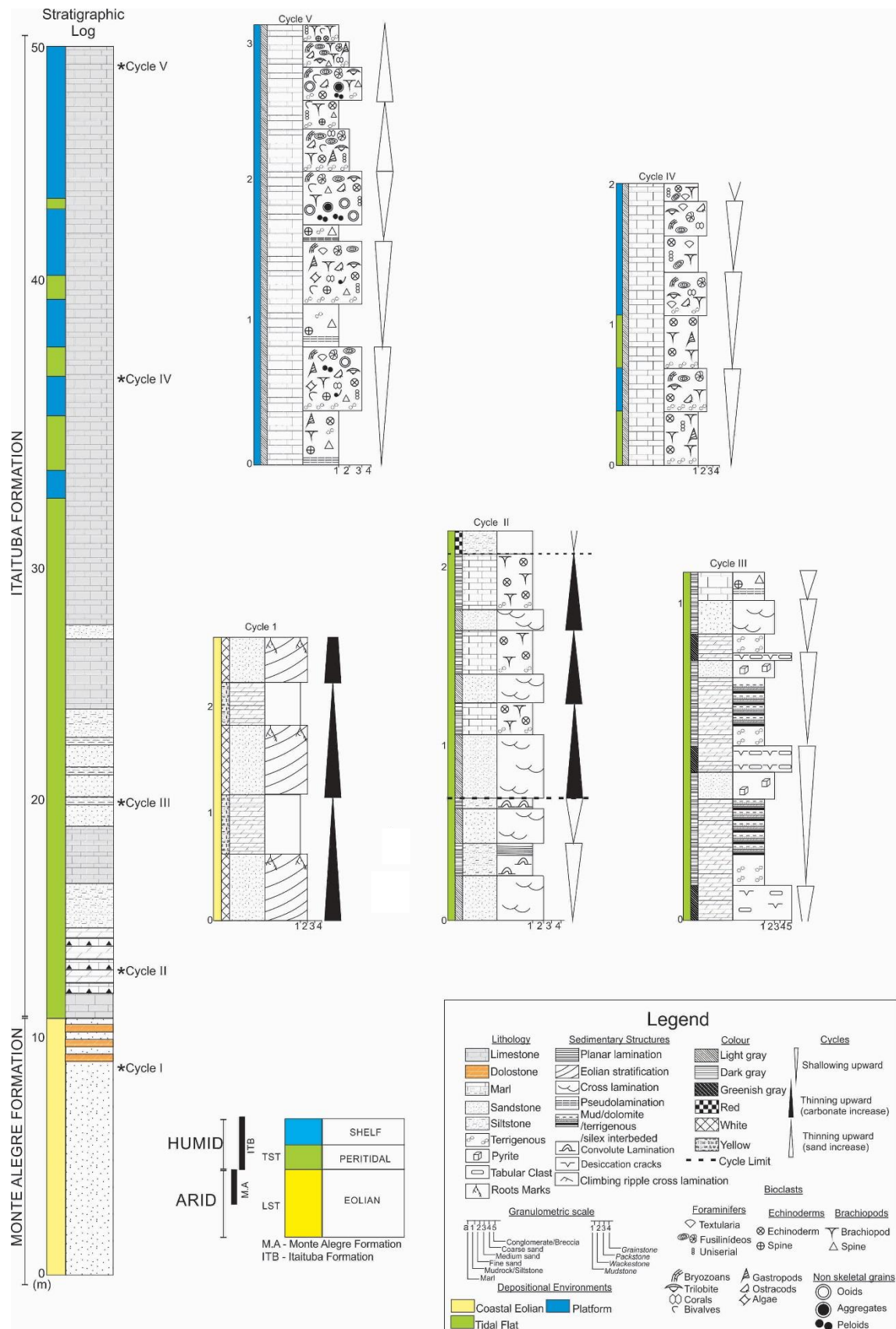
Figure 3- Composite profile of the carbonate - siliciclastic study area sedimentary succession, where the five cycles are positioned from the bottom to the top. Cycle I - sandstone / dolostone; Cycle II - sandstone / carbonate; Cycle III - dolostone / sandstone; Cycle IV - wackestone / lime mudstone; Cycle V cycle - wackestone / grainstone / lime mudstone.
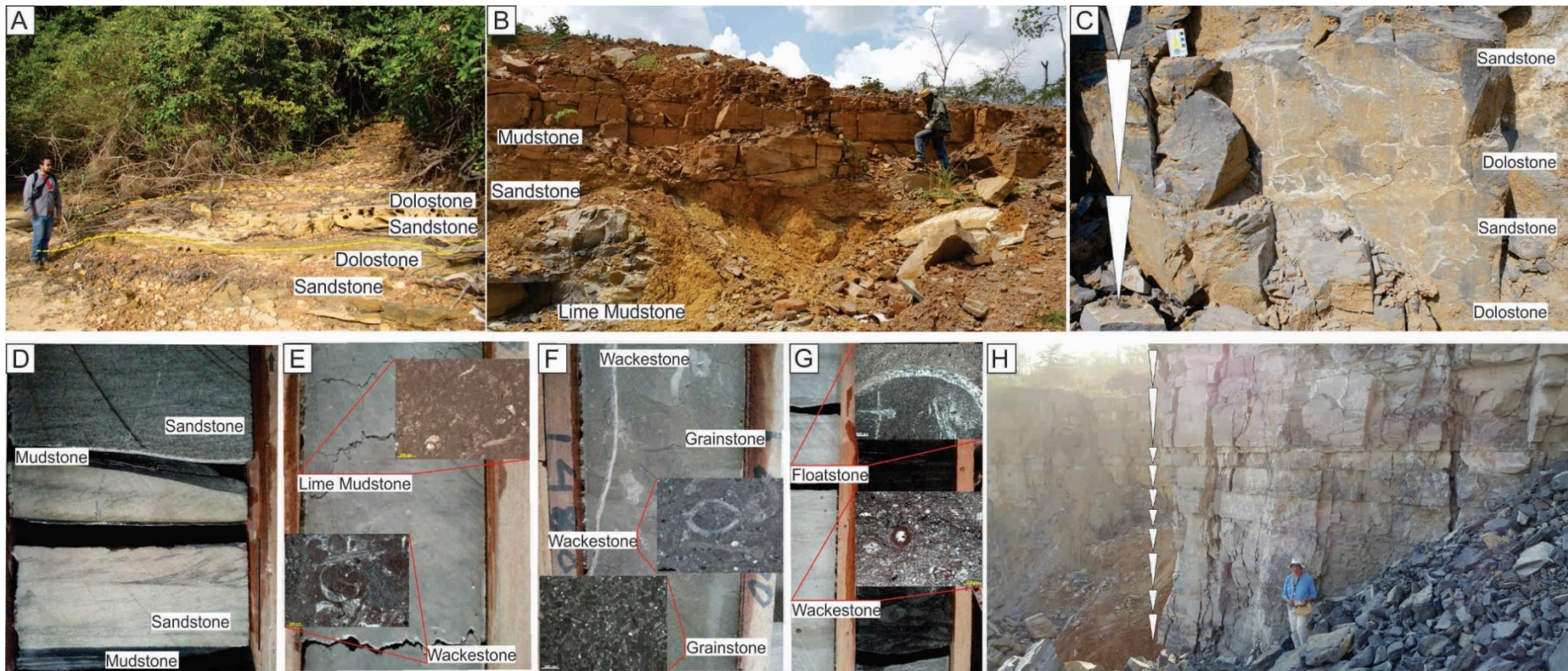
Figure 4- All cycles exhibiting a shallowing upward pattern of the study area, observed in outcrops and core. A- Cycle I, intercalation of marine dolostone with coastal deserts sandstones. B- Cycle II tidal channel sandstones and massive pelites. C- Cycle III alternation of dolostone and massive sandstones associated with the supratidal / intertidal boundary. D- Cycle II sandstones / lamites. E-Cycle IV -intercalation of carbonate layers of wackestone / lime mudstone, where the lime mudstone represents the lagoon and the shelf wackestone, in detail are the photomicrography of the respective facies. F- basal portion of Cycle V represented by grainstone / wackestone intercalation, in detail photomicrography of grainstone microfacies and photomicrography of wackestone microfacies. G- alternation of floatstone and lime mudstone of tidal flats, in detail the corresponding microfacies. H- general view of Caltarém quarry section in the region of Monte Alegre, representative of cycle V.

The glaciation is recorded only to the south of Gondwana and the deposition occurred as sedimentary pulses linked to expansion and retreat of glaciers throughout the Early Pennsylvanian (Caputo and Crowley 1985, Saltzman 2003). This waxing and waning of glaciers triggered more than fifty transgressive-regressive deposits (Ross and Ross 1987) that was directly reflected in the global sea level curve (Haq & Schutter 2008). Lima (2010) associates this mixed sedimentation with alternating pulses of marine flooding and subaerial exposure which is compatible with the generation of Cycle I. Is difficult to recognize in the base of the Monte Alegre-Itaituba succession an explicit reading of glaciogene influence in the cycles. Therefore, a lowstand phase can be inferred due the reduced thickness of the cycles that reflects a low space of accommodation of the basin margins, developing an aggradational to retrogradational pattern. The low accommodation corroborated by the presence of traces fossils typical of shallow waters with less than 10 m deep. In addition, the eolian sedimentation was gradually replaced by the shallow marine limestone of the Itaituba Formation revealing a post-glacial flooding (transgressive) correlated for hundreds of kilometers by the Amazonia basins, confirming the allogenic nature of Cycle I.

5.2. Cycle II - Sandstone / mudstone - Sandstone / lime mudstone

The maximum thickness observed of this cycle is 85 cm and in outcrops predominate sandstone with tidal bundles filling channel geometry, generally interbedded with lime mudstone while in cores is common the occurrence of lime mudstone and floatstone (Figures 3 and 4a). The lateral distribution of cycles is limited occurring only for dozens of meters observed in outcrops and cores. Echinoderms and brachiopods are the main body fossils. Bioturbations are found in the carbonate rocks and post-deformational structures are observed in the limit of beds (Figure 3).

The Cycle II occurs predominantly in the basal portion of the Itaituba Formation, previously interpreted as carbonate and mixed tidal flat/lagoon deposits (Caputo 1984, Figueiras & Truckenbrodt 1987, Matsuda 2002, Lima 2010, Silva 2014). The Bashkirian age of this cycles is based on conodonts found mainly in lagoon deposits (Moutinho *et al.* 2016b, Scomazzon *et al.* 2016). Autogenic processes inherent of depositional paleoenvironment such as channel migration on tidal flats and draining on lagoons was responsible by the origin of this cycle. The occurrence of mud drapes on cross beds of sandstone suggests alternation of current action and suspension processes, characteristic of tidal processes in coastal systems (cf. Visser 1980). The influence of flood and ebb tides is considered to the intertidal flat and tidal channels (Longhitano 2010, Longhitano *et al.* 2012). The presence of mudstone and fine-grained

sandstone of channel deposits indicates a probable meandering geometry of channel. Lime mudstone with root traces and bioturbations indicate installation of vegetation in the intertidal and supratidal zone (Matsuda 2002, Lima 2010). The shallowing up tendency of tidal flat cycles suggests a local progradational pattern into a transgressive (retrogradational) tendency (c.f. Tucker and Wright 1990). The generation of accommodation space can be also associated to the paleotidal range, estimated here, discarding the loss of volume by compaction during diagenesis of ~1m. This estimation of tidal range suggests microtidal regime compatible with an epicontinental sea. The presence of tidal systems or even evidence of tidal systems in epicontinental shallow seas is rare, however during the Paleozoic this occurrence is recorded as a system of islands and bars that border the edges of these seas (Pratt & James. 1986).

5.3. Cycle III - dolostone / sandstone

Cycle III represents the alternation of dolostone with massive sandstones exhibiting. shallowing upward tendency, thinning upward of dolostone beds and thickness upward of sandstone beds. The maximum thickness of cycle is 80 cm composed of fine dolostone with desiccation cracks and massive pyritous sandstones couplets (Figure 4e). These cycles are concentrated in the base of Itaituba Formation and overlies lagoonal limestones of Cycle II. Similarly, to Cycle II, they have limited lateral continuity.

The periodic subaerial exposure of the tidal flat deposition indicate sedimentation in the supratidal zone (Tucker & Wrigth 1990). The occurrence of massive sandstone interbedded with carbonates suggests periods of rapid flooding, possibly originating from the action of spring tides, flooding events fed by discharge of rivers or exceptional storms waves. The dolomitization of the matrix of the level with mud cracks with partial silicification suggest the mixing of meteoric waters and evaporation processes the formation of dolomite (cf. Warren 2000). The silicification depicts a replacement of evaporites by silica, like that found by Matsuda (2002) and Lima (2010) to the north border of Amazonas Basin. Matsuda (2002) identifies the same progradational pattern for this type of cycle found along of the cliffs of the Tapajós River and cores, interpreting as a product linked to the highstand phase. However, as interpreted to Cycle II, we consider an autogenic origin and the progradational tendency is local inserted a general retrogradational framework that record a transgressive system tract.

5.4. Cycle IV – Floatstone/lime mudstone and wackestone/lime mudstone

The Cycle IV has thickness up to 1.5 and consists of the intercalation of lime mudstone and wackestone beyond floatstone (Figure 4e). They are separated from cycle III by layers of siltstone and carbonates, corresponding to the basal portion of lagoon deposits. They represent floatstone or lime mudstone interbedded with wackestone and lime mudstone. The lime mudstone contains abundant fossils of brachiopod, echinoderm, monoseriate foraminifera and rare ostracodes, the micritic matrix presents an opaque appearance that indicate low intensity of neomorphism. Terrigenous grains are rare in this cycle.

The formation of this cycle is directly related to sea-level changes related to the Bashkirian post-glacial transgressive event. Local variations cause the installation of coastal environments gradually replaced by shallow to moderately deep waters shelf settings. The content of terrigenous is differentiated in the cycle couplets, they are abundant in lagoon deposits and absent in shelf deposits. The difference reflects the proximity with the continent and terrigenous input of the tidal channels and deltas. The terrigenous content is concentrated in the bioclastic bars deposits and rare inlets channels, whereas in the shelf deposits admits an eolian origin or clouds with silt size grains provided by storms. These shallowing upward cycles were previously interpreted as subtidal deposits composed of wackestone and lime mudstone, generated during highstand phase (Matsuda 2002). This cycle is reinterpreted here as a product of continuous generation of accommodation space linked to sea-level rise, a post-glacial transgression that affected the Amazonas Basin during Bashkirian-Moscovian. The marine nature of carbonate sedimentation is reinforced by the fossiliferous assembly composed of open sea individuals (Osleger 1991).

5.5. Cycle V - grainstone, wackestone and lime mudstone

The cycle V has thicknesses of up to 2 m, consists of ABC asymmetric cycles of grainstone, wackestone and lime mudstone interbedded, upsection, with asymmetric BC couplets composed of wackestone and lime mudstone (Figure 4f e 4h). The grainstone are composed of fragments of shelf bioclasts, terrigenous and allochemical. The wackestone are composed of micritic matrix, low content of terrigenous and a high diversity of bioclast represented by algae, brachiopod, bivalve, bryozoan, coral, echinoderm, greater diversity of foraminifera, gastropods, ostracodes and trilobite. The lime mudstone has a micritical matrix with brachiopod, bioclasts, foraminifera and trilobites, without terrigenous.

The Cycle V represents pure carbonate sedimentation with reduced terrigenous inflow recorded more frequently in grainstone beds and in the base of wackestone layers. The terrigenous in grainstone come from inlet channels incised on inner shelf, while the rare silt and fine-grained terrigenous in the base of wackestone were interpreted as eolian influx. In the grainstone microfacies the fossils are fragmented indicating reworked by waves and storms. In contrast, in the wackestone and lime mudstone predominate body fossils. Mudstone were deposited in moderately deep waters than grainstone that generally exhibits reworking by waves. The high fossiliferous diversity observed in wackestone confirms a shelf setting with more nutrients and expressive biological activity. The fossil assembly in these microfacies are characteristic of open sea shelf and confirms the transgressive tendency for this succession. The paleoecological studies of Moutinho et al. (2016a, 2016b) estimated in 60 meters depth for the Itaituba sea. Therefore, the limited thickness of cycles with approximately 1m-thick, discounting the loss of volume during burial diagenesis, suggest low accommodation space during deposition. This typical transgressive trend for carbonate cycles observed in the most upper succession that include cycles type V is similar those proposed by Handford & Loucks (1993) for shallow shelf sea settings. The retrogradational trend observed in this cyclic stacking pattern of Upper Itaituba Formation confirms the climax record of the Bashkirian-Moscovian post-glacial sea level rise occurred in the Amazonas Basin.

6. C AND O ISOTOPIC STRATIGRAPHY

6.1. Sampling and evaluation of the isotopic data

Samples were collected from a 32 m-thick succession and are representative of all facies associations (Table 1). Changes in the $\delta^{13}C$ values of carbonate rocks have been used as a proxy for understanding the global carbon cycle, as well as, in modeling the evolution of atmospheric carbon dioxide levels (Shackleton 1985, Veizer *et al.* 1999, Berner and Kothavala 2001, Macdonald et al. 2010). The O- isotopes has been used to determinate the sea-surface temperature changes related to the climate evolution of the Earth (Veizer *et al.* 1999, van Geldern *et al.* 2006). The definition of the isotopic secular trends is fundamental to define the extension of secondary alteration that modified the original the $\delta^{18}O$ and $\delta^{13}C$ composition of carbonates. Brachiopods shell (biogenic low-Mg calcite) and whole rock (matrix aragonite/calcite) are the main material for the acquisition of $\delta^{18}O$ and $\delta^{13}C$ data to evaluate the seawater signature and paleoceanographic changes in the Carboniferous epicontinental sea worldwide (Veizer *et al.* 1999, Saltzman *et al.* 2004, van Geldern *et al.* 2006, Brand *et al.* 2009).The whole rock samples for isotopic analysis of Pennsylvanian succession of Amazonas

Basin were collected in Caltarem quarry of Uruará region representative of stratigraphy for the Monte Alegre and Itaituba formations (Figure 5). C- and O-isotope analyses were performed on 30 fine-grained dolostone and limestone samples (Table 1). The analyzed core samples are fresh, show weak neomorphism with preserved primary textures and structures. The micritic matrix, either of dolomitic or calcitic composition, is opaque and when neomorphosed presents regular intercrystalline boundaries composing a fine-grained, hipidiotopic, equant mosaic. Homogeneous samples were preferred although the dolomitized samples were also analyzed. Fractured, mineral-filled, weathered and hornfels zones were discarded.

The $\delta^{13}C$ values of the ~30m-thick mixed siliciclastic-carbonate succession are positive ranging from ~+0.58 to ~+4.91‰ while the $\delta^{18}O$ values are negative between -8.27 to -3.88‰. Even when the isotopic data are integrated with previous isotopic data obtained in core samples by Matsuda (2002) and Parente (2014) the isotopic trend do not change. In this complete isotopic framework only two samples with negative $\delta^{13}C$ values of -2‰ in the base of the succession (Figure 6). Negative values of $\delta^{18}O$ are considered a strong indicator for signal alteration, but numerous studies have demonstrated that, whereas O isotopes can be readily altered by diagenesis, C-isotopes are typically buffered to primary rock values (Brand 2004, Korte *et al.* 2006, van Geldern *et al.* 2006). In fact, the $\delta^{18}O$ values are easily altered in carbonate rocks because it is controlled by temperature of precipitation, the $^{18}O/^{16}O$ relationship of water of precipitation while the $\delta^{13}C$ value is directly linked to the carbon cycle and CO_2 source and less susceptible to alteration (Mitchell *et al.* 1996).

Table 1: $\delta^{13}C$ e $\delta^{18}O$ values for representative limestone samples of the corresponding facies associations the Monte Alegre and Itaituba formations exposed in the Caltarém quarry.

Unit	Facies association	$\delta^{13}C$ (VPDB)	$\delta^{18}O$ (VPDB)
Monte Alegre Formation	Tidal flat associated with coastal desert	+1, 50	-8, 09
		+1, 57	-8, 27
		+1, 27	-8, 03
		+0, 58	-8, 09
Itaituba Formation	Tidal flat	+1, 98	-8, 02
		+2, 02	-8, 04
		+2, 03	-8, 14
		+2, 38	-7, 80
		+3, 22	-6, 93
		+3, 48	-7, 81
		+3, 77	-7, 58
		+3, 88	-7, 39
		+3, 94	-6, 08
		+4, 01	-6, 28
	Shelf	+3, 98	-4, 21
		+4, 91	-3, 88
		+5, 28	-4, 13
		+5, 23	-6,19
		+4, 79	-5,68
	Tidal flat	+4, 35	-6,34
		+4, 62	-6, 41
	Shelf	+4, 52	-4, 36
		+4, 41	-4, 38
		+4, 55	-5, 83
		+4, 19	-7, 68
		+3, 94	-5, 86
		+3, 77	-4, 90
		+3, 65	-6, 03
		+3, 70	-5, 77
	Tidal Flat	+2, 82	-4, 74
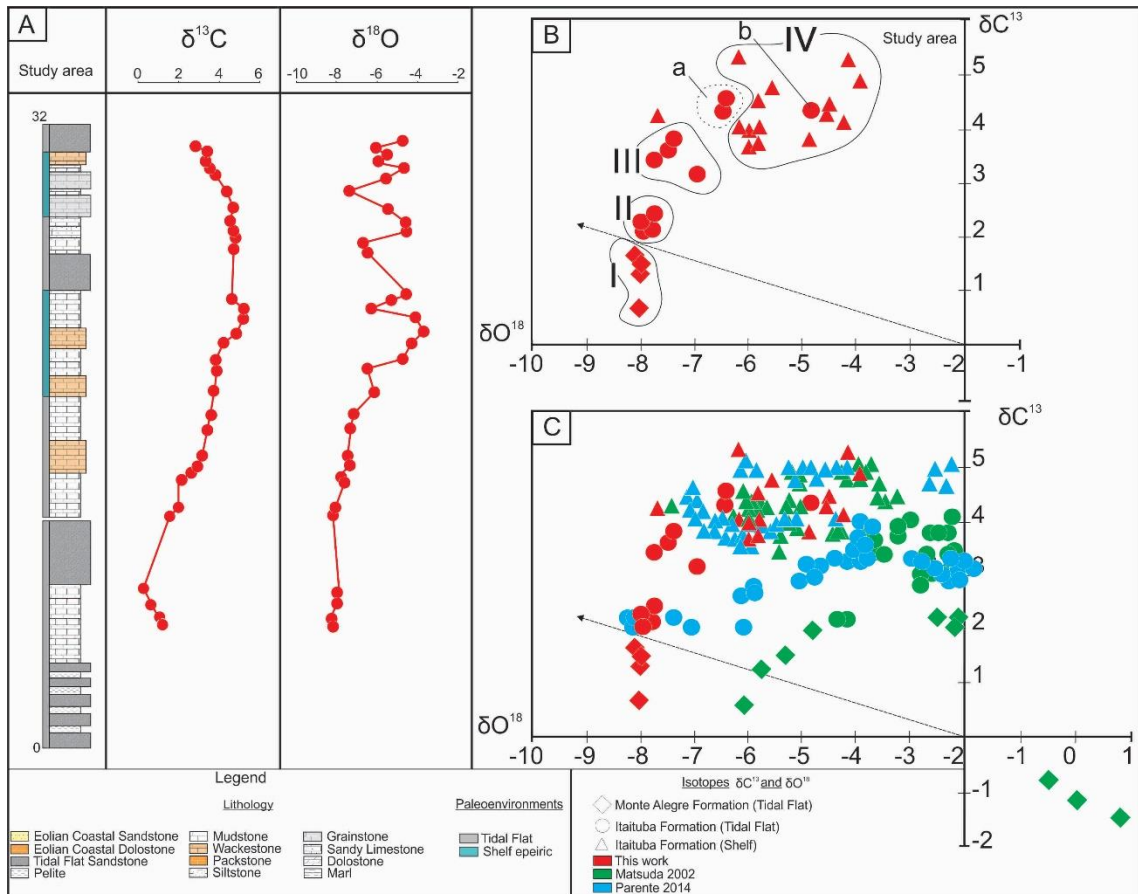
Figure 5: a) values of the carbon and oxygen isotopes for the carbonates of the Monte Alegre region, north border of the Amazonas Basin. The data vary from base to top according to the facies associations found, with $\delta^{13}C$ values between 0‰ to + 3‰ and $\delta^{18}O$ between -8‰ and -7‰, for the tidal plain carbonates, the $\delta^{13}C$ isotopic values for the shelf association ranges from + 3‰ to + 5‰ and δO^{18} from -8‰ to -4‰; b): Stability isotope distribution graph of $\delta^{13}C$ and $\delta^{18}O$ showing the presence of four main trends related to their respective environments and geological units.
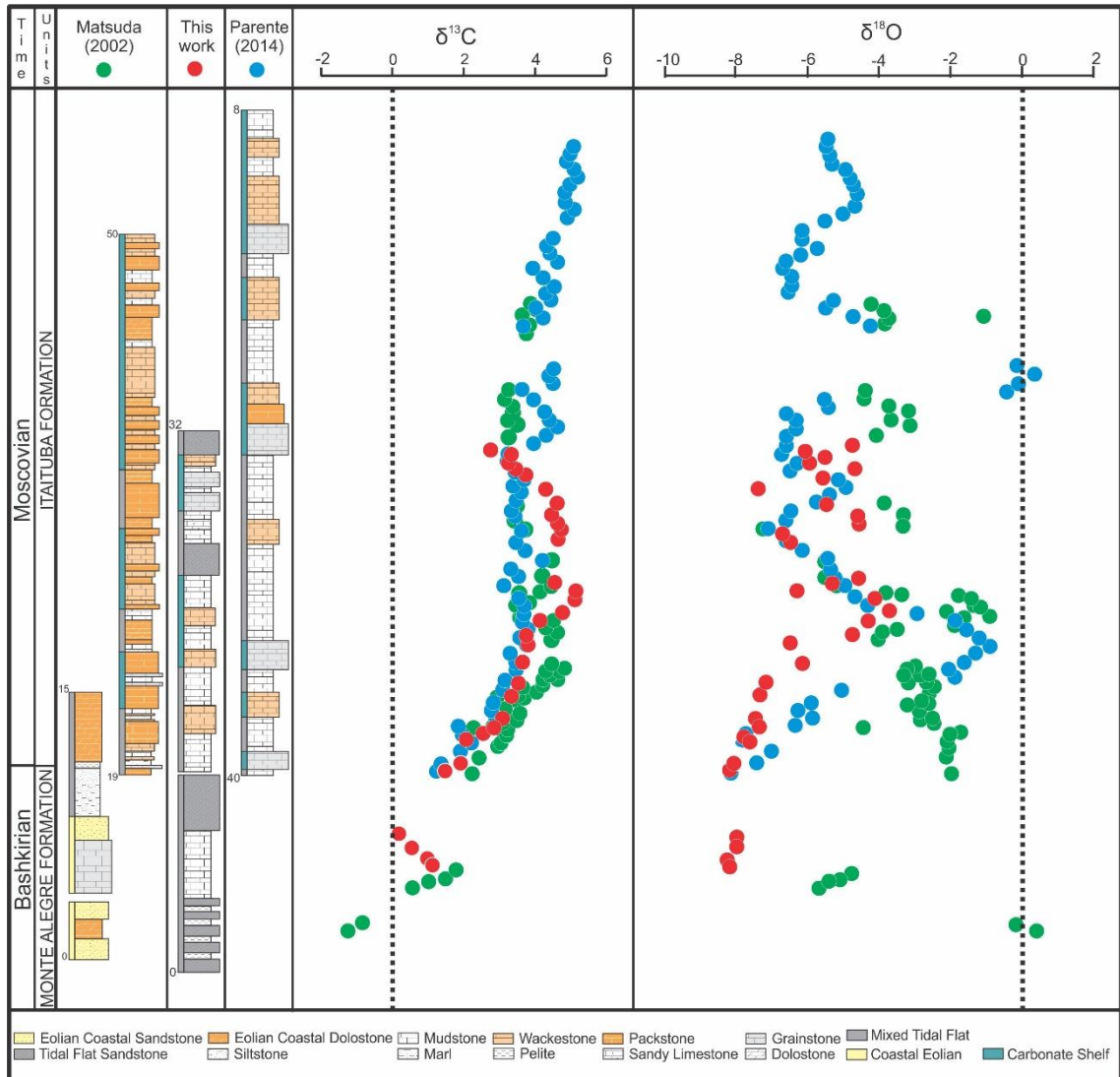
Figure 6: Distribution of $\delta^{13}C$ and $\delta^{18}O$ isotopes from the Monte Alegre-Itaituba succession and from Matsuda (2002) and Parente (2014) showing a general tendency for carbon data to be extremely positive, whereas the oxygen data present a tendency to change by the eodiagenetic processes. The positive values of $\delta^{13}C$ coincide with the increase in relative sea level, which occurs in the form of fluctuations, represented by thin cycles with predominance of marine deposits to the top, even with a glacial period registered for the Moscovian.

The $\delta^{13}C$ versus $\delta^{18}O$ cross plots were made for all the datasets (Figure5A) to check for simultaneous decreasing trends for both C- and O-isotope compositions, which would indicate diagenetic modification of the isotopic record (e.g., Jacobsen and Kaufman, 1999). The samples were grouped according to facies associations and are perfectly differentiated in $\delta^{13}C–\delta^{18}O$ cross plots (Figure 6). Dispersion in the O-isotope data between different facies indicate that diagenetic fluids did not modify all the facies, but specific facies have undergone modification by diagenetic fluids (Figure 6). Therefore, as commented previously the evidence of intense diagenesis was not observed in the studied succession and if was, affected mostly the O-isotope signal and the primary C-isotopic signal was retained. The co-variance found between $\delta^{13}C$ and

$\delta^{18}O$ values of quarry samples obtained in this work suggests a closed system behavior without influence of diagenetic fluids (Talbot & Kelts, 1989, Valero-Garcés *et al*. 1997). On the other hand, no correlation between $\delta^{13}C$ and $\delta^{18}O$ values are depicted within any facies association (Figure 5C). The large dispersion of negative $\delta^{18}O$ values suggests alteration by diagenetic fluids but were not able to modify the $\delta^{13}C$ original composition. The covariation between the bulk $\delta^{13}C$ and $\delta^{18}O$ values of shallow marine carbonates can reflect alteration within waters of varying isotopic composition into the mixing-zone (Allan & Matthews 1982) or reflects variable amounts of recrystallization/neomorphism and the addition of diagenetic cement (Swart, & Oehlert 2018). A lack of covariation between the bulk $\delta^{13}C$ and $\delta^{18}O$ values does not necessarily prove that the deposit maintains the original isotopic composition. Swart & Oehlert. (2018) have demonstrated that carbonate rocks pervasively altered in the vadose zone frequently present no covarying trend between $\delta^{13}C$ and $\delta^{18}O$ values and in the other instances exhibit strong covariance in unaltered material, which simply reflects, in this case, the mixing of material from sources with differing $\delta^{13}C$ and $\delta^{18}O$ values.

The isotopic variations observed in the studied succession can be explained by different interpretations, therefore the $\delta^{13}C$ up section enrichment trend of Monte Alegre-Itaituba succession, including values near of 0‰ up to +5.5‰, is compatible with the values found in Mississippian to Pennsylvanian periods (Veizer *et al*. 1999, Mii *et al* 1999, 2001, Saltzman 2005, van Geldern *et al*. 2006, Isozaki *et al*. 2007, Brand *et al*. 2015). Other lines of evidence support the pristine isotopic values, particularly the $\delta^{13}C$, observed in almost all analyzed samples from the Monte Alegre-Itaituba succession: (a) the original micritic texture is preserved in almost all samples, and (b) relation between $\delta^{13}C$ and $\delta^{18}O$ compositions is not covariant indicating diagenetic alteration mainly for $\delta^{18}O$ with predominant negative values. Finally, we consider the carbon isotopic framework likely represent the Pennsylvanian seawater isotopic composition of Itaituba epicontinental sea and can be used for local and global correlations.

6.2. Paleoceanography and correlation with carbon isotopic global curve

In general, the isotopic carbon trends along the Mississippian-Pennsylvanian show a clear decoupling of the ^{13}C oceanic sea water and epicontinental sea marked by large-scale fluctuations of this element when compared with examples of epicontinental seas (Veizer *et al*. 1999, Mii *et al*. 1999, 2001, Saltzman, 2005, van Geldern *et al*. 2006, Isozaki *et al*. 2007, Brand *et al*. 2015). Particularly, the overall record of the sea water isotopic composition during warm periods tends to range from ~ + 3.3 ‰ to + 5.3 ‰ VPDB, whereas during cold periods the range is from + 5.2 ‰ to 6.8 ‰ VPDB (Brand *et al*. 2009). In addition, these fluctuations seem to be

directly related to eustatic events (Haq *et al.* 1988, Haq & Shutter 1988), and can be used in the interpretation of stratigraphic sequences and as a marker of rapid sea level variations (Mitchell *et al.* 1996). The isotopic signal observed in the siliciclastic-carbonate deposits of the studied succession are in the general range for carbonate rocks. The isotopic carbon data that form the chemostratigraphic framework for the Itaituba epicontinental sea cyclic deposits of the central portion of the Amazonas Basin were summarized in an isotopic curve along the global carbon isotope curve for the Middle to Late Carboniferous (Figure 7).
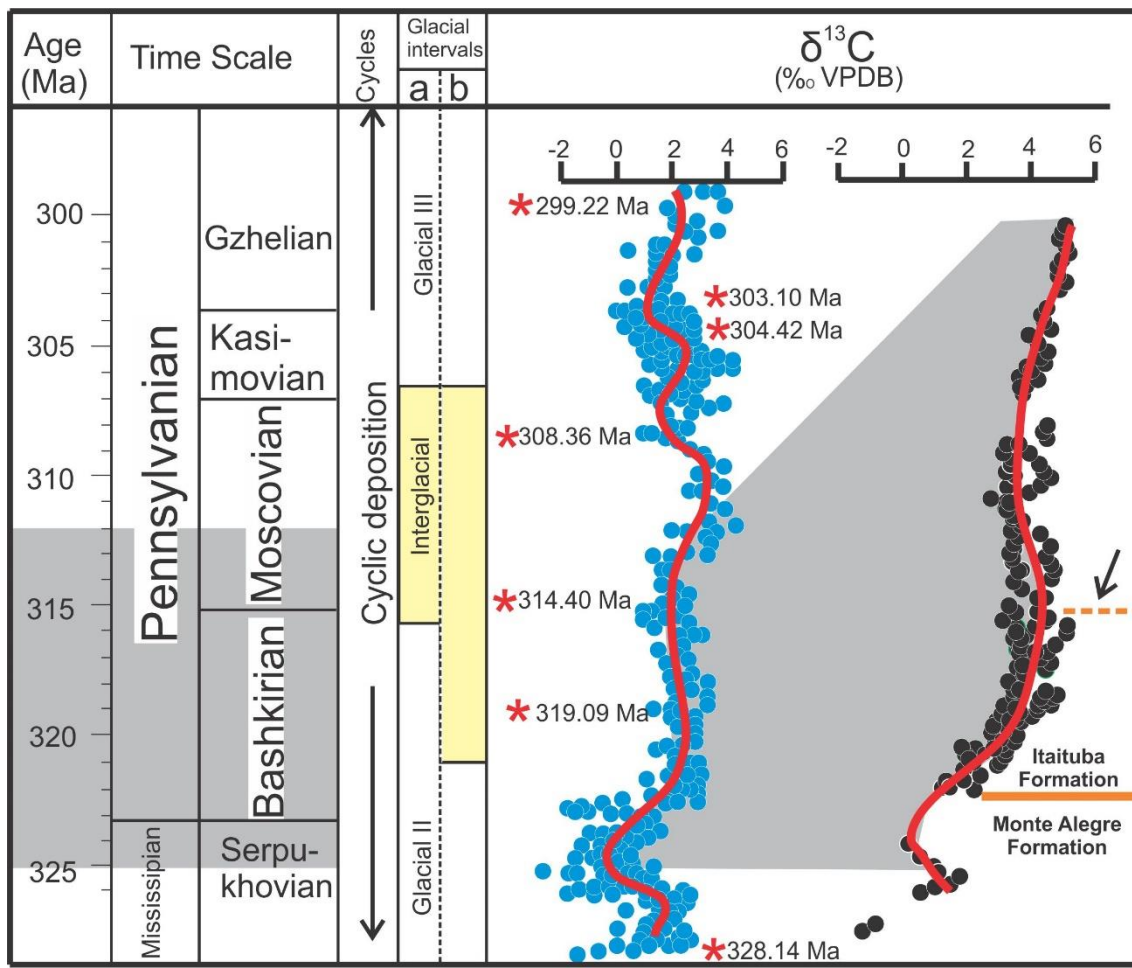
Figure 7. Correlation of carbon isotopic curves between for the Carboniferous (left) and the Monte Alegre-Itaituba succession from the Amazonas Basin. The generalized Carboniferous isotopic curve is combined with periods, stages, radiometric age (indicated by red asterisk), carbon isotopic records, cyclothems, glacial and interglacial (letter a) intervals (After Smith & Read, 2000, Isbell *et al.*, 2003, Menning *et al.*, 2006, Davydov *et al.*, 2012, Saltzman & Thomas, 2012). The interglacial interval for Bashkirian was enlarged in this work (letter b) based on correlation with the transgressive deposits of the Itaituba Formation with positive values of δ13C (see text for explanations). The limit between both formations previously close to the Bashkirian-Moscovian boundary (arrow) was repositioned in the base of Bashkirian suggesting that the Monte Alegre deposits include Mississipian (Serpukhovian) age. The age estimation for deposition of the studied succession is approximately 13 Ma (grey interval).

The results show that the δ^{13}C isotopic composition of the lagoon dolostone and tidal flats associated with the Monte Alegre Formation coastal desert deposits ranges from rare negative values of -1.5‰ to +0.58‰ while the δ^{18}O composition varies from -8, 27‰ to -8.03‰. The values of δ^{13}C are depleted, probably related to the reduced consumption of organic carbon (^{12}C) associated with low biological productivity and the paleoenvironmental restriction related to the continuous influx of continental siliciclastic. According to Moutinho (2016b) the brachiopods and echinoderms in the coastal facies of the Monte Alegre and Itaituba formations are tolerant to episodic continental terrigenous influxes and to salinity variations related to paleoenvironmental constraints or confinement. The increase in organic productivity coincides with the first transgressive pulse that floods the Amazonas Basin, precipitating the carbonates of the Monte Alegre unit upper part (Caputo 1984, Cunha *et al.* 2007). This siliciclastic unit is rapidly replaced by tidal plain deposits of the Itaituba Formation with δ^{13}C isotopic values varying from + 3.98‰ to +4.62‰. These values of δ^{13}C present a greater enrichment in relation to the Monte Alegre Formation.

In the supratidal/intertidal carbonates the values of δ^{13}C vary from + 1.98‰ to +2.03‰, the most depleted values of this unit. The carbon isotopes represent a positive excursion probably associated with high carbon consumption whose preservation in organic matter levels contained in the intertidal facies attest to a reducing environment indicated by the precipitation of pyrites. The lagoon carbonates reach values of δ^{13}C above + 3‰. This enrichment is directly associated to the depositional environment that provided an intense biological activity with the abundant proliferation of brachiopods and echinoderms, monoseriate foraminifera and rare ostracods. The partial confinement of those bounded by barrier islands and carbonate shoals that allowed interaction with open water and a homogenization of the isotopic signal. A significant enrichment of the ^{13}C isotopic signal for the shelf carbonates from + 3.65‰ to + 5.28‰ coincides with the transgressive trend of the Itaituba succession. The proximal + 3‰ values are associated with the bioclastic bar microfacies and the innermost portion of the shelf. The abundance of bioclasts and terrigenous from the shelf waves reworking processes and the extensive enrichment of ^{13}C indicates a strong colonization of the biota and high consumption of ^{12}C typically by organisms of open shallow seas of Pennsylvanian age. This positive excursion recorded in the Itaituba succession is more enriched than the average recorded for the Pennsylvanian Oceans.

According to Brand *et al.* (2009) this anomaly is related to the epicontinental nature of marine deposits with thicknesses lower than 80 m, with seas characterized by a wide reservoir

of carbon arising from the proliferation of specimens of shallow seas (Immenhauser *et al* 2002).This characteristic is observed in the epicontinental seas from the Mesodevonian to the Neopermian with extensive positive excursions in the Pennsylvanian and Permian and negative excursions during the Mississippi (Brand *et al*. 2009, Immenhauser *et al* 2003).

The values of $\delta^{13}C$ of $+3\%$ o reaching to $+3.88\%$ o coincide with the values proposed for the Bashkirian global oceanic curves, the same age is proposed by Scomazzon *et al* (2016) for the unit based on the occurrence of rare conodonts *Idiognathodus incurvus*. This period coincides with a relative increase in sea level originating from an interglacial interval and can be compared with the overall Pennsylvania curve and is similar to the isotopic data obtained for the initial portion of the Moscovian (Davydov *et al.* 2012). The age provided by conodonts is relatively large and ranges from the basal portion of the Bashkirian to the Moscovian age (Scomazzon *et al.* 2016, Moutinho *et al.* 2016b). A Bashkirian age was proposed for the top of the Monte Alegre Formation based on the stratigraphic positioning of conodonts (Matsuda 2002, Scomazzon *et al.* 2006, Moutinho *et al.* 2016a, 2016b). However, impoverished data of $\delta^{13}C$ ranging from $+0.58$ ‰ to $+1.57$ ‰ VPDB found in lagoon deposits of the Monte Alegre Formation, on the northern edge of the Amazonas Basin, located stratigraphically below the dolomitic and calcitic marine deposits of the Tapajós River region, are more consistent with the values of $\delta^{13}C$ proposed for the Serpukhovian-Bashkirian boundary (Davydov *et al.* 2012, Brand *et al.* 2015). Limarino *et al* (2011) describes Serpukhovian as one of the periods of greatest expansion of the southern glacial cover of Gondwana, which resulted in an eustatic sea level demotion and a continental aridification process.

The process of continental aridification marks paleotropical deposits from the end of the Mississippian (Serpukhovian) to Bashkirian represented by sea-level fluctuations with intercalation of continental and marine carbonate shallow deposits (Handford & Francka 1991, Aleeksev *et al.* 1996). Thus, the isotopic data associated with the presence of aeolian deposits suggests that the top of the Monte Alegre Formation may belong to the Serpukhovian-Bashkirian boundary. In fact, the lower and unexposed portion of the Monte Alegre Formation remains undetermined, but the possible recognition of the top of the Mississippian for the outcrop portion may suggest this age for the remainder of the unit that reaches 140 m thick (Cunha *et al.* 2007).

7. ORIGIN OF HIGH FREQUENCY CYCLES

7.1. Sea-level changes and stacking pattern of cycles

Global eustatic variations are observed in cycles of increase and decrease of sea level, observed in several localities, controlled directly by the availability of sediments, subsidence rate and tectonic activity (Catuneanu, 2006). Glacial and interglacial periods, combined with the effects of regional tectonics and eustasy, may control the high frequency cyclic stacking patterns, as is the case of the Pennsylvania deposits of the Amazonas Basin. The preparation of an isotopic carbon curve enhances stratigraphic resolution and can be used as a reference for assessing sea level high frequency variations in carbonate deposits (Mitchell *et al.* 1996, Haq *et al.* 1988, Haq & Schutter 2008, Hardenbol *et al.* 1998). In the carboniferous deposits of the southern border of the Amazonas basin, the variation in the isotope curve obtained in the transition of the Monte Alegre-Itaituba formations, suggest an onlap curve, evidencing regional increase and decrease of sea level, with metric shallowing upward cycles, inserted in aggradational and retrogradational intervals (Figure 8). The different patterns in the stratum stacking were identified using the fisher plot graphic (Fischer, 1964, Sadler *et al.* 1993, Tucker &Harland 2010).

The high frequency stratigraphy associate with Fisher plot graphic provides the meter-scale cycles origin, that include: i) autogenic sedimentary models associated with the tidal flat progradation and islands migration (James 1984, Lehrmann & Goldhammer 1999), ii) tectonic mechanisms that reflect subsidence or uplift of accommodation space controlled by local or regional tectonics (Bosence *et al.* 2009), iii) eustatic related the sea level variation in function orbital forcing and glacioeustasy (Goldhammer *et al.* 1990, Lehrmann & Goldhammer 1999). Thus, it was possible to determine two cycles along the studied sequence organized in a composite profile (Figure 9), combining with other proxies for the Carboniferous. A total of 53 asymmetric reassembly cycles with a mean of 1.13 meters thickness were identified, with a negative stacking pattern, and their genesis associated with reduced initial accommodation space (Tucker and Harland, 2010). Five types of tidal cycles are described, grouped in: a) costal/eolian cycles; b) supratidal cycles; c) intertidal cycles; d) lagoonal cycles; e) Shelf cycles. These cycles present a retrogradational and aggradational tendencies included within a transgressive system tract, formed by the intercalation of continental coastal deposits superimposed by shallow marine deposits, marking the initial phase of one of the several marine floods that affected the planet's Cratonic regions during the Pennsylvanian (Almeida &

Carneiro, 2004, Davydov *et al.* 2012). Individual cycles accumulated in an average of ~0.25 my (53 cycles/~13 my; see figures 8 and 9) and thus represent fourth order cycles linked to high-frequency fluctuations of relative sea level. Tucker & Harland (2010) propose that ages based on the fourth order glacial-eustatic cycles can vary from 20ky to 400ky depending on the type of movement responsible for their generation, which are consistent with 133ky to 210 ky ages proposed by Matsuda (2002), suggesting a long precession phase.

The cycles can be originated by autochthonous or allochthonous sedimentation processes (Strasser *et al.* 2006), where in the first, the change of cycles are caused by factors internal to the depositional environment, whereas in the later cycles change are due to external factors (Spencer & Tucker, 2007). In this way, the supratidal and intertidal cycles are autochthonous, formed by the migration of the tidal channels, the other cycles are allochthonous, formed by the marine influence in the Amazonas Basin, with an average thickness of approximately of 45 meters. The variation of the sea level curve in the work area, supported by the data of the δ^{13}C curve, position the Itaituba Formation in the Upper-Moscovian to Upper Serpukhovian range (320-309 Ma), linking the δ^{13}C isotopic curve with the global sea level curve (Haq &Schutter 2008).
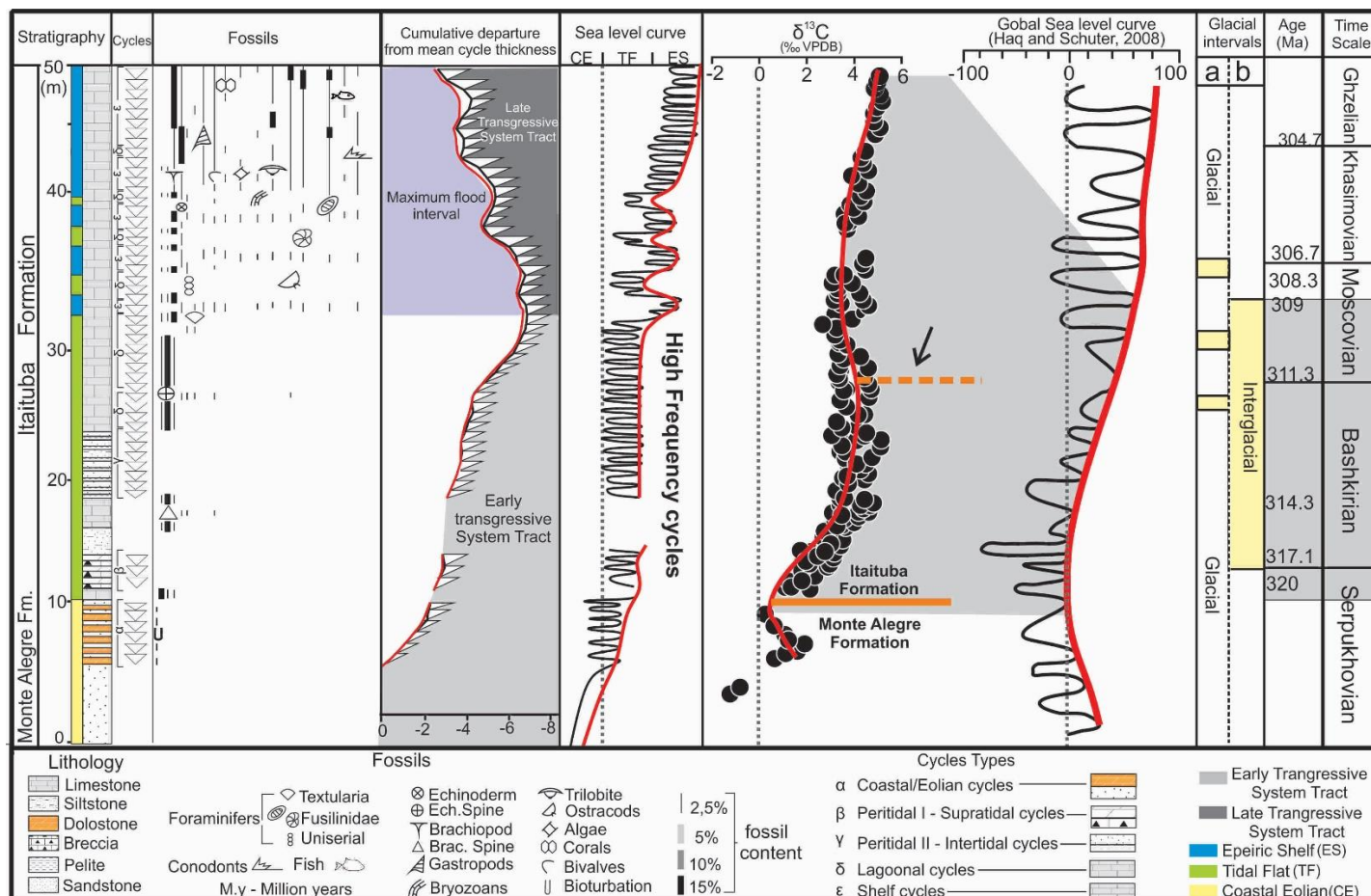
Figure 8- Stratigraphic analysis of Monte-Alegre-Itaituba succession of the Amazonas Basin. The analysis compares stacking pattern of mixed siliciclastic-carbonate cycles with frequency the fossils, fisher plot data, high frequency and $\delta^{13}C$ curves and the correlation with global relative sea-level curve for the Carboniferous. Fisher Plots graph associated with the composite profile of the study area, representing the stacking of 53 cycles with average 1.13 meters in thickness. Facies and facies associations are representative of a transgressive system tract. A single surface defining the point of maximum flooding may not be identified, and a maximum flooding zone is recognized instead. The previous interpreted interglacial interval for Bashkirian (letter a) was enlarged in this work (letter b) based on correlation between the Monte Alegre- Itaituba and the Carboniferous global sea-level curves. The enriched values of $\delta^{13}C$ upsection suggested high consume of ^{12}carbon coincident with increase of biological activity indicated by densely fossiliferous beds. These data allowed calibrate the stratigraphic position of both formations with limit previously close to the Bashkirian-Moscovian boundary (arrow) and now repositioned in the base of Bashkirian and top of Serpukhovian, confirming a Mississippian age for Monte Alegre Formation. The age estimation for deposition of the studied succession is approximately 13 Ma (grey interval).

7.2. Glacio-eustasy x thermal (flexural) subsidence

The origin of high-frequency cycles (fourth order cycles) is related to the relative sea-level rise with high potential of preservation, particularly during progradational events (Strasser 1991, James 1984, Pratt & James. 1986). The authigenic cause for cyclicity are the sedimentological and paloenvioronmental changes related to specific lateral variations of facies/microfacies, differences in terrigenous and allochemical content and, as well as, the Fossiliferous diversity (Einsele *et al.* 1991, Harland 2010, Tucker & Wright, 1990, Strasser *et al.* 2006, Bádenas *et al*. 2010). The more common autoghenic cycles are peritidal, controlled directed by marine influence (Strasser 1991), the most common models for its preservation are the tide plain progradation (James 1984) and the island model (Pratt & James. 1986). Nonetheless, allochthonous cycles are originated by changes in terrestrial obliquity, orbital precession or even Milankovitch cycles (Einsele *et al.* 1991, Schwarzacher 1993, Strasser *et al.* 2000, Berger 1977, Berger 1989). These changes would represent periods of sea level changes related to expansion and retreat of ice sheets, which gives a cyclic nature of deposits similar to those described for the Neogene to Recent (Abdul Aziz *et al.* 2003, Dinares-Turrel *et al.* 2003).

Cyclic sedimentation recorded in extensively exposed and well-studied Carboniferous cyclothems in the northern hemisphere reflect repeated fluctuation in base sea level (e.g. Ramsbottom, 1979, Ross & Ross, 1985, 1987, Caputo & Crowell, 1985, Heckel 1986,1994, Algeo & Wilkinson 1988, Dickinson et al. 1994). These rocks were deposited in equatorial regions of Pangea (cf. Scotese & McKerrow 1990), and, are primarily know in North America and Europe, where they form vertically stacked transgressive-regressive successions of nonmarine, nearshore and offshore clastic and carbonate deposits (e.g. Moore 1964, Ramsbottom 1979, Maynard &Leeder 1992, Heckel 1994). It is widely consensus that late Paleozoic sea-level fluctuations were caused by changes in ice sheet volume (e.g., Crowell 1978, Veevers & Powell, 1987). However, before the cause and effect between Gondwana glaciation and cyclothems can be accepted, at least two questions must be addressed: (1) was the glaciation penecontemporaneous to the interval of cyclic sedimentation? and (2) were the late Paleozoic ice sheets large enough to account for the inferred changes in sea level?

Gondwana strata contains at least three non-overlapping glacial successions. Glacial I (Frasnian to possibly Tournaisian) and Glacial II (Serpukhovian to Bashkirian) both strata deposited due to alpine glaciers (Figure 8). The duration of glacial and interglacial periods during the Carboniferous differs between authors (Figure 8 and 9). Haq & Shutter (2008) consider the predominance of glacial conditions of ten million years interchanged with reduced

stages of interglacial of thousands of years (Figure 9). In contrast, other authors consider glacial and interglacial intervals with similar amplitude of dozens of millions of years indicated by glacial stages I, II and III (Figure 8). There is a consensus between author that the glaciers waxing related to stages I and II was insufficient to change the base-level. In contrast, Upper Carboniferous (Kasimovian to Early Gzhelian) to lower Permian Glacial III rocks extensive ice sheets, that covered large parts of the Gondwana, generated a eustatic change of ~100m. With the new inferred age for the Monte Alegre-Itaituba successions in the Amazonas Base–Late Serpukhovian to Early Moscovian- it is untenable to argue that Glacial II influenced in the deposition of these high-frequency cycles. In addition, glaciogene strata was never observed interbedded with coastal plain and shelf carbonate deposits of these succession, coadunate with little or no influence of Glaciation II in the northern part of the South America continent.

Aggradational to retrogradational stacking pattern observed in the carbonate deposits of Monte Alegre succession are better explained as a record of long-term post-glacial transgression. And, as mentioned above, the interglacial interval in the Amazonas basin was adjusted to Bashkirian to early Moscovian age. The long-term post glacial transgression (glaciation II) from the Panthalassa Ocean, from the west, entered Gondwana affecting an area of more than 1,000,000 km2 encompassing the west border basins of Gondwana (Acre, Solimões, Amazona basins) and a little portion of the North part of the Parnaíba Basin (Millani & Thomaz Filho 2000, Cunha, 2007, Wanderley Filho *et al.* 2007, Cunha *et al.* 2007, Palagi, 2009, Medeiros *et al.* 2019).

The origin of the cycles is intrinsically related to the sedimentary evolution of the Monte Alegre-Itaituba succession. The Cycle type I is allogenic generated during the transition between lowstand and early transgressive phase, where the icehouse conditions were replaced by greenhouse period during Late Mississippian and Early Bashkirian. The beginning of the transgression is marked by the progressive burial of the coastal dunes and the implantation of the mixed and carbonate tide plains (Cycle I) generating aggradational cycles. These deposits may indicate the end of a lowstand sea system tract still related to the end of the glaciation II phase. The cycles II and III were formed by autochthonous processes linked to installation of tidal flats/lagoon settings and tidal channel migration. Periods of subaerial exposure and local erosion in these settings were inherent to paleoenvironmental modifications. The cycles IV and V were strongly influenced by Bashkirian-Moscovian post-glacial sea-level rise. A slow thermal subsidence typical of the intracratonic basin, together with the transgressive pulses generated the asymmetric cyclicity observed in the Monte-Alegre Itaituba succession. This

continuous subsidence can has amplified the marine transgression and suppress the marine regression, culmination in a retrogradational tendency upsection (Cycles IV and V). Additionally, no tectonic causes of regional marine regression were identified in the time for the deposition of a single cycle.

The continuous flooding of the Itaituba epicontinental sea expands its limits reaching the northern portion of the Parnaíba Basin (see Medeiros *et al.* 2019). The continuous aggregation of the Pangea provided several collision events which in turn promoted the uplift and regressive pulses that can influenced the morphology of epicontinental seas at the end of the Moscovian. The predominant carbonate sedimentation was gradually replaced by a carbonaceous / evaporitic sedimentation, represented by the Nova Olinda Formation, interpreted as great saline lakes and *sabkha* plains (Cunha *et al.* 1994, Matsuda *et al.* 2004, Vaz *et al.* 2007). The isolation of the internal seas was accentuated during the Permian with formation of the Variscan orogeny that uplift great part of the region continentalization again the basin. The continental aggregation process is completed with the formation of the Pangea supercontinent, completely uplifting the Northwest portion of Gondwana.
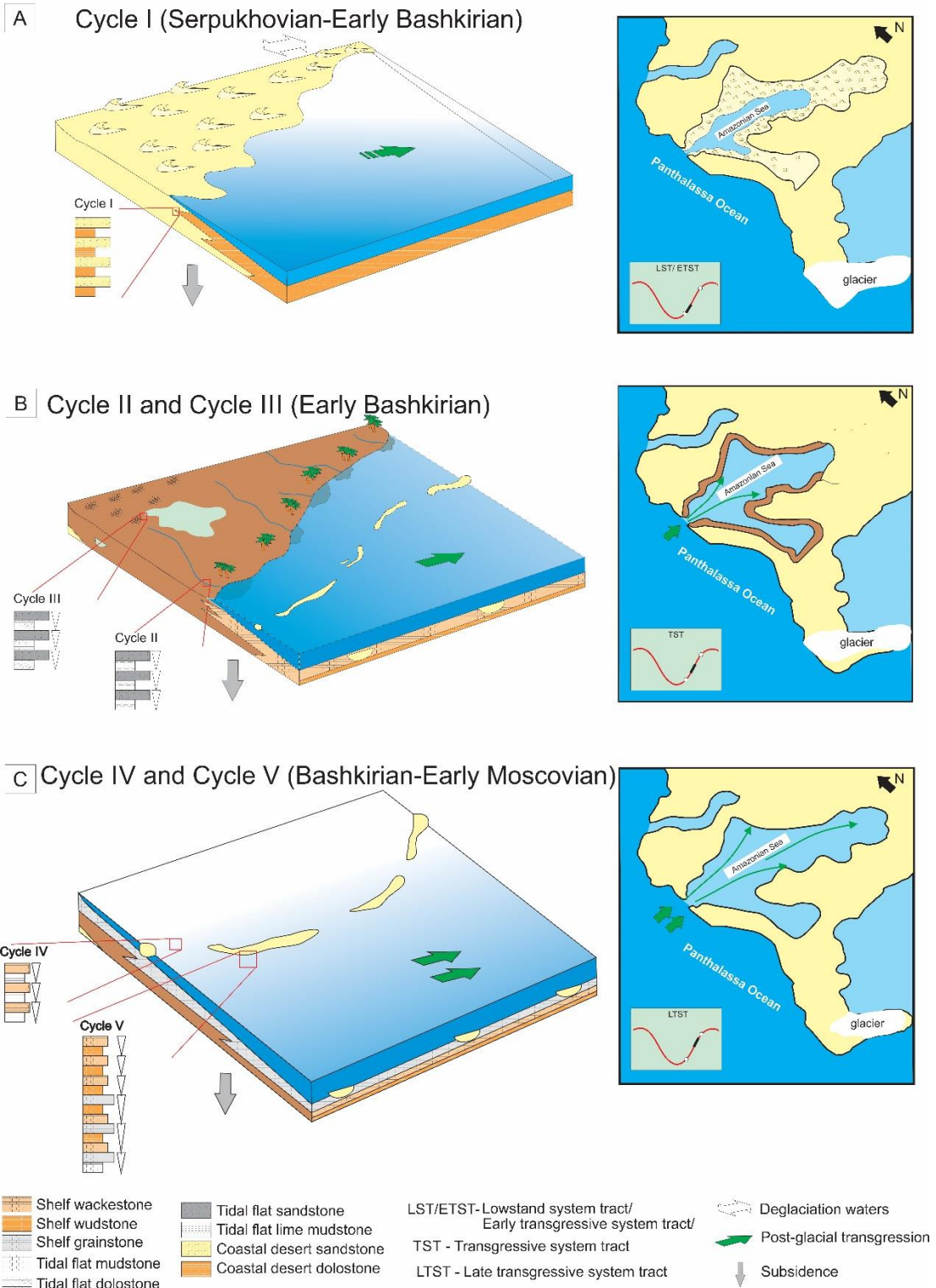
Figure 9: Late Mississippian to Early Pennsylvanian high frequency fluctuations in the Western Gondwana. A- The final lowstand phase was characterized by large dune fields developed in the margin of epicontinental sea. The coastal plain was progressively flooded triggered by deglaciation waters recorded mainly in tidal flat and lagoon aggradational cycles. B- The slow transgression combined with constant and progressive subsidence caused a period of stagnation in the sea margin with low accommodation space that propitiated the development of tidal flats with tidal channels recorded in autogenic cycles. The Itaituba epicontinental sea become larger but its extension not trespassing the Central Amazonia. C- The post-glacial transgression is amplified causing the invasion of the Panthalassa waters and the enlargement of Itaituba epicontinental sea that reach the inland portions of Western Gondwana. The increase of accommodation space resulted in the deposition of shallow marine carbonate cycles characterized by proliferation of a marine benthic assembly and paleoceanographic modifications in the carbon cycle.

8. CONCLUSIONS

Mixed-carbonate-siliciclastic high-frequency cycles represents the main pattern to recognize the factors controlling deposition in Paleozoic carbonate shelf in the Gondwana. The example used here from the Amazonas Basin, 50m-thick Late Mississippian-Pennsylvanian Monte Alegre-Itaituba succession shows a pervasive cyclicity trend that include coastal desertic, tidal flat and marine shelf deposits typical of an epicontinental sea. Five types of fourth order shallowing upward cycles were described: I) alternance of dolostone and sandstone; II) interbedded of sandstone-mudstone and sandstone-mudstone-floatstone rhythmites; III) dolostone interbedded with sandstone; IV) rhythmite formed by wackestone/lime mudstone couplets; and V) consisting by alternance of grainstone, wackestone and mudstone passing upsection for asymmetric cycles composed by wackestone and lime mudstone.

The stacking of 53 cycles with average thickness with average of 1,1 m, combined with *Fisher plot diagram*, indicated an aggradational to retrogradational stacking pattern. The cycles were accumulated in an approximately 0.25 my and thus represent fourth order cycles related to high-frequency fluctuations of relative sea level. The lowermost succession recorded a lowstand to early transgressive system tracts (Cycles I-III) while the uppermost portion represents a prominent late transgressive system tract (Cycles IV and V). The $\delta^{13}C$ curve exhibits enriched trend upward ranging from ~+0.58 to ~+5.28‰, interpreted as representative of Pennsylvanian epicontinental seawater. The facies succession presents the following $\delta^{13}C$ values: 1) peritidal in coastal desertic siliciclastic deposits ranging from -1.5 to +0.3‰; 2) tidal flat and lagoon deposits ranging from +3,98‰ to +4, 62‰; and 3) shelf deposits ranging from +3,65‰ a +5,28‰. The $\delta^{13}C$ values is more enriched than values found to Panthalassa waters and must be local variation as resulted of the high proliferation of organism in the upper carbonate succession coadunate with maximum flooding and high productivity of organic carbon. The correlation between the isotope record and the relative sea-level curves supports the close association between paleoceanographic changes and paleoenvironmental evolution during the Pennsylvanian.

The explanation of high frequency cycles in Monte Alegre-Itaituba succession was completely disconnected of fluctuations of glacial ice volume in Gondwana. This premise used the waxing and waning of these massive ice sheets have produced the changes in base level recorded by cyclothems. Although the Pennsylvanian was a glacial period, the glaciers were restricted to continental portions of the South Pole and not influenced significantly the increase of the relative level of the sea in the Itaituba epicontinental sea. The reevaluation of studied

succession age based on the calibration of $\delta^{13}C$ curve combined with high frequency cycles analysis that were compared with the global Carboniferous $\delta^{13}C$ and sea-level curves. This procedure allowed the stratigraphic position adjustment of Monte Alegre-Itaituba succession. The previously Bashkirian to Moscovian age based only in conodonts was refined for Late Serpukhovian to Early Moscovian. The possible end of glacial influence, if occurred, was recorded in the Serpukhovian to Early Baskhirian Monte Alegre deposits (Cycle I), possibly during the end of lowstand phase. In contrast, the interglacial interval was marked by prominent post-glacial transgressive pulses (Cycles IV and V) combined with slow and continuous subsidence of the basin. Although, the succession analyzed in the Amazonas basin is not complete was possible the use of high-resolution procedures that revealed an important part of evolutionary history of Itaituba Formation open perspectives to guide future studies with the same focus showed here and to understand the Pennsylvanian events post-implantation of the Itaituba epicontinental sea that preceded the formation of Pangea.

Acknowledgements

CAPÍTULO 6 CONSIDERAÇÕES FINAIS

O estudo das fácies e microfácies sedimentares, dos dados de conodontes, dos processos diagenéticos, da ciclicidade e os resultados obtidos para os isótopos estáveis de δ^{13}C e δ^{18}O permitiram traçar a reconstrução paleoambiental juntamente com a gênese da ciclicidade e assim posicionar corretamente as unidades estudadas nas bordas Norte e Sul da bacia do Amazonas no limite Mississipiano-Pensilvaniano.

As análises de fácies sedimentares e microfácies carbonáticas revelaram a ocorrência de três paleoambientes deposicionais: deserto costeiro (AF1), planície de maré mista (AF2) e plataforma carbonática epicontinental (AF3). O deserto costeiro é composto por arenitos muito finos a médios, pelitos e dolomitos, subdividido em cinco subambientes, representados por: campo de dunas eólica, lençol de areia, canal fluvial, interduna e a porção carbonática bioturbadas por *Palaeophycus*, *Lockeia*, *Thalassinoides* e *Rosselia*. A planície de maré mista é constituída por arenitos finos a médios, pelitos, folhelhos, siltitos e calcários caracterizados por subambientes de supramaré, canais de maré, delta de maré, laguna siliciclástica e laguna carbonática, a ocorrência de bioclastos de braquiópodes e equinodermas indicam uma conexão marinha restrita deste ambiente, diretamente associado aos processos de maré. A plataforma carbonática epicontinental é composta por *lime mudstones, wackestones, packstones* e *grainstones*, subordinadamente arenito carbonático, correspondentes a um sistema de barras e baixios carbonáticos conectados a plataforma colonizada por organismos marinhos bentônicos, como: braquiópodes, briozoários, conodontes, corais, equinodermas, foraminíferos, gastrópodes, ostracodes, trilobitas e peixes. A ocorrência dos conodontes *Neognathodus symmetricus, Streptognathodus sp. e Ellisonia sp*. em AF3 posiciona a porção basal da Formação Itaituba, registrada na área de estudo, como pertencente ao intervalo Baskiriano-Moscoviano, o qual é descrito em diversas biozonas em Gondwana.

A análise dos dados diagenéticos revelou que os arenitos das formações Monte Alegre e Itatiuba foram submetidos aos processos de compactação física, porosidade, cimentação de calcita equigranular, cimentação de sílica, dolomitização, piritização, formação de óxidos e hidróxidos de ferro e a alteração mineral. Os processos mesodiagenéticos se restringem apenas aos contatos côncavos-convexos dos grãos nos arenitos. Já os carbonatos das duas unidades, apresentam uma sequência de eventos com composta por micritização, nemorfismo, compactação física, porosidade, cimento de calcita fibrosa, cimento de calcita em *bladed*, cimento de calcita equigranular, cimento de

calcita espática, cimento de sílica, a dolomitização e a Piritização. Os processos mesodiagenéticos são associados a compactação química e a silicificação. Esta sequência de eventos diagenéticos e ampla precipitação de cimentos fazem com que os carbonatos das duas unidades apresentem uma baixa porosidade e permeabilidade associando estas feições a ampla precipitação de carbonatos, indicando que os sinais isotópicos de carbono e oxigênio, que corroboram com a assinatura original dos valores de δ^{13}C. Estes valores de isótopos variam de -2‰~ a +5, 28‰. Esta tendência enriquecida se coaduna com a alta produtividade orgânica, desencadeada pelo florescimento maciço de organismos bentônicos de controle eufótico, principalmente em AF3.

A análise estratigráfica de alta frequência identificou cinco tipos de ciclos de raseamento ascendente e assimétricos na sucessão Monte Alegre-Itaituba. Ciclos de perimaré em deserto costeiro (ciclo I), formados pela alternância de dolomitos e arenitos com valores de δ^{13}C variando de -1, 5‰ a +0, 3‰. Os ciclos II consistem em intercalações de arenito pelito e arenito *floatstone* e o ciclo III é composto por alternância de dolomitos e arenitos. Estes ciclos são interpretados como depósitos de planície de maré e laguna com valores de δ^{13}C alcançando de +3, 98‰ a +4, 62‰. O ciclo IV é um ritmito formado por pares de *wackestone/lime mudstone,* enquanto o ciclo V consiste na alternância de *grainstones, wackestones* e *lime mudstones* (ciclicidade ABC) passando para ciclos compostos por *wackestones* e *lime mudstones* (ciclicidade AB). Os ciclos IV e V são depósitos de plataforma com valores de δ^{13}C variando de +3, 65‰ a 5, 28‰. O padrão de empilhamento dos 53 ciclos com uma média de 1, 13 m, através do gráfico de *Fischer plot diagram,* consistiu em uma média de 1, 13m*,* refletindo uma tendência agradacional a retrogradacional. Os ciclos foram acumulados em aproximadamente 0, 25 ka associados a flutuações do nível do mar de alta frequência. típicos de ciclos de quarta ordem. Estes dados foram correlacionados com as curvas globais de δ^{13}C e do nível do mar, que posicionaram a sucessão Monte Alegre-Itaituba no Serpukhoviano Superior ao Moscoviano inferior. A influência da glaciação Mississipiana foi insignificante nestes depósitos, mas a transgressão pós-glacial associada a lenta subsidência da Bacia do Amazonas gerou os ciclos I, IV e V, enquanto os demais ciclos foram gerados por processos autóctones ao ambiente deposicional. A sucessão Monte Alegre-Itaituba é o registro de um grande mar epicontinental amazônico que estava diretamente ligado ao Oceano *Panthalassa* durante o Pensilvaniano.

REFERÊNCIAS

Abdul Aziz, H. Hilgen, F. Krijgsman, W. Calvo, J. 2003. An astronomical polarity time scale for the late middle Miocene based on cyclic continental sequences. *Journal of geophysics research.* **108**. 1-16 p.

Adams, A. Mackenzie, W. Guilford, C. 1984. Atlas of sedimentary rocks under the microscope. 2. ed. Harlow. Longman. 104p.

Ahlbrandt, T. & Fryberger, S. 1982. Introduction to eolian deposits. In: Scholle, P. A., Spearing, D. (Eds.), *Sandstone Depositional Environments*. The Am. Ass. Pet. Geologists, Tulsa, OK, pp. 11-14.

Albuquerque, O. R. 1922. Reconhecimentos geológicos no vale do Amazonas. *Boletim do Serviço Geológico Mineral*. Rio de Janeiro, 3:1-84.

Algeo, T. & Wilkinson, B. 1988. Periodicity of mesoscale Phanerozoic sedimentary cycles and the role Milankovitch orbital modulation. *Journal of geology*. **26**: 515-542.

Allan, J.R., Matthews, R.K., 1982. Isotope signatures associated with early meteoric diagenesis. *Sedimentology*, 29(**6**):797-817.

Allen, J. 1982. Sedimentary structures: Their character and physical basis volume1. Elsevier. Amsterdam. 594p.

Almeida, F. & Hasui, Y. 1984. O Precambriano do Brasil. Ed. Edgard Blucher, São Paulo. 378p.

Almeida, F. F. M. & Carneiro, C. D. R. 2004. Inundações marinhas fanerozóicas no Brasil e recursos minerais associados. In: V. Mantesso-Neto, A. Bartorelli, C. D. R. Carneiro, B. B.Brito-Neves (Orgs.). *Geologia da continente Sul-Americano: Evolução da obra de Fernando Flávio Marques de Almeida.* São Paulo: Beca. p. 43-58.

Anelli, L. 1999. *Invertebrados Neocarboníferos das formações Piauí (bacia do Parnaíba) e Itaituba (bacia do Amazonas), taxonomia e análise cladística das subfamílias Oriocrassatellinae (Crassatellacea, Bivalvia) e Neospiriferinae (Spiriferoidea, Brachiopoda).* Tese de dourado. Instituto de Geociências. Universidade de São Paulo. São Paulo. 184p.

Athy, L.F. 1930 Density, Porosity and Compaction of Sedimentary Rocks. AAPG Bulletin. **14.** 1-24.

Bádenas, B. Aurell, M. Bosence, D. 2010. Continuity and facies heterogeneities of shallow carbonate ramp cycles (Sinemurian, Lower Jurassic, (Northeast Spain). *Sedimentology*. **57** (4). 1021-1048.

Barale, L. Bertok, C. Talabani, N. Atri, A. Martire, L. Piana, F. Préat, Al. 2013. Very hot, very shallow hydrothermal dolomitization: Na example of Maritimi Alps (North-western Italy-South-East France). *Sedimentology*. **63** (7). 2037-2065.

Bathurst, R. 1971. Carbonate sediments and their diagenesis. Developments in sedimentology 12. Amsterdam. Elsiever. 658p.

Berger, A. 1977. Long term variations of the Earth's orbital elements. *Celestial Mechanics.* **15**:53-74.

Berger, A. 1989. Astronomical frequencies over the Earth's history for paleoclimate studies. *Terra Nova*. **1**:474-479.

Berner, R. & Raiswell, R. 1983. Burial of organic carbon and pyrite sulfur in sediments over Phanerozoic time: a new theory. *Geochim. Cosmochim. Acta.* **47**. 855-862.

Berner, R. A. & Kothavala, Z. 2001. GEOCARB III: a revised model of atmospheric CO2 over Phanerozoic time. *American Journal of Science*, 301(**2**):182-204.

Berner, R. A. 1983. Sedimentary pyrite formation: An update. Geochimica et cosmochimica Acta. Vol 48. 605 – 615p.

Bezerra, I. S. 2018. *O Cenozoico Superior do Centro-Leste da Bacia do Amazonas: Paleobotânica do embasamento Cretáceo e evolução do rio Amazonas*. Tese de doutorado. Instituto de Geociências. Universidade Federal do Pará. Belém. 144p.

Boardman, D.R., II, and Heckel, P.H., 1989, Glacial-eustatic sea-level curve for early Late Pennsylvanian sequence in north-central Texas and biostratigraphic correlation with curve for midcontinent North America. *Geology*. 17(**9**):802-805

Boggs JR. S. 1992. Petrology of sedimentary rocks. New York. Bookmark. 707p.

Boggs, S. 2006. Petrology of Sedimentary rocks. 2nd edition. Cambridge press. 600p.

Boggs, S. and D. Krinsley, 2006, *Application of Cathodoluminescence Imaging to the Study of Sedimentary Rocks*: Cambridge University Press, Fig. 4.5, p. 65,

Bosence, D., Procter, E., Aurell, M., Bel Kahla, A., Boudagher-Fadel, M., Casaglia, F., Scherreiks, R. 2009. A dominant tectonic signal in high-frequency, peritidal carbonate cycles? A regional analysis of Liassic platforms from Western Tethys. *Journal of Sedimentary Research*, 79(**6**):389-415.

Brand, U., 2004. Carbon, oxygen and strontium isotopes in Paleozoic carbonate components: an evaluation of original seawater-chemistry proxies. *Chemical Geology*. **204**:23-44.

Brand, U., Azmy, K., Griesshaber, E., Bitner, M.A., Logan, A., Zuschin, M., Ruggiero, E., Colin, P.L. 2015. Carbon isotope composition in modern brachiopod calcite: A case of equilibrium with seawater? *Chemical Geology*. **411**:81-96.

Brand, U., Tazawa, J. I., Sano, H., Azmy, K., & Lee, X. 2009. Is mid-late Paleozoic ocean-water chemistry coupled with epeiric seawater isotope records? *Geology*, 37(**9**):823-826.

Bridge, J. & Demicco, R. 2008 (Eds.). *Earth surface processes, landforms and sediments deposits. Cambridge university press*. 1st edition 815p.

Brookfield M. 1992. Eolian systems. In Walker R. James, N (eds) *Facies models: response to sea level change,* Geological Association of Canada. Geotext 1: 143-156p.

Brookfield, M. & Silvestro, S. 2010. Eolian system. In James, N. Dalrymple, R (eds) *Facies Model 4*. Geological association of Canada. Geotext 6.139-166p.

Caputo, M. 1984. *Stratigraphy, tectonics, paleoclimatology and paleogeography of northern basins of Brazil*. PhD Thesis. University of California. Santa Barbara. 583p.

Caputo, M. Crowell, J. 1985. Migration of glacial centers across Gondwana during Paleozoic Era. *Geological society of America Bulletin*. **96**:1020-1036.

Caputo, M. Rodrigues, R. Vasconcelos, D. 1971. Litoestratigrafia da bacia do Amazonas. Petrobrás. Relatório interno, 641p.

Catuneanu, O. 2006. *Principles of sequence stratigraphy*. Elsevier. Amsterdam. 375p.

Cheel, R.J., Leckie, D.A. 1992. Coarse-grained storm beds of the Upper Cretaceous Chungo Member (Wapiabi Formation), southern Alberta, Canada. *Journal of Sedimentary Petrology*, 62(**6**):933-945

Choquette, P.W. & Pray, L.C. 1970. Geologic nomenclature and classification of porosity in sedimentary carbonates; *AAPG Bulletin*. 54(**2**):207-250

Clemmensen, L. Pye, K. Murray, A. Heinemeier, J. 2001. Sedimentology, stratigraphy and landscape Evolution of a Holocene coastal dune system. Lodbjerg, NW Jutland, Denmark. *Sedimentology*. 48. 3-27p.

Cordani, U. G., Brito Neves, B. B. D., Fuck, R. A., Porto, R., Thomaz Filho, A., & Cunha, F. M. B. (1984). Estudo preliminar de integração do Pré-Cambriano com os eventos tectônicos das bacias sedimentares brasileiras. Ciência. Técnica. Petróleo. Seção: Exploração de Petróleo, 14:1-70.

Costa, A. 2002. Tectônica Cenozóica e movimentação salífera na Bacia do Amazonas e suas relações com a geodinâmica das placas da América do Sul, Caribe, Cocos e Nazca. Belém. CG/UFPA. Dissertação de Mestrado. 238p.

Costa, M. & Selbach, H. 1981. Estudo sedimentológico da Formação Monte Alegre na área de Autás-Mirim, Bacia do Amazonas. Relatório Interno. Rio de Janeiro, PETROBRÁS/DEPEX/LABOR/DENOR/DINTER, 38 p.

Crowell, J.C. 1978. Gondwanan glaciation, cyclothems, continental positioning, and climate change. *American Journal of Science*, 278(**10**):1345-1372.

Crowley T.J., Yip K-J.J., Baum S.K., Moore S.B. 1996. Modelling Carboniferous coal formation. *Paleoclimates* 2:159–77

Cunha, P. 2007. Bacia do Acre. *Boletim de Geociências da Petrobrás*. 15(**2**):207-215

Cunha, P. R. C.; Gonzaga, F. G.; Coutinho, L.F.C. Feijó, F. J. 1994. Bacia do Amazonas, *Boletim de Geociências Petrobrás*, 8. n1. 47 – 55p.

Cunha, P., Melo, J. & Silva, O. 2007. Bacia do Amazonas, *Boletim de Geociências*. Manaus. Petrobrás. 15(**2**):227-254.

Curtis, C. & Coleman, M, 1986: Controls on the precipitation of early diagenetic calcite, dolomite and siderite concretions in complex depositional sequences. In: Gautier, D. L. (Ed.), Roles of organic matter in sediment diagenesis. Society of Economic Paleontologists & Mineralogists, Special Publication 38, 23-33.

D'Alpaos, A. Lanzoni, S. Marani, M, Fagherazzi, S. Rinaldo, A. Tidal network ontogeny: channel initiation and early development. *Journal of geophysics research*. vol110. 1-14p.

Daemon, R. & Contreiras C. 1971. Zoneamento palinológico da Bacia do Amazonas. In: SBG Congresso brasileiro de geologia. 25. São Paulo. Anais. 3. 79 – 92p.

Dalrymple, R. 1992. Tidal depositional systems. In Walker, R. James, N. (eds) *Facies models: a response to sea level change.* Geological association of Canada. Ontario. p. 195-218.

Dalrymple, R. Choi, K. 2007. Morphologic and facies trends through the fluvial-marine transition in the tide-dominated depositional systems: a sistematic framework for environmental and sequence-stratigraphic interpretation. *Earth Science reviews*. 81:135-174.

Davydov, V. Korn, D. Schimitz, M. 2012. The Carboniferous periods. In Gradstein, F. Ogg, J. Schimitz, M. Ogg, G. (eds). *Geological time scale*. Amsterdam. Elsevier. p. 603-651.

Dickinson, W. Soreghan, G. Giles, K. 1994. Glacio–eustatic origin of Permo–Carboniferous stratigraphic cycles: Evidence from the Southern Cordillerean foreland region. In Dennison, J. Ettensohn, F. (eds) *Concepts in sedimentology and paleontology*. Vol 4. Society for sedimentary geology. Tulsa. 25 - 34p.

Dietrich, R., Hobbs Jr, C., Lowry, W. 1963. Dolomitization interrupted by silicification. *Journal of Sedimentary Petrology*. 33(**3**):646-663.

Dinares – Turrell, J. Baceta, J. Pujalte, V. Orue – Etxebarria, X. Bernaola, G. Lorito, S. 2003. Untangling the Paleocene climatic rhythm: an astronomically calibrated Early Paleocene magnetostratigraphy and biostratigraphy at Zumaia (Basque basin, Northern Spain). *Earth planetary science letters*. **216**. 483-500p.

Dunham, R. 1962. Classification of carbonate rocks according to deposicional texture. In: Ham, W. (ed). *Classification of carbonate rocks*. Tulsa: AAPG. (Memoir 1). p. 108-121.

Einsele, G. Ricken, W. Seilacher, A. (1991). *Cycles and events in stratigraphy*. Springer –Verlag. Heidelberg. 955p.

Embry, A. Klovan, J. 1971. Late Devonian reef tracts on northeastern Banks Islands, Northwest Territories. *Canadian Petrology and Geology Bulletin*, 19:730-781.

Enos, P. 1983. Shelf. In Scholle, P. Bebout, D. Moore, C. (eds) *Carbonate depositional environments.* AAPG, Memoir 33. p. 267-296.

Figueiras, A. & Truckenbrodt, W. 1987. *Petrologia dos carbonatos da Formação Itaituba, na região de Aveiro – PA*. Belém. Boletim do Museu Emílio Goeldi: Nova Série. Geologia. 31:1-56.

Figueiras, A. 1983. *Petrologia dos carbonatos da Formação Itaituba, na região de Aveiro-PA. Universidade Federal do Pará*. Tese de mestrado, 135p.

Fischer, A. G. 1964. The Lofer cyclothem of the Alpine Triassic: *Kansas Geological Survey Bulletin* 169, p. 107-149.

Fisher, S. 1986. Pyrite replacement of mollusc shells from the Lower Oxford Clay (Jurassic) of England. *Sedimentology*. **33**. 575–586.

Flügel, E. 2004. Microfacies of carbonate rocks: analysis, interpretation and application. London. Springer Verlag. 995p.

Folk, R. L. 1962. Spectral subdivision in limestone type. Tulsa Memoir AAPG. n.1. 62–84p.

Folk, R.L. 1974. *Petrology of Sedimentary Rocks*. Hemphill's Pub., Austin, TX. 159p.

Freydank, H. G. 1957. Limited investigation along eastern and southern flank of the Monte Alegre Dome. Relatório interno. Belém, PETROBRÁS/DENOR. n. p.

Fryberger, S., Ahlbrandt, T., Andrews, S. 1979. Origin, sedimentary features, and significance of low-angle eolian "sand sheet" deposits, Great Sand Dunes National Monument and vicinity, Colorado: *Journal of Sedimentary Petrology*, v. 49, p. 733-746p.

Fúlvaro, V. 1965. *Conodontes do calcário Itaituba, do Carbonífero do Rio Tapajós, Estado do Pará*. Boletim da Sociedade Brasileira de Geologia. São Paulo. v.14, p. 29-440

Gawthorpe, R.L. 1987. Burial dolomitization and porosity development in a mixed carbonate-clastic sequence: an example from the Bowland Basin, Northern England. *Sedimentology*. **34**. 533-558.

Ginsburg, R.N. 1971. *Landward movement of carbonate mud: new model for regressive cycles in carbonates. In:* Am. Ass. Petr. Geol. Bull. Tulsa, **55**, 340–340

Gleannie, K. 1970. Desert sedimentary environments. Elsevier. Amsterdam. Developments in sedimentology 14. 222p.

Goldhammer, R. K. 1987. Platform carbonate cycles, Middle Triassic of northern Italy: The interplay of local tectonics and eustasy: Ph.D. dissertation, The John Hopkins University, Baltimore, Maryland, 468p.

Goldhammer, R. K., Dunn, P. A., & Hardie, L. A. 1990. Depositional cycles, composite sea-level changes, cycle stacking patterns, and the hierarchy of stratigraphic forcing: examples from Alpine Triassic platform carbonates. *Geological Society of America Bulletin*, 102(**5**):535-562.

Goldhammer, R. K., Lehmann, P. J., Tood, R. G., Wilson, J. L., Ward, W. C., Johnson, C. R. 1991. Sequence stratigraphy and cyclostratigraphy of the Mesozoic of the Sierra Madre Oriental, northeast Mexico, a fild guid-book: Gulf Coast Section, Society of Economic Paleontologists and Mineralogists, 85 p.

Goodbred, S. & Saito, Y. 2012. *Tide-dominated deltas*. In Davis Jr, R. Dalrymple, R. (eds) Principles of tidal sedimentology. Springer. New York. 1st edition. 129-150p.

Haas, J. 2004. Characteristics of peritidal facies and evidences for subaerial exposures in Dachstein-type cyclic platform carbonates in the Transdanubian range, Hungary. Facies. (50). 263-286p.

Handford, C. & Loucks, R. 1993. *Carbonate depositional sequences and system tracts– responses of carbonate platforms to relative sea level changes*. In Loucks, R. Sarg, J. (eds) Carbonate sequence stratigraphy. AAPG Memoir 57. Tulsa. p. 3-41.

Handford, C. R., & Francka, B. J. 1991. *Mississippian carbonate-siliciclastic eolianites in southwestern Kansas. In*: Lomando, A.J. and Harris, P.M. eds. Mixed Carbonate-Siliciclastic Sequences: SEPM, Core Workshop 15, p. 205-243.

Haq, B. & Schutter, S. 2008. A chronology of Palaezoic sea level changes. *Science*. **322**:64-68.

Haq, B.U., Hardenbol, J. and Vail, P.R. 1988 Mesozoic and Cenozoic Chronostratigraphy and Cycles of Sea Level Change. In: Wilgus, C.K., et al., Eds., *Sea Level Changes: An Integrated Approach*, SEPM Special Publication, Houston, p. 71-108.

Hardenbol, J., Thierry, J., Farley, M.B., Jacquin, T., de Graciansky, P.C. and Vail, P. (1998) *Mesozoic and Cenozoic Sequence Chronostratigraphic Framework of European Basins*. In: De Graciansky, P.C., et al., Eds., Mesozoic and Cenozoic Sequence Stratigraphy of European Basins, 60, charts 1-8, SEPM Special Publication, Houston, p. 3-13.

Harms, J., Southard, J., Walker, R. 1982. Structures and sequences in clastic rocks. Tulsa, Soc. Econ. Paleont. Miner. (Short Course, 9).

Harries, P. 2011. Earth system: history and natural variability. Epeiric Seas: A Continental Extension of Shelf Biotas. Encyclopedia of Life Support Systems. v.4, p 1-17.

Harrington, H. 1962. Paleogeographic development of South America. *Bulletin of American association of petroleum geologists*. 46(**10**):1773-1814.

Heckel, P. 1986. Sea-level curve for Pennsylvanian eustatic marine transgressive-regressive depositional cycles along midcontinent outcrop belt, North America. *Geology*. 14:330-334.

Heckel, P. H. 1994. Evaluation of evidence for glacio-eustatic control over marine Pennsylvanian cyclothems in North America and consideration of possible tectonic effects. Tectonic and Eustatic Controls on Sedimentary Cycles: SEPM, *Concepts in Sedimentology and Paleontology,* 4:65-87.

Hessel, R. 1990. Early diagenetic pore water/sediment interaction: modern offshore basin. In: Mcllrealth, I. & Morrow, D. (eds) *Diagenesis*. Ottawa. Geoscience Canada. 277-316.

Holmden, C.; Panchuk, K.; Finney, S. C. 2012. Tightly coupled records of Ca and C isotope changes during the Hirnantian glaciation event in an epeiric sea setting. *Geochimica et Cosmochimica Acta*, 98:94-106.

Hughes, Z. 2012. Tidal channels on tidal flats and marshes. In Davis Jr, R. Dalrymple, R. (eds) *Principles of tidal sedimentology*. Springer. New York. 1st edition. p. 269-300.

Hummel, G. and Kocurek, G. 1984. Interdune areas of the back-Island dune field, North Padre Island, Texas: *Sedimentary Geology*, v. 39, p. 1-26p.

Hunter, R. 1977. Basic types of stratification in small eolian dunes. *Sedimentology*. (24). 361-387p.

Hurtado, C., Roddaz, M., Santos, R. V., Baby, P., Antoine, P. O., & Dantas, E. L. 2019. Cretaceous-early Paleocene drainage shift of Amazonian rivers driven by Equatorial Atlantic Ocean opening and Andean uplift as deduced from the provenance of northern Peruvian sedimentary rocks (Huallaga basin). *Gondwana Research*, **63**. 152-168.

Husinec, A., Basch, D., Rose, B., & Read, J. F. 2008. FISCHERPLOTS: An Excel spreadsheet for computing Fischer plots of accommodation change in cyclic carbonate successions in both the time and depth domains. *Computers & geosciences*, 34(**3**): 269-277.

Immenhauser, A., Della Porta, G., Kenter, J. A., Bahamonde, J. R. 2003. An alternative model for positive shifts in shallow-marine carbonate δ13C and δ18O. *Sedimentology*, 50(**5**):953-959.

Immenhauser, A., Kenter, J. A., Ganssen, G., Bahamonde, J. R., Van Vliet, A., Saher, M. H. 2002. Origin and significance of isotope shifts in Pennsylvanian carbonates (Asturias, NW Spain). *Journal of Sedimentary Research*, 72(**1**):82-94.

Irwin, M.L. 1965. General theory of epeiric clear water sedimentation. *AAPG Bulletin*. 49:445-459.

Isbell, J.L., Miller, M.F., Wolfe, K.L., and Lenaker P.A. 2003. Timing of late Paleozoic glaciation in Gondwana: Was glaciation responsible for the development of northern hemisphere cyclothems? In: Chan, M.A., and Archer, A.W., eds., Extreme depositional environments: Mega end members in geologic time: Boulder, Colorado, *Geological Society of America Special Paper* 370:5-24.

Isozaki, Y., Kawahata, H., & Minoshima, K. 2007. The Capitanian (Permian) Kamura cooling event: the beginning of the Paleozoic–Mesozoic transition. *Palaeoworld*, 16(**1-3**):16-30.

isozaki-Garcés, B.L., Laird, K.R., Fritz, S.C., Kelts, K., Ito, E., Grimm, E.C. 1997. Holocene climate in the Northern Great Plains inferred from sediment stratigraphy, stable isotopes, carbonate geochemistry, diatoms, and pollen at Moon Lake, North Dakota. *Quaternary Research*, 48**(3)**:359-369.

Issler, R.S. A. Montalvão, R. Guimarães, G., Silva, G. Lima, M. I. C. 1974. Geologia da Folha SA.22. Belém, Brasil. In: Departamento Nacional de Produção Mineral. Projeto RADAMBRASIL. Rio de Janeiro, DNPM. v. 5, p. 1-60p.

Jacobsen, S. B., & Kaufman, A. J. 1999. The Sr, C and O isotopic evolution of Neoproterozoic seawater. *Chemical Geology*, 161**(1-3)**:37-57.

James, N. & Choquette, P. 1990. Limestones – Introduction. In: Mcllreath, I. & Morrow, D. (eds) *Diagenesis*. Geoscience of Canada.

James, N. 1984. Shallowing-upward sequences in carbonate. In: Waker, R (ed) *Facies Models*. Geoscience Canada reprint series. **1**:213-228.

Jipa, D. C., & Olariu, C. 2013. Sediment routing in a semi-enclosed epicontinental sea: Dacian Basin, Paratethys domain, Late Neogene, Romania. *Global and planetary change*, v. 103, p. 193-206.

Kerans, C. & Tinker. S.W. 1997. Sequence stratigraphy and characterization of carbonate reservoirs. *Society for Sedimentary Geology*. SEPM. v. 40. 137p.

Kiessiling, W. Flügel, E. Golonka, J. 2003. Patterns of Phanerozoic carbonate platform sedimentation. *Lethaia.* 36:195-226.

Kocurek, G. & Nielson, J. 1986. Conditions favourable for the formation of warm climate aeolian sand sheets. *Sedimentology*. 33:795-816.

Kocurek, G. 1996. Desert aeolian systems. In Reading, H. (ed) *Sedimentary environments: Processes, facies and stratigraphy*. Blackwell publishing. 3rd edition. 125-153p.

Korte, C., Jasper, T., Kozur, H. W., & Veizer, J. 2006. 87Sr/86Sr record of Permian seawater. *Palaeogeography, Palaeoclimatology, Palaeoecology*, 240**(1-2)**:89-107.

Kremer. 1956. Geological report in the Monte Alegre structure. Relatório Interno. Belém, PETROBRÁS/DENOR. 16p.

Lane, G. & Straka II, J.J. 1974. Late Mississipian and Early Pennsylvanian Conodonts, Arkansas and Oklahoma. *Geological Society of America Special Paper*, 152:144.

Laporte, L. F. 1969. Recognition of a transgressive carbonate sequence within an epeiric sea: Helderberg Group (Lower Devonian) of New York State, in Friedman, G.M. *Depositional environments in carbonate rocks*: Society of Economic Paleontologists and Mineralogists Spacial Publication 14:98-119.

Lee, H. S., & Chough, S. K. 2011. Depositional processes of the Zhushadong and Mantou formations (Early to Middle Cambrian), Shandong Province, China: roles of archipelago and mixed carbonate–siliciclastic sedimentation on cycle genesis during initial flooding of the North China Platform. *Sedimentology*, 58**(6)**:1530-1572.

Lehrmann, D.J. and R.K. Goldhammer, 1999, Secular variation in parasequence and facies stacking patterns of platform carbonates: a guide to application of stacking-patterns analysis in strata of diverse ages and settings, in P.M. Harris, A.H. Saller, and J.A. Simo, eds., Advances in carbonate sequence stratigraphy: application to reservoirs, outcrops,

and models: SEPM (Society for Sedimentary Geology) Special Publication No. 63, p. 187-225.

Lemos, V. & Medeiros, R. 1989. Transgressões e regressões cíclicas e ocorrência de conodontes no Morrowano e Atokano da Bacia do Amazonas. *11º Congresso Brasileiro de Paleontologia*. Curitiba. 2:961-969.

Lemos, V. B., Scomazzon, A. K. 2001. Carboniferous biochronostratigraphy of the Amazonas Basin, Brazil based on conodonts. Ciência, Técnica, Petróleo. Seção Exploração de Petróleo, Rio de Janeiro, 2:131-138.

Lemos, V.B. & Medeiros, R.A. 1996. O Limite Morrowano/Atokano na Bacia do Amazonas, Brasil, com base em conodontes. *Boletim de Geociências da Petrobras*, 10 **(14)**:165-173.

Lemos, V.B. 1990. *Assembléia de conodontes do Carbonífero da Bacia do Amazonas*. Porto Alegre: Universidade Federal do Rio Grande do Sul. Tese de doutorado, 259p.

Lemos, V.B. 1992. Conodontes do Carbonífero das bacias do Amazonas e Solimões: taxonomia, parte I. *Pesquisas*, Porto Alegre. 19:75-93.

Lima, H. 2010. *A sucessão siliciclástica–carbonática Neocarbonífera da Bacia do Amazonas, regiões de Monte Alegre e Itaituba (PA)*. Dissertação de mestrado. Instituto de Geociências. Universidade Federal do Pará. Belém. 121p.

Limarino, C. Césari, S. Spalletti, L. Taboada, A. Isbell, J. Geuna, S. Gulbranson, E. 2014. A paleoclimatic review of Southern South American during the late Paleozoic: A record from icehouse to extreme greenhouse conditions. Gondwana Research. (25). 1396-1421.

Lindholm, R. 1987. *A Practical Approach to Sedimentology*. London. Ed. Allen & Unwin. 276p.

Loczy, L. 1966. Contribuições à paleogeografia e história do desenvolvimento geológico da Bacia do Amazonas. Rio de Janeiro. *Boletim da Divisão de Geologia e Mineralogia*. 223:1-96.

Longhitano, S. 2011. The record of tidal cycles in mixed silici – bioclastic deposits: examples from small Plio – Pleistocene peripheral basins of the microtidal central Mediterranean sea. *Sedimentology*. **58 (3)**. 691 – 719p.

Longhitano, S. Mellere, D. Steel, R. Ainsworth, B. 2012. Tidal depositional systems in the record: A review amd new insights. *Sedimentary geology*. 279:2-22.

Lupia, R. and Armitage, J. 2013. Late Pennsylvanian-Early Permian vegetational transition in Oklahoma: Palynologival record. International Journal of Coal Geology. 119:165-176.

Macdonald, F. A., Schmitz, M. D., Crowley, J. L., Roots, C. F., Jones, D. S., Maloof, A. C., Schrag, D. P. 2010. Calibrating the cryogenian. *Science*, 327**(5970)**:1241-1243.

MacEachern, J. Pemberton, S. Gingras, M. Bann, K. 2010.Ichnology and facies models. In James, N. Dalrymple, R (eds) *Facies Model 4*. Geological association of Canada Geotext. 6:19-58.

Maliva, R. & Siever, R. 1986. Mechanism and controls of silicification on fossils in limestones. *The journal of geology*. **96(4).** 387-398.

Matsuda, N. 2002. *Carbonate sedimentation cycle and origin of dolomite on the Lower Pennsylvanian intracratonic Amazon Basin, Northern Brazil*. Tese de Doutorado. Tókio, Department of Earth and Planetary Science. 231 p.

Matsuda, N. Dino, R. Wanderley Filho, J. 2004. Revisão litoestratigráfica do Grupo Tapajós, Carbonífero Médio – Permiano da Bacia do Amazonas. Manaus. *Boletim de Geociências da Petrobrás,* **12** (2):435-441.

Matsuda, N. Winter, W. Wanderley Filho, J. Cancela, A. 2010. Roteiros geológicos– O paleozoico da borda Sul da Bacia do Amazonas, Rio Tapajós, Estado do Pará. *Boletim de Geociências da Petrobrás.* **18** (1):123-152.

Maynard, J. R., & Leeder, M. R. 1992. On the periodicity and magnitude of Late Carboniferous glacio-eustatie sea-level changes. *Journal of the Geological Society*, 149(**3**):303-311.

Mazzullo, S. J., Boardman, D. R., Grossman, E. L., Dimmick-Wells, K. 2007. Oxygen-carbon isotope stratigraphy of upper carboniferous to lower Permian marine deposits in Midcontinent USA (Kansas and ne Oklahoma): Implications for sea water chemistry and depositional cyclicity. *Carbonates and Evaporites*, 22(**1**):1-55.

McBride, E. 1989. Quartz cement in sandstone-a review. *Earth science reviews.* **26**. 69-112.

Mcllreath, I. A. and Morrow, D. W. 1990. Diagenesis. Reprint. Series 4. Geoscience of Canada. *Geological Association of Canada*, 338p.

Medeiros, R. 2015. *Depósitos carbonáticos–siliciclásticos da porção superior da Formação Piauí, Carbonífero da bacia do Parnaíba, região de José de Freitas–PI*. Dissertação de Mestrado. Instituto de Geociências. Universidade Federal do Pará. Belém. 120p.

Medeiros, R. S. P., Nogueira, A. C. R., da Silva Junior, J. B. C., Sial, A. N. 2019. Carbonate-clastic sedimentation in the Parnaiba Basin, northern Brazil: Record of carboniferous epeiric sea in the Western Gondwana. *Journal of South American Earth Sciences*. 91:188-202.

Medeiros, R., P. Nogueira, A. C. Bandeira, J, B. Sial, A., N. 2019. Carbonate-clastic sedimentation in the Parnaíba Basin, Northern Brazil: Record of Carboniferous epeiric sea in the Western Gondwana. *Journal of South American earth science.*

Menning, M., Alekseev, A., Chuvashov, B., Davydov, V., Devuyst, F., Forke, H., Grunt, T., Hance, L., Heckel, P., Izokh, N. 2006. Global time scale and regional stratigraphic reference scales of Central and West Europe, East Europe, Tethys, South China, and North America as used in the Devonian-Carboniferous-Permian Correlation Chart 2003 (DCP 2003). *Palaeogeography, Palaeoclimatology. Palaeoecology* 240, 318e372.

Merril, G. Von Bitter, P. 1984. Facies and frequencies among Pennsylvania conodonts: apparatuses and abundances. *Geological Society of America special paper*. (**96**). 251-261p.

Miall, A. D. 1977. A review of the braided-river depositional environment. *Earth-Science Reviews,* 13(**1**):1-6p.

Mii, H. S., Grossman, E. L., & Yancey, T. E. 1999. Carboniferous isotope stratigraphies of North America: implications for Carboniferous paleoceanography and Mississippian glaciation. *Geological Society of America Bulletin*, 111(**7**):960-973.

Mii, H. S., Grossman, E. L., Yancey, T. E., Chuvashov, B., & Egorov, A. 2001. Isotopic records of brachiopod shells from the Russian Platform—evidence for the onset of mid-Carboniferous glaciation. *Chemical Geology*, 175**(1-2)**:133-147.

Milani, E. J., & Thomaz Filho, A. 2000. Sedimentary basins of South America. In Cordani, U. Milani, E. Thomaz Filho, A. Campos, D. (eds.) *Tectonic evolutions of South America.* Rio de Janeiro. 31:389-449.

Millani, E. J. & Zálan, P. V. 1999. An outline of the geology and petroleum system of Paleozoic interior basins of South American. *Episodes.* **3** (22). 199-205.

Mitchell S.F., Paul C.R., Gale, A.S. 1996. Carbon isotopes and sequence stratigraphy. In: Howell, J.A., Aitken, J.F. eds. High resolution stratigraphy: innovations ans applications. *Geological Society Special Publication.* 104:11-24.

Moore, D. G. & Curray, J. R. 1964. Wave-base, marine profile of equilibrium, and wave-built terraces: discussion. *Geological Society of America Bulletin*, 75**(12)**:1267-1273.

Morad, S. 1998 *Carbonate Cementation in Sandstones.* Spec. Publs Int. Assoc. Sediment. Blackwell Science, Oxford. **26.** 511p.

Morad, S., MarfiL, R., Al-Aasm, I.S. & Gomez-Gras, D. 1992) The role of mixing-zone dolomitization in sandstone cementation: evidence from the Triassic Buntsandstein, the Iberian Range, Spain. *Sedimentary geology.* **80. 53-65**

Morrow, D. 1990a. Dolomite-part 1: The chemestry of dolomitization and dolomite precipitation. In McRealth, I. Morrow, D. (eds) *Diagenesis*. Geoscience Canada. Repreint series 4. 113-124p.

Morrow, D. 1990b. Dolomite-part 2: Dolomitization models and ancient dolostones. In McRealth, I. Morrow, D. (eds) *Diagenesis*. Geoscience Canada. Repreint series 4. 125-140p.

Mountney, N. 2006. Eolian Facies Models. In Posamentier, H. Walker, R. (eds). *Facies Models revisited.* SEPM. 84:19-83.

Moutinho, L. P. 2006. *Assinaturas tafonômicas dos invertebrados da Formação Itaituba – Aplicação como ferramenta de análise estratigráfica e paleoecológica na seção Pensilvaniana aflorante na porção sul da Bacia do Amazonas, Brasil*. Tese de doutorado. Instituto de Geociências. Universidade Federal do Rio Grande do Sul. Porto Alegre. 346 p.

Moutinho, L., Nascimento, S., Scomazzon, A., Lemos, V. 2016a. Trilobites, scolecodonts and fish remains occurrence and the depositional paleoenvironment of the upper Monte Alegre and Itaituba formations, Lower – Middle Pennsylvanian of the Amazonas basin, Brazil. *Journal of South America earth science*. 72:76-94.

Moutinho, L., Scomazzon, A., Nascimento, S., Lemos, V. 2016b. Taphofacies of Lower – Middle Pennsylvanian marine invertebrates from the Monte Alegre and Itaituba formations, part of the outcropped marine sequence of the Tapajós Group (Southern Amazonas basin, Brazil) – regional palaeocological models. *Journal of South America earth science.* 70:83-114.

Nascimento, S. 2008. Conodontes e a cronoestratigrafia da base da seção Pensilvaniana, na região de Itaituba, porção Sul da Bacia do Amazonas, Brasil. Tese de doutorado. Universidade Federal Rio Grande do Sul. Porto Alegre. 247p.

Nascimento, S.; Lemos, V.B.; Scomazzon, A.K.; Matsuda, N.S.; Silva, C.P. 2010. First occurrence of Ellisonia, Gondolella and Ubinates (Conodonts) in Itaituba Formation, Pennsylvanian of Amazonas Basin, Brazil. Gaea, 6(**2**):56-62.

Nogueira, A. C. R. 2008. Guinada para o Atlântico. In: Furtado, R. (coord.). *Scientific América Brasil*. Coleção Amazônia Origens, 1:22-27.

Nogueira, A. C. R. Silveira, R. Guimarães, J. F. 2013. Neogene–Quaternary sedimentary and paleovegetation history of the eastern Solimões Basin, central Amazon region.*Journal of South American Earth Sciences*. **46.** 89-99.

Olsen, H. Due, P. Clemmensen, L. 1989. Morphology and genesis of asymmetric adhesion warts-a new adhesion surface structure. *Sedimentary geology*. v61. 277-285p.

Osleger, D. 1991. Subtidal carbonate cycles: implications for allocyclic vs. autocyclic controls. *Geology*. **19**. 917-920p.

Palagi, P. 2009. Evaporitos no Brasil e na América do Sul. In Mohriak, W. Szatmari, P. Anjos, S. (eds) Sal geologia e tectônica exemplos das bacias brasileiras. Editora Beca. Porto Alegre. p. 190-209.

Panchuk, K. M., Holmden, C., & Kump, L. R. 2005. Sensitivity of the epeiric sea carbon isotope record to local-scale carbon cycle processes: tales from the Mohawkian Sea. Palaeogeography, Palaeoclimatology, Palaeoecology, 228(**3-4**):320-337.

Parente, A. 2014. Paleoambiente e quimioestratigrafia da Formação Itaituba, carbonífero da borda sul da Bacia do Amazonas, região de Uruará – Pará. Dissertação de mestrado. Instituto de Geociências. Universidade Federal do Pará. Belém. 120 p.

Pereira, E. Carneiro, C. Bergamaschi, S. Almeira, F. 2012. Evolução das sinéclises Paleozoicas: Províncias Solimões, Amazonas, Parnaíba e Paraná. In: Geologia do Brasil. Hasui, Y. Carneiro, C. Almeida, F. Bartorelli, A. (eds). São Paulo. Editora Beca. 374-394.

Perlmutter, M.A. & Azambuja Filho, N.C. 2005. Cicloestratigrafia: Teoria e Técnicas. *Revista Brasileira de Geociências*. **35**:1-12.

Playford, G. & Dino, R. 2000. Palynostratigraphy of Upper Paleozoic Strata (Tapajos Group), Amazonas Basin, Brazil: Part One. Stuttgart, *Paleontographica Abt. B*, **255**:1-46.

Pomar, L. 2001. Types of carbonate platforms: a genetic approach. *Basin research*. 13:313-334.

Posamentier, H. & James, N. 1993. Sequence stratigraphy–uses and abuses. In sequence stratigraphy and facies associations. Posamentier, H. Summerhayes, C. Haq, B. Allen, G. (eds) *International associations of sedimentologists special publications*. **18**:3-18.

Pratt, R. & James, N. 1986. The St. George Group (Lower Ordovician) of western Newfoundland: tidal flat island model for carbonate sedimentation in shallow epeiric seas. *Sedimentology*. **33**:313-343.

Purkis, S. J., Rowlands, G. P., & Kerr, J. M. 2015. Unravelling the influence of water depth and wave energy on the facies diversity of shelf carbonates. *Sedimentology*, 62(**2**):541-565.

Qing, H. & Mountjoy, Eric. 1994. Formation of coarsely crystalline, hydrothermal dolomite reservoirs in the Presqu'ile barrier, Western Canada sedimentary basin. AAPG bulletin. **78** (1). 55-77.

Ramsbottom, W. H. 1979. Rates of transgression and regression in the Carboniferous of NW Europe. *Journal of the Geological Society*, 136**(2)**:147-153.

Rodríguez-López, J. Clemmensen, L. Lancaster, N. Mountney, N. 2014. Archean to recent aeolian sand systems and their sedimentary record: current understanding and future prospects. *Sedimentology*. 61:1487-1534.

Ross, C. & Ross, J. 1985. Late Paleozoic depositional sequences are synchronous and worldwide. *Geology*. **13**. 194 - 197p.

Ross, C.A. & Ross, J.R. 1988. Late Paleozoic transgressive-regressive deposition. In Wilgus, C. Hastings, B. Posamentier, H. Van Wagoner, J. Ross, C. Christopher, G. Kendall, C. (eds) *Sea-level changes*: An integrated approach. SEPM. 227-248p.

Ross, C.A., & Ross, J.R. 1987. Late Paleozoic sea levels and depositional sequences. Cushman Foundation for Foraminiferal Research. Western Washington University 137p.

Rowley, D. Raymond, A. Parrish, J. Lottes, A. 1985. Carboniferous palaeogeographic and phytogeographic and palaeoclimatic reconstructions. *International. Journal of Coal Geology.* 5:7-42.

Rutter, E.H., 1983. Pressure solution in nature, theory and experiment. *J. Geol. Soc. London*. **140**. 725-740.

Sadler, P.M., Osleger, D.A., Montanez, I.P. 1993. On the labeling, length, and objective basis of Fischer plots. *Journal of Sedimentary Research*, 63**(3)**:360-368.

Saltzman, M. R. 2005. Phosphorus, nitrogen, and the redox evolution of the Paleozoic oceans. *Geology*, 33**(7)**:573-576.

Saltzman, M. R., & Thomas, E. 2012. *Carbon isotope stratigraphy*. The geologic time scale, **1**:207-232.

Saltzman, M.R., Groessens, E., Zhuravlev, A.V. 2004. Carbon cycle models based on extreme changes in δ13C: an example from the lower Mississippian. *Palaeogeography, Palaeoclimatology, Palaeoecology*. 213**(3-4)**:359-377.

Schckleton, N. J. 1986. Paleogene stable events. *Paleogeography, Paleoclimatology and Paleoecology*. **57** (1). 91-102.

Scholle, P. Scholle, D. 2003. *A colour guide to the petrography of carbonate rocks: grains, textures, porosity, diagenesis*. Tulsa. AAPG Memoir 77. 470p.

Scholle, P. Scholle, D. 2003. A colour guide to the petrography of carbonate rocks: grains, textures, porosity, diagenesis. Tulsa. AAPG Memoir 77. 470p.

Schwarzacher, W. 1993. Cyclostratigraphy and the Milankovitch theory. *Development in sedimentology*. Amsterdam. 52. 225p.

Scomazzon, A. 2004. *Estudo dos conodontes em carbonatos marinhos do Grupo Tapajós, Pensilvaniano inferior a médio da Bacia do Amazonas com aplicação de isótopos de Sr e Nd neste intervalo.* Tese de Doutorado. Universidade Federal do Rio Grande do Sul. Porto Alegre. 114 p.

Scomazzon, A. K., Koester, E., Moutinho, L. P., Nascimento, S., Matsuda, N., Lemos, V. B. 2005. *Sr and Nd isotopic analysis in fossils and carbonatic rocks of Itaituba and Nova Olinda Formations, Pensylvanian of Amazonas Basin*. In: Gondwana 12, Mendoza. p. 328-328.

Scomazzon, A. Moutinho, L. Nascimento, S. Lemos, V. Matsuda, N. 2016. Conodont bioestratigraphy and paleoecology of the marine sequence of the Tapajós Group, Early–Middle Pennsylvanian of the Amazonas basin, Brazil. *Journal of South America earth science*. 65:25-42.

Scomazzon, A.K., & Lemos, V.B. 2005. Diplognathodus occurrence in the Itaituba Formation, Amazonas Basin, Brazil. *Revista Brasileira de Paleontologia*. **8** (3):203-208.

Scotese, C. R., & McKerrow, W. S. 1990. Revised world maps and introduction. Geological Society, London, *Memoirs*, 12(**1**):1-21.

Scotese, C.R., 2001. Atlas of Earth History, Volume 1, Paleogeography, PALEOMAP Project, Arlington, Texas, 52 p.

Sharma, G.D., 1965. Formation of silica cement and its replacement by carbonates. J. Sediment. Petrol., 35:733-745.

Shinn, E. 1983. Tidal Flat Enviroment. In: Scholle, P. Bebout, D. Moore, C. 1983. *Carbonate Depositional Environments*. Tulsa. AAPG Memoir 33. SEPM. 171-210p

Silva, O. 1997. *Ciclicidade sedimentar do Pensilvaniano da bacia do Amazonas e o controle dos ciclos de sedimentação na distribuição estratigráfica dos conodontes, fusulinídeos e palinomorfos.* Tese de doutorado. Instituto de Geociências, Universidade Federal do Rio Grande do Sul. Porto Alegre. 331p.

Silva, P. 2014. *Paleoambiente e diagênese da Formação Itaituba, Carbonífero da bacia do Amazonas, com base em testemunho de sondagem, região de Uruará, Pará.* Dissertação de mestrado. Instituto de Geociências. Universidade Federal do Pará. Belém. 78p.

Silva, P. Afonso, J. Soares, J. Nogueira, A. 2015. Depósitos de plataforma mista, Neocarbonífero da bacia do Amazonas, região de Uruará, Estado do Pará. *Geologia Usp-série científica.* São Paulo. 15(**2**):79-98.

Smith, L. B., & Read, J. F. 2000. Rapid onset of late Paleozoic glaciation on Gondwana: Evidence from Upper Mississippian strata of the Midcontinent, United States. *Geology*, 28(**3**): 279-282.

Solomon, S. T., & Walkden, G. M. 1985. The application of cathodoluminescence to interpreting the diagenesis of an ancient calcrete profile. *Sedimentology,* 32(**6**), 877-896.

Spencer, G.H. & Tucker, M.E. 1997. Genesis of limestone mega-breccies and their significance in carbonate sequence stratigraphic models: a review. *Sedimentary Geology*. 112:163-193.

Spencer, G.H. & Tucker, M.E. 2007. A proposed integrated multi – signature model for peritidal cycles in carbonates. *Journal of sedimentary research*. 77:797-808.

Strasser, A. 1991. Lagoonal-peritidal sequences in carbonate environments: autocyclic and allocyclic processes. In: Einsele, G., Ricken, W. & Seilacher, A. (eds.): *Cycles and events in stratigraphy.* Springer-Verlag, p. 709-721.

Strasser, A. Hillgärtner, H. Hug, W. Pittet, B. 2000. Third – order depositional sequences reflecting Milankovitch cyclicity. *Terra Nova*. 12:303-311.

Strasser, A., Hilgen, F. J., & Heckel, P. H. 2006. Cyclostratigraphy–concepts, definitions, and applications. *Newsletters on Stratigraphy*, 42(**2**), 75-114.

Swart, P.K. & Oehlert, A.M. 2018. Revised interpretations of stable C and O patterns in carbonate rocks resulting from meteoric diagenesis. *Sedimentary Geology*, 364:14-23.

Tada, R. & Siever, R. 1989. Pressure solution during diagenesis. *Annual review of earth and planetary sciences*. **17.** 89-118.

Talbot, M.R. & Kelts, K.R. 1989. The Phanerozoic record of lacustrine basins and their environmental signals. *Palaeogeog. Palaeoclimat. Palaeoecol*. 70:1-304.

Torres, A, M. 1989. *Litofácies e evolução diagenética dos arenitos da Formação Monte Alegre na Região do Rio Tapajós, Bacia do Amazonas*. Tese de mestrado. Instituto de Geociências. Universidade Federal do Pará. Belém. 144p.

Tucker, M. & Garland, J. 2010. High–frequency cycles and their sequence stratigraphic context: orbital forcing and tectonic controls on Devonian cyclicity, Belgium. *Geological Belgica*. 13(**3**):213-240.

Tucker, M.E. & Wright, V.P. 1990. *Carbonate Sedimentology*. Oxford: Blackwell Scientific Publications. 482 p.

Tucker, M.E. 1988. Techniques in Sedimentology. Blackwell Scientific Publications, Oxford, 394 p.

Tucker, M.E. 1991. Sequence stratigraphy of carbonate-evaporite basins: models and application to the Upper Permian (Zechstein) of northeast England and adjoining North Sea. *Journal of the Geological Society*, 148(**6**):1019-1036.

Tucker, M.E. 1992. *Sedimentary Petrology: an introduction*. 2a ed. London: Blackwell Scientific Publications. 252 p.

Tucker, M.E. 2013. Rochas sedimentares: guia prático de campo. Bookman. Porto Alegre. 4a edição. 336p.

Van Geldern, R., Joachimski, M. M., Day, J., Jansen, U., Alvarez, F., Yolkin, E. A., & Ma, X. P. 2006. Carbon, oxygen and strontium isotope records of Devonian brachiopod shell calcite. *Palaeogeography, Palaeoclimatology, Palaeoecology*, 240(**1-2**):47-67.

Vasconcellos, A. 2000. Bacia do Amazonas-uma via marítima durante o carbonífero médio. *Boletim do museu Emílio Goeldi*. vol12. 3-61p.

Vaz, P. Rezende, N. Wanderley Filho, J. 2007. Bacia do Parnaíba. *Boletim de Geociências da Petrobrás*.**15**:253-260.

Veevers, J. Powell, M. 1987. Late Paleozoic glacial episodes in Gondwanaland reflected in transgressive – regressive depositional sequences in Euramerica. *Geological society of America bulletin*. **98**:475-487.

Veizer, J., Ala, D., Azmy, K., Bruckschen, P., Buhl, D., Bruhn, F., Jasper, T. 1999. 87Sr/86Sr, δ13C and δ18O evolution of Phanerozoic seawater. *Chemical geology*, *161*(**1-3**):59-88.

Visser, M. 1980. Neap spring cycles reflected in Holocene subtidal large scale bedform deposits: a preliminary note. *Geology*. 8(**11**):543-546.

Walker, R. 1992. Facies, facies models and modern stratigraphic concepts. In: Walker, R. & James, N. (Eds.) *Facies Models – Response to sea Level Change*. Ontario, Geological Association of Canadá. 265-275p.

Wanderley filho, J. 1991. *Evolução estrutural da Bacia do Amazonas e sua correlação com o embasamento*. Belém, CG/UFPA. Dissertação de Mestrado. 125p.

Wanderley Filho, J. Eiras, J. Cunha, P. Van der Vem, P. 2010. The Paleozoic Solimões and Amazonas basins and the Acre foreland basin of Brazil. In Hoorn, C. Wesselingh, F. (eds) Amazonia: landscape and species evolutions A look into the past. Willey–Blackwell. Amsterdam. p. 29-37.

Wanderley Filho, J. Eiras, J. Vaz, P. 2007. Bacia do Solimões. *Boletim de Geociências da Petrobrás.* 15(**2**):217-225.

Wanderley filho, J. Travassos, W. Alves, D. 2006. O diabásio nas bacias paleozoicas amazônicas-herói ou vilão? *Boletim de Geociências*. PETROBRÁS, 14(**1**):177-184.

Wang, Z. H.; Qi, Y.P. 2002. Report on the Pennsylvanian conodont zonation from the Nashui section of Luodian, Guizhou, China. *Newsletter on Carboniferous Stratigraphy*. 26:29-33.

Warren, J. 2000. Dolomite occurrence, evolution and economically importance. *Earth science reviews.* 52:1-81.

Warren, J. 2010. Evaporites through time: Tectonic, climatic and eustatic controls in marine and nonmerine deposits. *Earth Science review*. 98:217-268.

Waugh, B., 1970. Formation of quartz overgrowths in the Peurith sandstone (Lower Permian) of northwest England as revealed by scanning electron microscopy. Sedimentology, 14: 309-320.

Weimer, R. Howard, J. Lindsay, D. 1982. Tidal flats and associated tidal channels. In Scholle, P. Spearing, D. (eds) *Sandstone depositional environments*. AAPG. 31:191-245.

Wilson, J. 1975. *Carbonate fácies in geologic history*. Berlin, Springer-Verlag. 471p.

Witzke, B. 1987. Models for circulation patterns in epicontinental seas aplied to Paleozoic facies of North America Craton. *Paleoceanography*. 2(**2**):229-248.

Wopfner, H. 1999. The early Permian event deglaciation event between East Africa and Northwestern Australia. *Journal of African earth science*. 29:77-90.

Worden, R & Burley, S. 2003. Sandstone diagenesis: the evolution of sand to Stone. In: Burley, S & Worden, R. (eds). *Sandstones diagenesis*: recent and ancient. Blackwell publishing. Berlin. 649p.

Wright, V. P. 1992. A revised classification of limestones: *Sedimentary Geology*. 76:177-185.

Zalán P.V. 2004. A Evolução Fanerozoica das Bacias Sedimentares Brasileiras. In: Montesso- Neto, V., Bartorelli A., Carneiro C. Brito-Neves B. *Geologia do Continente Sul-Americano*: evolução da obra de Fernando Flávio Marques de Almeida. São Paulo. Ed. Becca, p.595- 612.
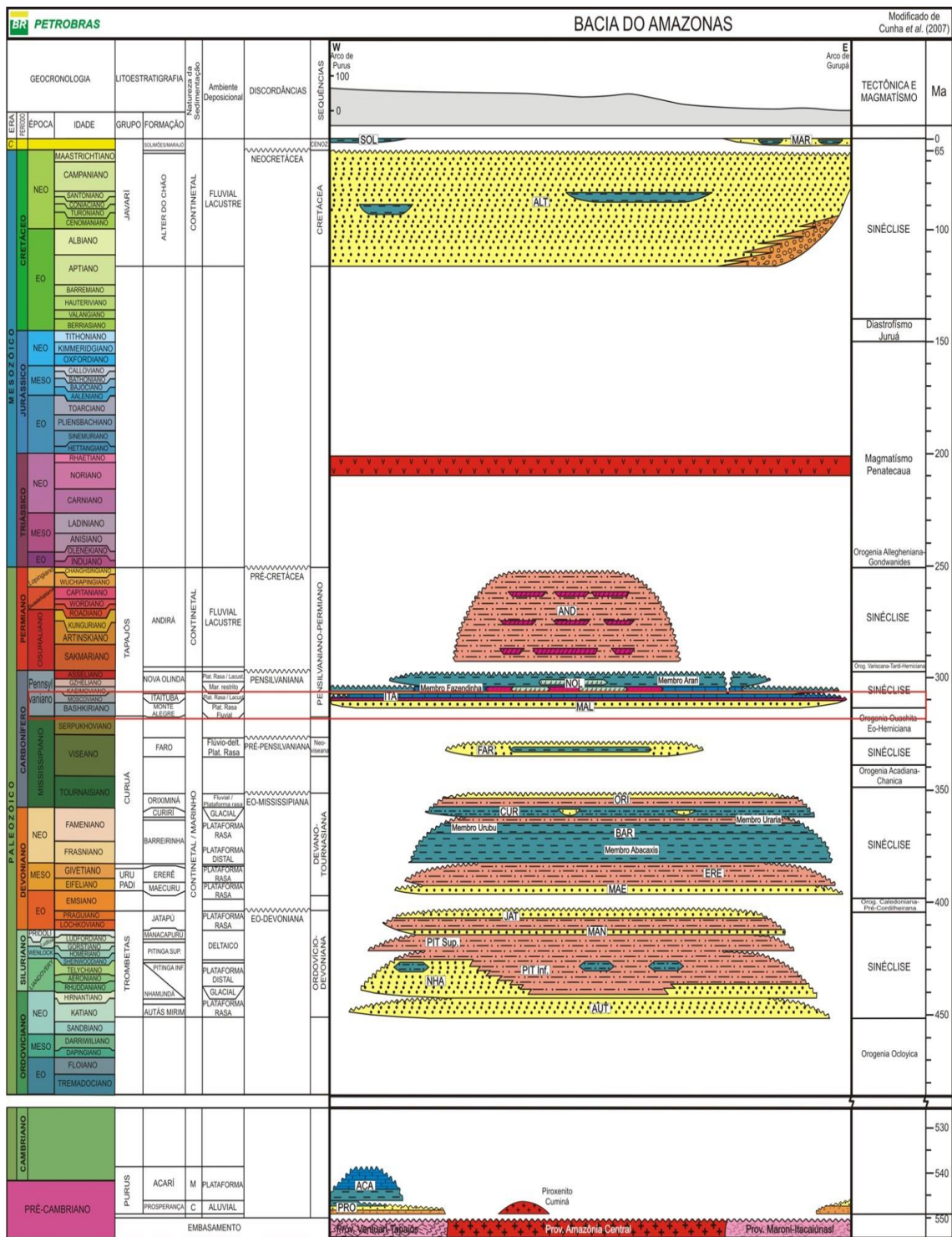
Anexo 1- Carta litoestratigráfica da Bacia intracratônica do Amazonas, apresentando o preenchimento sedimentar e vulcanosedimentar das sequências sedimentares, sendo hierarquizado em membros, formações e grupos. Em vermelho destaque para as formações Monte Alegre e Itaituba, de idade Pensilvaniana (Bashikiriano-Moscoviano). Fonte :Cunha *et al* (2007).

Amostra	Microfácies	AF	Matriz	Bioclasto	Aloquímico	Terrígenos	Cimento	Pirita
1	Dm	AF1	87	x	x	5	x	8
2	Dm	AF1	93	x	x	2	x	5
3	Dm	AF1	90	x	x	8	x	2
4	Dm	AF1	90	x	x	3	x	7
5	Ds	AF1	80	x	x	20	x	x
6	Ds	AF1	82	x	x	18	X	x
7	Ds	AF1	77	x	x	20	x	3
8	Ds	AF1	75	x	x	23	x	2
9	Dm	AF2	91	x	x	5	x	4
10	Dm	AF1	92	x	x	3	x	5
11	Dm	AF1	88			x	x	5	7
12	Dm	AF1	87	x	x	x	5	8
13	Dm	AF1	88	x	x	x	4	8
14	Dt	AF1	90	x	x	9	x	1
15	Dt	AF2	90	x	x	8	x	2
16	Dt	AF2	92	x	x	8	x	x
17	Dt	AF2	89	x	x	7	x	4
18	Dt	AF2	89	X	x	11	x	x
19	Lm	AF2	91	x	x	4	x	5
20	Lm	AF2	94	x	x	3	x	3
21	Lm	AF2	91	x	x	5	x	4
22	Lm	AF2	93	X	x	4	x	3
23	Fb	AF2	70	25	X	x	x	5
24	Fb	AF2	73	20	x	x	x	7
25	Fb	AF2	70	21	x	x	x	9
26	Fb	AF2	72	23	x	x	x	5
27	Fb	AF2	71	19	x	x	x	10
28	Wt	AF2	78	8	x	10	x	2
29	Wt	AF2	80	8	x	9	x	3
30	Wt	AF2	76	9	x	11	x	4
31	Wt	AF2	77	8	x	12	x	3
32	Wt	AF2	80	8	x	10	x	2
33	Gbo	AF3	x	36	54	8	x	2
34	Gbo	AF3	x	37	60	x	2	1

35	Gbo	AF3	x	38	55	x	4	3
36	Gbo	AF3	x	35	62	x	3	x
37	Gbo	AF3	x	37	60	x	2	1
38	Gbo	AF3	x	38	57	x	2	1
39	Gbo	AF3	x	35	60	x	4	1
40	Gbt	AF3	x	60	4	20	10	6
41	Gbt	Af3	x	62	3	25	7	3
42	Gbt	Af3	x	58	2	28	7	5
43	Gbt	Af3	x	60	4	20	10	6
44	Gbt	Af3	x	65	x	15	12	8
45	Gbt	Af3	x	65	5	15	8	7
46	Gbt	Af3	x	62	x	20	10	8
47	Gbt	Af3	x	55	x	30	12	3
48	Gbt	Af3	x	60	3	22	10	5
49	Gbt	Af3	x	60	x	30	10	x
50	Gbt	Af3	x	58	x	27	14	1
51	Wb	AF3	40	55	x	x	x	5
52	Wb	AF3	42	50	x	2	x	6
53	Wb	AF3	47	42	x	3	x	8
54	Wb	AF3	44	41	5	5	x	5
55	Wb	AF3	41	49	x	4	x	6
56	Wb	AF3	44	46	x	3	x	7
57	Wb	AF3	42	47	x	3	x	8
58	Wb	AF3	40	48	x	2	x	2
59	Wb	AF3	43	51	x	x	x	6
60	Wb	AF3	46	44	x	2	x	8
61	Wb	AF3	44	50	x	x	x	6
62	Wb	AF3	45	42	x	3	x	10
63	Wb	AF3	48	41	x	1	x	10
64	Wb	AF3	47	43	x	2	x	8
65	Wb	AF3	49	41	x	3	x	7
66	Pbt	AF3	21	69	x	8	x	2
67	Pbt	AF3	25	63	x	7	x	5
68	Pbt	AF3	25	65	x	5	x	5
69	Pbt	AF3	27	68	x	8	x	7

70	Pbt	AF3	29	61	x	7	x	3
71	Pbt	AF3	28	67	x	5	x	x
72	Pb	AF3	30	58	x	2	x	10
73	Pb	AF3	31	59	x	2	x	8
74	Pb	AF3	28	65	x	3	x	4
75	Pb	AF3	27	65	x	x	x	8
76	Pb	AF3	28	65	x	x	x	7
77	Pbt	AF3	30	67	x	x	x	3
78	Pbt	AF3	29	65	x	x	x	6
79	Pb	AF3	28	61	x	2	x	9
80	Lb	AF3	90	5	x	x	x	5
81	Lb	AF3	92	8	x	x		x
82	Lb	AF3	92	4	x	2		2
83	Lb	AF3	95	4	x	x	x	1
84	Lb	AF3	90	4	x	3	x	3
85	Lb	AF3	91	4	x	x	x	5
86	Lb	AF3	97	2	x	x	x	1
87	Lm	AF3	95	2	x	x	x	3
88	Lm	AF3	93	5	x	x	x	2
89	Lm	AF3	94	4	x	x	x	2
90	Lm	AF3	93	4	x	x	x	3
91	Lm	AF3	92	5	x	x	x	3
92	Lm	AF3	94	4	x	x	x	2
93	Lm	AF3	93	4	x	x	x	3
94	Lm	AF3	92	3	x	x	x	5
95	Lm	AF3	94	3	x	x	x	3
96	Lm	AF3	92	5	x	x	x	3
97	Lm	AF3	91	5	x	2	x	2
98	Dm	AF2	91	x	x	5	x	4
99	Dm	AF2	90	x	x	6	x	4
100	Dm	AF2	92	x	x	5	x	3
101	Dm	AF2	90	x	x	5	x	5
102	Dm	AF2	91	x	x	3	x	6
103	Lm	AF2	93	x	x	7	x	x
104	Lm	AF2	92	x	x	6	x	2

105	Lm	AF2	94	x	x	3	x	3
106	Lm	AF2	94	x	x	2	x	4
107	Lm	AF2	93	x	x	5	x	2
108	Lm	AF2	90	2	x	4	x	4
109	Lm	AF2	92	1	x	5	x	2
110	Lm	AF2	92	2	x	4	x	2
111	Lm	AF2	95	2	x	3	x	x
112	Gbt	AF3	x	58	2	22	11	7
113	Gbt	AF3	x	61	5	18	10	6
114	Gbt	AF3	x	65	3	25	7	x
115	Gbt	AF3	x	57	x	28	14	11
116	Gbt	AF3	x	58	x	32	8	2
117	Gbt	AF3	x	55	3	28	10	4
118	Gbt	AF3	x	57	x	19	11	3
119	Gbt	AF3	x	61	2	25	9	3
120	Gbt	AF3	x	65	x	28	7	x
121	Gbt	AF3	x	60	x	30	6	4
122	Gbt	Af3	x	62	3	25	7	3
123	Gbo	AF3	x	36	52	17	x	x
124	Gbo	AF3	x	35	52	13	x	x
125	Gbo	AF3	x	36	54	8	x	2
126	Wb	AF3	40	55	x	x	x	5
127	Wbt	AF3	40	28	5	22	x	5
128	Wbt	AF3	39	31	x	25	x	5
129	Wbt	AF3	40	30	4	26	x	x
130	Wbt	AF3	40	31	x	29	x	x
131	Wbt	AF3	40	32	x	28	x	x
132	Wbt	AF3	45	25	5	20	x	5
133	Wbt	AF3	42	43	x	12	x	3
134	Pb	AF3	27	63	x	2	x	8
135	Pb	AF3	30	59	x	2	x	9
136	Pbt	AF3	22	65	x	8	x	5
137	Pb	AF3	20	70	x	9	x	1
138	Pbt	AF3	24	68	x	6	x	2
139	Pbt	AF3	25	70	x	5	x	x

140	Pbt	AF3	21	73	x	6	x	x
141	Lb	AF3	94	5	x	x	x	1
142	Lb	AF3	90	4	x	x	x	6
143	Lb	AF3	93	4	x	x	x	3
144	Lb	AF3	91	5	x	x	x	4
145	Lm	AF3	95	2	x	x	x	3
146	Lm	AF3	93	3	x	x	x	4
147	Lm	AF3	97	1	x	x	x	2
148	Lm	AF3	95	2	x	x	x	3
149	Lm	AF3	93	x	x	x	x	7
150	Lm	AF3	95	2	x	x	x	3

ANEXO I- tabela com as médias das microfácies descritas e contadas para a área de estudo e foram plotadas em seus respectivos pontos nos perfis estratigráficos. Os valores correspondem a porcentagem de cada constituinte.
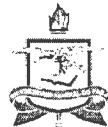
PARECER

Sobre a Defesa Pública da Tese de Doutorado de
PEDRO AUGUSTO SANTOS DA SILVA

A banca examinadora da Tese de Doutorado de **PEDRO AUGUSTO SANTOS DA SILVA** orientando do Prof. Dr. Afonso César Rodrigues Nogueira (UFPA), composta pelos professores doutores Ana Maria Góes (USP), Isaac Daniel Rudnitzki (UFOP), Werner Truckenbrodt (UFPA) e Moacir José Buenano Macambira (UFPA), após apresentação da sua tese intitulada "**O MAR EPICONTINENTAL ITAITUBA NA REGIÃO CENTRAL DA BACIA DO AMAZONAS: PALEOAMBIENTE E CORRELAÇÃO COM OS EVENTOS PALEOCLIMÁTICOS E PALEOCEANOGRÁFICOS DO CARBONÍFERO**", emite o seguinte parecer:

O documento do candidato apresenta um volume significativo de dados, porém necessita de melhor organização, redação e revisão bibliográfica, que podem ser corrigidas nos artigos submetidos. Na apresentação da tese e arguição o candidato demonstrou maior segurança na temática desenvolvida, em particular, sobre o paleoambiente da sucessão Monte Alegre – Itaituba, exposta nas bordas norte e sul da Bacia do Amazonas, por meio de análise de fácies, petrologia sedimentar e isótopos estáveis. O candidato demonstrou domínio sobre o tema da tese e os métodos aplicados.

Finalmente, a banca examinadora decidiu por unanimidade aprovar a tese de doutorado de Pedro Augusto Santos da Silva.

Belém, 14 de março de 2019.

_____
Prof. Dr. Afonso César Rodrigues Nogueira (Orientador – UFPA)
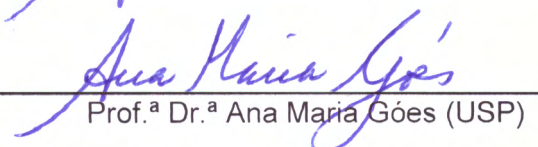
_____
Prof.ª Dr.ª Ana Maria Góes (USP)

_____
Prof. Dr. Isaac Daniel Rudnitzki (UFOP)

_____
Prof. Dr. Werner Truckenbrodt (UFPA)

_____
Prof. Dr. Moacir José Buenano Macambira (UFPA)